PREDICTION OF TENSILE STRENGTH OF COLD ASPHALT EMULSION MIXTURES USING THE MATURITY METHOD

MAGDALENE NAFULA OTIENO

Master of Science

(Construction Engineering and Management)

JOMO KENYATTA UNIVERSITY OF

AGRICULTURE AND TECHNOLOGY

2019

Prediction of Tensile Strength of Cold Asphalt Emulsion Mixtures Using the Maturity Method

Magdalene Nafula Otieno

A thesis submitted in partial fulfillment for the degree of Master of Science in Construction Engineering and Management in the Jomo Kenyatta University of Agriculture Technology

2019

DECLARATION

This thesis is my original work and has not been presented for a degree in any other university.

Signature: ……Date:…….

Magdalene Nafula Otieno

This thesis has been submitted for examination with my/our approval as the university supervisors.

Signature: ……Date:…….

Prof. James Wambua Kaluli, PhD.

JKUAT, Kenya

Signature: ……Date: …….

Dr. Eng. Charles K. Kabubo, PhD.

JKUAT, Kenya

DEDICATION

This work is dedicated to my family, friends and colleagues in the engineering field.

ACKNOWLEDGEMENT

I first acknowledge The Almighty God for the blessing of life, good health, sanity, strength, funds and a constructive team to undertake this study. I am very grateful.

I wish to express my heartfelt gratitude to my supervisors, Prof. James Wambua Kaluli and Dr. Eng. Charles K. Kabubo for their consistent guidance, constructive judgement and encouragement.

I am very grateful to my loving parents Mr. & Mrs. Otieno, my sister Diana Otieno, other family members and friends for their understanding, support and prayers.

Thank-you.

ABSTRACT

Lack of universal design standards for CMA has led to the use of Laboratory-Field Curing Correlation techniques to predict the performance (strength) in CMA. Such techniques involve performance-based tests that were originally developed for hot mix asphalt. Laboratory-Field curing correlation techniques disregard the gradual strength gain in CMA, which is affected by curing time and temperature. Moreover, they have demonstrated considerable inconsistencies in the prediction of strength in CMA during curing. The main objective of this study was to predict the indirect tensile strength (ITS) of cold asphalt emulsion mixtures (CAEMs) produced using siliceous aggregates and a cationic bitumen emulsion. Materials characteristics were determined and mix designs were developed using virgin and recycled aggregates from Reclaimed Asphalt Pavement (RAP). The Marshall method was used to produce specimens of size 100 mm diameter and 63.5 mm thickness. Specimens were subjected to isothermal curing regimes at temperatures of 25, 40 and 60 ºC. The curing periods considered were 3, 8, 13, 18 and 23 days for each temperature. ITS was subsequently measured for each of those curing regimes. After 3 days of curing, the ITS of RAP mix cured at low temperature of 25 ºC was 47.04% lower than that of the virgin mix. However, for all temperature regimes, the difference in ITS of the virgin and RAP mix was 3% for specimens cured for 23 days and a maximum of 6% for specimens cured for 18 days. The temperature sensitivity factor (B) of the RAP mix was 94% higher than that of the virgin mix. This work determined that a linear-hyperbolic strength maturity function predicts the ITS of CAEMs produced using siliceous aggregates and a cationic bitumen emulsion with an accuracy of more than 95%. The study recommends the use of Maturity method to predict tensile strength of CAEMs during design and to monitor gradual strength gain in CAEMs during construction

.

TABLE OF CONTENTS

LIST OF TABLES

LIST OF FIGURES

LIST OF APPENDICES

LIST OF ABBREVIATIONS

AC	Asphalt Concrete
ACV	Aggregates Crushing Value
ASTM	American Society for Testing and Materials
BC	Bitumen Content
BSI	British Standards Institution
CAEMs	Cold Asphalt Emulsion Mixtures
CHI	Concrete Hardening Index
CMA	Cold Mix Asphalt
FHWA	Federal Highway Administration
FI	Flakiness Index
HMA	Hot Mix Asphalt
IBC	Initial Bitumen Content
IEC	Initial Emulsion Content
ITSM	Indirect Tensile Stiffness Modulus

ITS	Indirect Tensile Test
LAA	Los Angeles Abrasion
MT&RD	Materials Testing & Research Division
OBC	Optimum Bitumen Content
O/W	Oil in Water
RAP	Reclaimed Asphalt Pavement
RMC	Residual Moisture Content
TTF	Time-Temperature Factor
TRB	Transportation Research Board
TRL	Transport Research Laboratory
VA	Virgin Aggregates
VHM	Vibrating Hammer Method
WMA	Warm Mix Asphalt
W/O	Water in Oil

CHAPTER ONE

INTRODUCTION

1.1 Background to the study

The use of cold mix asphalt (CMA) for surfacing of flexible pavements is accompanied by sustainable environmental and economic benefits. Environmental benefits of using cold mix asphalt include reduced pollution, reduced depletion of natural resources through recycling of aggregates and reduced landfill requirement. CMA is produced and used at ambient temperatures hence energy consumption is limited and overall cost of production is reduced (D'Angelo et al., 2008; You, Goh & Qingli, 2011). Use of CMA at ambient temperatures enables safer working environment compared to hot mix asphalt and has significantly influenced the employment of labor-based methods that create employment especially in developing nations like Kenya.

The performance of CMA is significantly affected by the level of curing (Kuna, Airey & Thom, 2016). Lack of universal standards for design and evaluation of CMA has led to the use of Laboratory-Field Curing Correlation techniques to determine the level of curing in CMA (Doyle, McNally, Gibney & Tabaković, 2013; Kim, Im & Lee, 2011). These techniques predict the performance (strength) of CMA by correlating the moisture content of CMA specimens cured in the laboratory with the moisture content of a CMA pavement layer subjected to in-situ curing conditions (Lee, 1981). The correlation is done using the Residual Moisture Content (RMC) and minimal curing age. The RMC method considers the amount of moisture in CMA after a predetermined curing regime while the minimal curing age method assumes that CMA has effectively cured after a predetermined curing age (Kim et al., 2011).

Laboratory-Field Curing Correlation techniques have illustrated a variety of arbitrarily selected isothermal curing regimes used by different researchers based on their objectives, level of expertise, and locally available materials. Moreover, performance-based tests such as: rutting resistance, stiffness and moisture resistance tests (Zaumanis, Poulikakos & Partl, 2018; Asphalt Institute, 2008) are done at the end of pre-determined isothermal curing regimes hence the gradual strength gain nature of CMA is not considered. As a result, the use of Laboratory-Field Curing Correlation techniques is accompanied by considerable inconsistencies in the simulation of field curing and prediction of actual the performance of CMA pavements (Maccarone, Holleran & Ky, 1995; Kishore, Amar, Amarantha & Sudhakar, 2008; National Roads Authority, 2011; Acott, 1979; Kim, Lee & Heitzman, 2007; Ruckel, Acott & Bowering, 1983).

Maturity method used in cement concrete takes into consideration two important factors that affect strength gain of CMA. These are the combined effect of curing time and temperature on the strength gain of CMA and gradual strength gain in cold mix asphalt during curing (Carino & Lew, 2001; Doyle et al., 2013; Kuna et al., 2016; Chelelgo, Gariy & Shitote, 2019). Doyle et al. (2013) developed a logarithmic strength-maturity function for emulsified asphalt that overestimated the long-term strength of emulsified asphalt concrete. Using a logarithmic strength-maturity function, Kuna et al. (2016) obtained overestimated stiffness of foamed bituminous mixtures (FBMs) cured for 296 days and they recommended the use of parabolic-hyperbolic strength maturity functions for the prediction of stiffness of FBMs. Chelelgo et al. (2019) concluded that there is a strong correlation between the fatigue maturity of cold mix asphalt and the actual fatigue strength using the parabolic-hyperbolic strength-maturity function.

From the foregoing, there is no literature correlating the Maturity method and the tensile strength of cold asphalt emulsion mixtures produced from siliceous basaltic aggregates and a cationic bitumen emulsion. Engineering significance of indirect tensile strength in

asphalt concrete includes: simulation of tensile stresses at the base of asphalt concrete surface course when subjected to loading. Moreover, ITS demonstrates the strength and adherence of asphalt concrete against fatigue failure, temperature cracking and rutting failure. From the foregoing, this study used the Maturity method to predict the indirect tensile strength of cold asphalt emulsion mixtures produced using siliceous basaltic aggregates commonly found in Kenya and a slow setting cationic bitumen emulsion.

1.2 Problem statement

Use of cold mix asphalt has economic, environmental and social benefits. Cold mix asphalt gains strength gradually through curing, hence strength in CMA is directly proportional to the level of curing. Laboratory-Field Curing Correlation techniques which are currently used to predict the strength of CMA have produced considerable variations of results with regard to determination of gradual curing and strength prediction in CMA. Examples of such variations include; estimation of similar field curing age of 365 days of emulsified CMA subjected to different isothermal curing regimes of 40 ºC for 28 days (Kishore et al., 2008) and 20 ºC for 100 days (Brown & Needhem, 2000). Foamed CMA subjected to similar isothermal curing regimes of 40 ºC for 3 days estimated different field curing age of 30 days (Ruckel et al., 1983) and 180 days (Kim et al., 2007). Strength prediction statistical models like the Michaelis-Menten and Exponential model have only demonstrated strength evolution in CMA during curing. Studies on application of Maturity method on CMA have demonstrated strong correlations between maturity and stiffness modulus of CMA. They however, have not shown how strength-maturity functions can be used to predict the tensile strength of emulsified asphalt produced from siliceous basaltic aggregates and a cationic bitumen emulsion. From the foregoing, this study used hyperbolic strength-maturity functions to predict the indirect tensile strength of cold asphalt emulsion mixtures (CAEMs).

1.3 Justification

Inability to determine the performance of CMA during curing is one of the factors limiting their use. CMA is produced at ambient temperature hence The use of CMA for

pavement of flexible pavement is accompanied by reduced pollution, reduced fuel consumption and employment of labor based methods required in developing countries like Kenya. This study used Maturity method to predict the tensile strength of cold mix asphalt. Knowledge from this study will instill confidence in the use of CMA which is currently shunned by professionals in the road construction sector.

1.4 Research objectives

1.4.1 General objective

To predict the tensile strength of cold asphalt emulsion mixtures using the Maturity method.

1.4.2 Specific objectives

1. Characterization of materials and mix design
2. To determine the effect of curing time and temperature on indirect tensile strength of cold asphalt emulsion mixtures.
3. To predict the indirect tensile strength of cold asphalt emulsion mixtures using the Maturity method.

1.5 Research Questions

1. What are the material characteristics and mix design parameters required for the study?
2. What are the effects of curing time and temperature on the indirect tensile strength of cold asphalt emulsion mixtures?

3. Can the Maturity method accurately predict the indirect tensile predict the strength of cold asphalt emulsion mixtures?

1.6 Scope and Limitation

1.6.1 Scope

The research scope was done at the Materials Testing & Research Division (MT&RD) of the Ministry of Transport, Infrastructure, Housing & Urban Development located at Nairobi, Kenya. Virgin and recycled aggregates were considered to produce 120 sample specimens of CAEMs produced using basaltic siliceous aggregates and a cationic bitumen emulsion. Indirect tensile strength tests coupled with hyperbolic strength-maturity empirical equations were used to predict the tensile strength of cold asphalt emulsion mixtures.

1.6.2 Limitation

Available tests used to evaluate tensile characteristics of asphalt concrete pavement layers include: direct tensile test, bending test and indirect tensile tests. Due to unavailability of flexural and cohesiometer equipment to evaluate the bending moment and modulus of rapture in CAEMs during failure the indirect tensile strength test was used to determine tensile strength.

1.7 Significance of the Study

A maturity-based strength prediction in CMA pavement layers enables timely knowledge of actual early-age tensile strength gained by CAEMs during curing. This enables the making of important and safe decisions like the earliest time a pavement layer can be overlaid by a wearing course or be opened to traffic. Knowledge from this study will enhance for effective planning and management of road construction projects.

CHAPTER TWO

LITERATURE REVIEW

2.1 Introduction

The study reviewed theoretical and empirical literature. Theoretical literature reviewed included: a brief description of asphalt concrete and detailed review of materials, production process and available design manuals developed for cold mix asphalt. The empirical section of the literature review covers the currently used strength prediction techniques that include: Laboratory-Field Curing correlation techniques and statistical models. Statistical strength prediction models outlined are Michaelis-Menten (MM) model, Exponential (EX) model, Maturity method. Lastly, the application of the Maturity method in cold mix asphalt is reviewed.

2.2 Asphalt Concrete

Asphalt concrete is a complex heterogeneous mixture of aggregates, fillers, asphalt binder and air voids used surfacing of modern road pavement (Aragão, Kim, Lee, & Allen, 2011). There are three types of asphalt concrete categorized based on how they are produced: hot mix asphalt (HMA) produced at high temperatures ranging from 138 - 180ºC; warm mix asphalt (WMA) produced at moderate temperatures ranging from 66 - 135 ºC and cold mix asphalt (CMA) produced at ambient temperatures (Read & Whiteoak, 2003). HMA is conventionally used for road pavement and its production is accompanied by adverse effects to the environment, natural resources and the human health (You et al., 2011). Some of these negative effects include emission of particulate matter such as dust, smoke, poisonous bituminous fumes and gases like CO_2, SO_2 and NO_2 that pollute the air, cause greenhouse effect and pose health risks to the humans

(Al-Hdabi, 2014). Moreover, the production of HMA consumes a lot of energy that contributes to high production cost (D'Angelo et al., 2008).

2.3 Cold Mix Asphalt

Cold mix asphalt is batched, mixed, laid and compacted at ambient temperature of approximately 23-30 ºC (Dash, 2013). Some of the benefits of using CMA include:

i. Reduced energy and fuel consumption during production (Bouteiller, 2010).
ii. Reduced emission of smoke, greenhouse gases and other particulate matter like dust that cause air pollution, global warming and pose health risks to human health. (You et al., 2011; Al-Hdabi, 2014).
iii. Reduced depletion of natural resources by incorporation of recycled aggregates from reclaimed asphalt pavement (Arimilli, Jain & Nagabhushana, 2016; Thanaya, Negara & Suarjana, 2014). Recycling reduces landfill requirements for waste during pavement renovation (Ma, Wang, Zhao, Huang & Pi, 2015; Thanaya et al., 2014).
iv. The CMA production is independent of the mix temperature. Hence, they are suitable for construction and maintenance of rural roads using labor based methods (Thanaya, Zoorob & Forth, 2009).

Some of the factors limiting the use of cold mix asphalt for construction of flexible pavements include:

i. Lack of universal standards for their design and evaluation (Bessa, Almeida, Vasconcelos & Bernucci, 2016).
ii. Time-consuming curing process required for gain strength (Kim et al., 2011; Thanaya, 2007).

iii. High air void content above 7% that makes the pavement susceptible to water ingress (Oluwasenyi, 2011; Thanaya et al., 2014; 2009). Moreover, the porosity of the RAP mix after in-situ compaction has been found to range above 10% (Valentin, Čížková, Suda, Batista, Mollenhauer & Simnofske, 2016; Moloto, 2010)

Cold mix asphalt can either be an emulsified mixture or a foamed mixture depending on the type of binder used. Foamed asphalt binder is produced by injecting water into hot bitumen to produce a spontaneous binder foam, which is mixed with aggregates in an expansion chamber to produce cold foamed asphalt mixtures (Kuna, 2015). Emulsified asphalt binder is produced by mixing asphalt with water in a colloid rotor at controlled temperature causing asphalt droplets to be dispersed in water as an emulsion (Transport Research Board, 2006). The asphalt emulsion is mixed with aggregates at ambient temperature to produce cold asphalt emulsion mixtures.

2.4 Components of cold Asphalt Emulsion Mixtures

Cold asphalt emulsion mixtures (CAEMs) are composed of well-graded mineral aggregates that are bound together by a bitumen emulsion.

2.4.1 Aggregates

Aggregates are mineral materials such as gravel, ballast, crushed stone, blast furnace slag, quarry dust and sand. They can be naturally occurring or artificially obtained through physical and chemical processes on industrial by-products (O'Flaherty, 2002). Aggregates are mixed with binders such as bitumen, cement, lime and other hydraulic components to form bound materials used for construction of engineering structures. There are two categories of aggregates namely coarse aggregates and fine aggregates. The size of coarse aggregates ranges from 2.36 - 37.5 mm while that of fine aggregates

range from 0.075 - 2.36 mm. Aggregates that pass sieve size 0.075 mm are called inert fillers (Transport Research Laboratory, 2002). According to Federal Highway Administration (FHWA) tech brief, 90 – 95% of asphalt concrete is composed of aggregates, the remaining 5 - 10% is a summation of binder and air voids (West et al., 2010). Grading is the physical blending of aggregates of different sizes to fit the blend within a specific band. It determines the concrete mix matrix which can be dense-graded, open graded or gap-graded (Sterling & Zamhari, 1997). The mix matrix of asphalt concrete determines the mechanical properties of the pavement layer constructed. This study used a dense-graded mixture of nominal size 20 mm.

2.4.2 Bitumen Emulsion

An emulsion is a two-phase co-existence of immiscible fluids represented by the dispersion of one fluid in the form of fine droplets in another continuous fluid. Emulsions are categorized into three groups: oil-in-water (O/W), water-in-oil (W/O) and multiphase emulsions (Figure 2.1, TRB, 2006). For oil-in-water emulsions, the dispersed phase is an oily fluid and water is the continuous fluid. The water-in-oil emulsion has the water as the dispersed fluid in a continuous oily fluid and the multiphase emulsion has a third phase, which contains globules of both the dispersed and the continuous fluids. Bitumen emulsion is an oil-in-water emulsion with bitumen droplets of approximately 0.1 - 20 microns representing the dispersed fluid while water is the continuous fluid (Al-Hdabi, 2014).

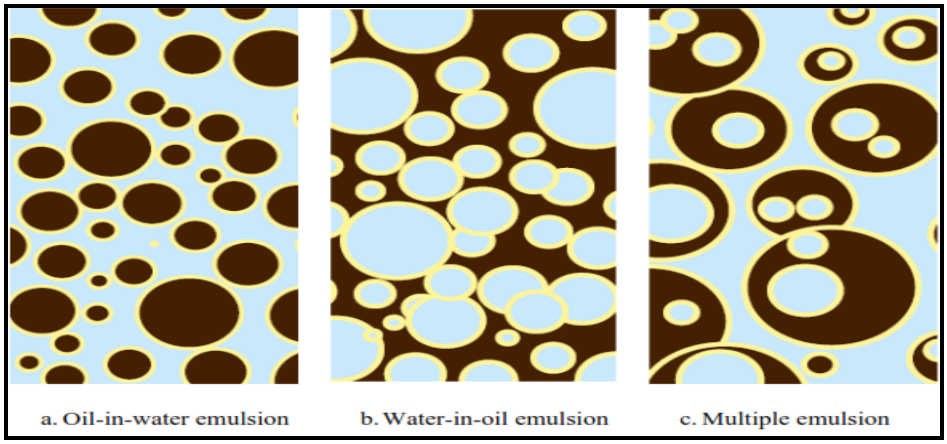

Figure 2.1: Types of emulsions

(Source: TRB, 2006)

Bitumen and water have different chemical composition hence they are immiscible. A chemical emulsifier also known as a surfactant is a surface-charge activating agent that enables mutual co-existence of bitumen and water at ambient temperatures. Transportation Research Board (TRB, 2006) defined an emulsifier as a water-soluble component that alters the properties of a solvent and the surface they contact. In the case of bitumen emulsion, the emulsifier coats the dispersed bitumen droplets to prevent them from coalescing prior to the required function of the emulsion. Bitumen emulsions have a range of 40 - 80% bitumen content depending on the purpose of the emulsion. Visually, the bitumen emulsions are brown in color prior to breaking.

2.4.3 Breaking mechanism of bitumen emulsion

Breaking of bitumen emulsion is also known as setting. It involves the expulsion of water from a bitumen emulsion allowing the bitumen droplets to coalescence and form a continuous bitumen binder. The speed at which the bitumen droplets coalescence is known as the breaking rate or setting rate (TRB, 2006). The setting rate of a bitumen

emulsion is influenced by the chemical reaction of the emulsion and environmental factors like temperature, humidity, wind speed and mechanical action (Meyer, 1999). Some of the breaking mechanisms of bitumen emulsion include:

i. Emulsifier abstraction – This is the withdrawal of the emulsifier from the bitumen-water interface by the aggregates. The positively charged surfactant coating the bitumen droplets is attracted to the negatively charged aggregate surface. This renders the bitumen droplets unstable causing them to coalesce for stability.
ii. Emulsifier deprotonation- This is the adsorption of protons from the acidic surface of the bitumen droplets by the basic sites on aggregate surface. The bitumen droplets become unstable and they coalesce to form a continuous binder.
iii. Droplet Migration – The positively charged bitumen droplets are attracted to the negatively charged aggregate surface causing the bitumen droplets to spread over the aggregate surface. The spreading of bitumen causes them to coalesce in to a continuous film that coats the aggregates.
iv. Emulsifier adoption - The aggregate surface adsorbs free emulsifier coating the bitumen droplets and from the bitumen-water interface. The adsorption causes the surface of the aggregates to be lipophilic (oil loving) in nature which attracts the unstable bitumen droplets. As a result, the bitumen droplets coalesce to form a continuous binder.

For the production of cold asphalt emulsion mixtures, one or more of the aforementioned breaking mechanisms occurs when bitumen emulsion is mixed with aggregates (Figure 2.2).

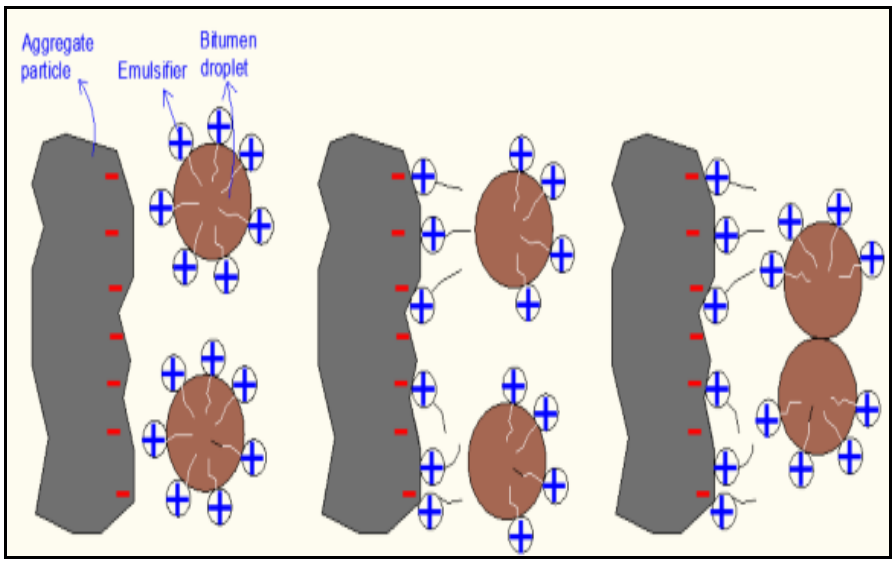

Figure 2.2: Breaking mechanism of bitumen emulsion

(Source: Al-Hdabi, 2014)

2.4.4 Classification of bitumen emulsions

Bitumen emulsions are classified in accordance to their electrical charge and their rate of breaking (Al-Hdabi, 2014; TRB, 2006). Bitumen emulsions defined by their electrical charge include:

i. Anionic bitumen emulsion – The bitumen molecules contain negatively charged electrons that move to the anode on application of an electric potential.
ii. Cationic bitumen emulsion – The bitumen molecules contain positively charged electrons that move to the cathode on application of an electric

potential. They are commonly used to produce cold asphalt emulsion mixtures.

iii. Non-ionic bitumen emulsion - The bitumen molecules have a neutral charge hence they do not move to any pole on application of electrical potential.

iv. Clay-stabilized bitumen emulsions – The bitumen molecules have a neutral charge. They are used for industrial works and products.

Bitumen emulsions defined by their rate of breaking when in contact with the aggregates include:

i. Rapid setting bitumen emulsions – They set quickly when in contact with aggregates especially of low surface area. Their rapid breaking nature does not allow effective mixture of binder and aggregate. They are suitable for spray application like tack coat between two asphalt layers.

ii. Medium setting bitumen emulsion – They set at a slower rate than the rapid setting emulsions. They can be used with coarse aggregate mixtures containing little or no fines.

iii. Slow setting bitumen emulsions –They are the most suitable for production of cold asphalt emulsion mixtures because they set at slow rate. The slow rate of setting enables the aggregates to be effectively coated with the emulsion during mixing. Furthermore, it enables CAEMs pavement layers to be well mixed, laid and compacted prior to setting.

This study used a slow setting cationic bitumen emulsion as the binder for cold asphalt emulsion mixtures.

2.5 Cold Mix Asphalt Design Guides

There is no universal mix design standards for cold mix asphalt. Therefore, countries that use cold mix asphalt for road pavements have to do preliminary mix designs by modifying the Marshall mix design standard (ASTM-D6926-10, 2010) which was originally developed for hot mix asphalt in accordance to their locally available resources (Bessa et al., 2016; Moghadam & Farhad, 2017; Tebaldi et al., 2014; Thanaya, 2007). Some of the available mix design manuals include:

i. Performance Based Specifications for Emulsified Asphalt Mixes (Serfass, 2012)
ii. Cold Mixed Granular Materials Guide (Bullen, John, Lancaster, Maccarrone, Mungan & Rebbechi, 1997)
iii. Standard Specification for Road and Bridge Construction in Kenya (Ministry of Roads and Public Works, 1986)
iv. Asphalt Cold Mix Manual (Asphalt Institute, 1989)
v. Basic Asphalt Emulsion Manual (Asphalt Institute, 2008)

i. Performance Based Specifications for Emulsified Asphalt Mixes

Cationic asphalt emulsions are used to prepare cold mix asphalt for road pavement in France. Aggregate selection and characterization is the first step of the mix design. The aggregate sizes recommended for the production of CMA are outlined in Table 2.1.

Table 2.1: Aggregates size for the cold mix asphalt

Type	Aggregate Gradation (mm)	Thickness Range (mm)
Very Thin	0/6, 0/10, 0/14	20 – 30
Thin	0/6, 0/10, 0/14	30 – 50
Thick	0/10, 0/14	50 – 80

(Source: Serfass, 2012)

After aggregate selection and characterization, trial blends called “bowl tests” are developed using empirical formulas. The bowl tests are visually observed to assess the aggregate grading, the pre-mix water and bitumen content. The mix is selected based on the quality of aggregate coating, the workability of the mix and the achieved mix compaction level. After compaction, the selected specimens are subjected to isothermal curing at accelerated temperatures. Isothermal curing involves subjecting of CMA specimens to controlled curing temperatures for a specified curing time. Cured specimens are then tested for moisture sensitivity using the compressive strength test and stiffness modulus test.

The procedures outlined in this guide are consistent with the Asphalt Cold Mix Manual (Asphalt Institute, 1989). This manual recommends the use of the CMA as a surface course while the Asphalt Cold Mix Manual recommends the use of CMA as a binder course of low to medium volume traffic roads because of inferior mechanical properties especially at early curing age. To enhance the mechanical properties of CMA, hydraulic additives like ordinary Portland cement are added during production (Bessa et al., 2016; Kuna, 2015). This mix design manual does not clearly outline the effect of the additives on the mix for it to be sufficient for use as a surface course of a road pavement.

ii. Cold Mixed Granular Materials Guide

The Cold Mixed Granular Materials Guide outlines the design specifications of cold mix asphalt in Australia using either the emulsified or the foamed bitumen as the binder (Bullen et al., 1997). The guide also predicts the in-situ performance of the cold mix asphalt under various conditions of traffic and environment. The guide recommends compaction using the gyratory compactor. The mix stiffness, resistance to permanent deformation, resistance to fatigue cracking and durability are the main variables considered during the mix design. The curing regimes outlined in the manual are:

i. Early age curing simulated by isothermal curing of specimens in the oven at temperatures of 40 ± 2 ^{o}C for 4 hours before indirect tensile strength test.

ii. Long-term curing simulated by isothermal curing of specimens in the oven for 4 days at temperatures of 60 ± 2 ^{o}C.

The use of the aforementioned curing regimes to simulate short and long term in situ curing disregards the residual moisture content (RMC) in the mix after curing that affects the performance of CMA. Furthermore, in situ weather conditions fluctuates, meaning that both the early age and long term curing are not well simulated by isothermal curing regimes in the laboratory. Moisture sensitivity is done using the indirect tensile strength (ITS) method where cured specimens are soaked in water at 23 ^{o}C for 18 hours followed by 2 hours under vacuum de-airing. The ratio between the strength of soaked specimen to that of dry specimen is called the tensile strength ratio (TSR). TSR is an indicator of moisture susceptibility of the mix. Moisture assessed of this mix design guide is consistent with the French manual (Serfass, 2012).

iii.Standard Specification for Road and Bridge Construction in Kenya

The Standard Specification for Road and Bridge Construction in Kenya, (Ministry of Roads and Public Works, 1986) recommends the use of cold mix asphalt for patching and surfacing of low volume traffic roads. This standard does not have a clear outline of the mix design procedure for CMA. Therefore, mix properties like stability, air voids and moisture susceptibility are not well described. With the above note, this standard was not used in this study.

iv. Asphalt Cold Mix Manual

The Asphalt Cold Mix Manual (Asphalt Institute, 1989) outlines a mix design procedure for emulsified asphalt concrete. The mix design commences with material quality tests that determine the physical and mechanical properties of the materials. The mix binder demand is approximated using either the Centrifuge Kerosene Equivalent test (C.K.E) or an empirical equation. The ability of the bitumen emulsion to coat the aggregates is determined using the coating test. The proposed binder should coat at least 50% of the aggregates for it to be used for production of CMA. Moisture density relationships are determined in terms of maximum dry density (MDD) and optimum total fluid content (OTFC). The total fluid content affects the aggregate pre-mix water and the bitumen content required. The optimal bitumen content is selected based on how it effects on the stability, stability loss, porosity, dry density and moisture absorption of cold asphalt emulsion mixtures. The design criteria are outline in Table 2.2.

Table 2.2: Mix design criterion

Test Property	Minimum	Maximum
Stability (N) at 22.2 ºC for paving mixtures	2224N	-
Stability Loss (%)	-	50
Aggregate Coating (%)	50	-

(Source: Asphalt Institute, 1989)

v. Basic Asphalt Emulsion Manual

The proposed CMA mix design procedures outlined in the Basic Asphalt Emulsion Manual (Asphalt Institute, 2008) are a replica of the procedures in the Asphalt Cold Mix Manual (Asphalt Institute, 1989) with a few modifications that include:

i. The coating test where the loosely coated cold asphalt emulsion mixtures are subjected to isothermal curing in the oven for 24 hours at 60 ^{o}C. After curing, the loose aggregates are boiled, stirred and air-dried for 24 hours. After curing for 24 hours, the percentage and quality of aggregates coated is visually assessed.

ii. Air curing is introduced during mixing to allow the specimen to be compacted at optimal moisture content based on visual inspection. Isothermal curing is done with the specimen in the moulds for 48 hours at 60 ^{o}C.

iii. Compaction of specimen is increased to 75 blows on each face of the specimen to represent medium volume traffic roads. Further compaction is done after curing using a double plunger.

This study used the asphalt institute manuals MS-14 (1989) and MS-19 (2008) to develop cold asphalt emulsion mixtures.

2.6 Techniques Used to Predict Strength of Cold Mix Asphalt

2.6.1 Curing of Cold Mix Asphalt

The performance (strength) of a cold mix asphalt pavement is directly related to its level of curing. Curing is the process of water expulsion from a cold mix asphalt that enables the bitumen and the aggregates to bond (Moloto, 2010; Serfass, Poirier, Henrat & Carbonneau, 2004). The two main sources of water in cold mix asphalt are aggregate pre-mix (pre-wetting) water and the water phase in the bitumen emulsion (TRB, 2006). The aggregate pre-mix water activates the surface charges on the aggregates and improve the workability of cold mix asphalt during production. Curing occurs in two stages; emulsion breaking and water expulsion. Emulsion breaking occurs when the bitumen emulsion is mixed with the aggregates as explained in section 2.4.3. Water in the emulsion evaporates hence the suspended bitumen droplets flocculate and coalesce

into a continuous bitumen film that coats the aggregates (TRB, 2006). The rate of emulsion breaking depends on the setting time of the emulsion used. Water expulsion is a gradual, time-consuming process, which begins during mixing and proceeds long after compaction (Graziani, Godenzoni, Cardone & Bocci, 2016; Kuna et al., 2016).

Lack of universal standards for design and evaluation of CMA has led to the use of Laboratory-Field Curing Correlation techniques and statistical models to determine the level of curing in CMA for strength prediction.

2.6.2 Laboratory-Field Curing Correlation techniques

Laboratory-Field Curing Correlation techniques involve subjecting CMA specimens to isothermal curing regimes in the laboratory and correlating their level of curing to in-situ curing conditions (Lee, 1981). Isothermal curing involves subjecting CMA specimens to controlled curing temperatures, humidity and pressure for a pre-determined time (Kuna et al., 2016). Isothermal curing regimes above room temperature are used during design to accelerate the rate of curing of CMA and enable the determination of expected performance of CMA (Carino, 1984; Serfass et al., 2004; Kuna et al., 2016; Ojum, Kuna, Thom & Airey, 2014).

Correlations between laboratory curing and field curing are currently assessed using the residual moisture content (RMC) and minimal curing age of CMA (Kim et al., 2011). The RMC method proposed by Lee (1981) considers the amount of moisture in CMA after a predetermined curing regime. As a result, different regions and states like Iowa, Arizona, Washington and Vermont are currently using a range of 1.0 - 1.5% RMC. Spain has less than 1.0% RMC requirement prior to placement of an overlay while Kansas has set its limits to 2% RMC (Kim et al., 2011). The use of RMC to assess the in-situ performance of CMA at the end of curing disregards the effect of curing temperature on the gradual strength development of CMA.

Minimal curing age method is another way of assessing the in situ performance of CMA pavements. Spain has set a minimum age of 7 days of in situ curing while the United Kingdom has a minimal age requirement of 36 hours of curing depending on the in situ climatic conditions. States like Idaho, Ontario, Maine, New York and Delaware have specified different curing durations ranging from 4 - 45 days (Kim et al., 2011). Application of the minimal curing age method does not account for the fluctuating in situ conditions. Moreover, it does not consider the effect of curing temperature on strength development of cold mix asphalt.

Laboratory-Field Curing Correlation techniques have used a variety of arbitrarily selected isothermal curing regimes used by different researchers based on their objectives, level of expertise, and locally available materials. As a result, there are considerable inconsistencies/deviations in the simulation of field curing which ultimately affects accurate prediction of strength in CMA during curing (Table 2.3).

Table 2.3: Laboratory-Field curing correlations of cold asphalt mix

Binder Type	Isothermal curing regimes		In-situ Curing (days)	Deviation Curing days predicted	Study
	Temp (ºC)	Time (days)			
Emulsion	60	3	365	similar	(Maccarone et al., 1995)
Emulsion	40	28	365	similar	(National Roads Authority, 2011)
Emulsion	20	100	365	similar	(Brown & Needhem, 2000)
Foam	60	3	365	165	(Maccarone et al., 1995)
Foam	60	3	200		(Acott, 1979)
Foam	40	3	180	150	(Kim et al., 2007)
Foam	40	3	30		(Ruckel et al., 1983)

CMA specimens subjected to similar isothermal curing regimes simulated different curing ages under in situ conditions (Table 2.3). For example, foamed bituminous mixtures cured at 40 ºC for 3 days by Ruckel et al. (1983) and Kim et al. (2007) and simulated in situ curing age of 30 days and 180 days respectively. Studies by Maccarone et al. (1995) and Accot (1979) cured foamed CMA specimens 60 ºC for 3 days and simulated in situ curing age of 60 days and 200 days respectively. Lastly, emulsified CMA cured at different isothermal regimes of 40 ºC for 28 days (Kishore et al., 2008) and 20 ºC for 100 days (Brown & Needhem, 2000) simulated similar in situ curing age of 365 days. Additional limitations of using Laboratory-Field Curing Correlation techniques include:

i. Isothermal curing regimes in the laboratory are controlled and their results cannot be compared to in situ fluctuating conditions (Doyle et al., 2010; 2013).
ii. Performance-based tests such as; rutting resistance, stiffness and moisture resistance tests (Zaumanis et al., 2018) are done at the end of pre-determined curing regime hence the gradual strength gain nature of CMA is not considered.

Knowledge of gradual strength development in CMA pavements under construction enable important and safe decisions to be made on time like the earliest time to overlay a CMA pavement layer with a wearing course or to allow traffic on the pavement.

2.6.3 Statistical Models used to predict curing in CMA

Statistical models are mathematical functions that simulate the asymptotic response of the mechanical properties of CMA during curing. Three statistical models outlined in literature include Michaelis-Menten (MM) model, Exponential (EX) model and Maturity method. Michaelis-Menten (MM) model and Exponential (EX) model were used to

demonstrate the evolution of physical and mechanical properties of CMA as a function of curing time (Graziani et al., 2016). Physical property analyzed was evaporated water (DW) and Mechanical properties analyzed were Indirect Tensile Stiffness Modulus (ITSM) and Indirect Tensile Strength. Both the MM and the EX models demonstrated gradual strength gain in CMA during curing. The EX model however underestimated the asymptotic values of the measured response (DW, ITSM and ITS) and had lower precision compared to the MM model. The study concluded that overtime loss of water (curing) improves the ability of cold mix to resist failure (Graziani, Godenzoni, Cardone, Bocci & Bocci, 2017). The study however did not asses the effect of curing temperature on strength development in cold mix asphalt and the models did not predict the strength of CMA.

2.7 The Maturity Method

The Maturity method is non-destructive approach used to analyze the performance of cement concrete under in situ conditions. The Maturity method uses the combined effect of curing time and temperature to predict the strength of cement concrete (Carino & Lew, 2001; Wilde, 2013). The extent of the developed strength in cement concrete is called maturity. Maturity index (*M*) is an indicator of maturity that is calculated from the temperature history of the cementitious mixture by using a maturity function (ASTM C1074-11, 2011).

The origin of the maturity method can be traced back to researchers from England in 1949 who used steam to accelerate the curing process of cement concrete produced for commercial use (McIntosh, 1949; Nurse, 1949). McIntosh (1949) observed that any curing temperature, which was above the datum temperature, had a direct influence on the rate of concrete hardening for a particular mix. He concluded that the curing temperature of cement concrete affects the rate of strength gain. With this knowledge, he

developed a model called the Concrete Hardening Index (CHI), which was correlating the basic age of concrete and its relative compressive strength within a temperature range of 15 - 93 °C. Nurse (1949) accelerated the curing temperature of cement concrete by subjecting the specimens to steam curing. He developed a Time-Temperature Factor (TTF) that used the combined effect of time and temperature to estimate the strength of concrete.

The improvement of the Temperature-Time Factor (TTF) led to the development of the Nurse-Saul maturity function (Nurse, 1949; Saul, 1951). The maturity rule states that concrete drawn from the same batch will have approximately the same strength at the same maturity index (Figure 2.3). This is the case despite the fact that concrete drawn from the same batch could be subjected to different combinations of curing temperature and time (Carino & Lew, 2001). M1 and M2 represent the maturity indices of two concrete batches subjected to cold and hot curing regimes respectively. At the same maturity, concrete mixtures cured under different regimes will have similar strength (Nixon, Schindler, Barnes & Wade, 2008).

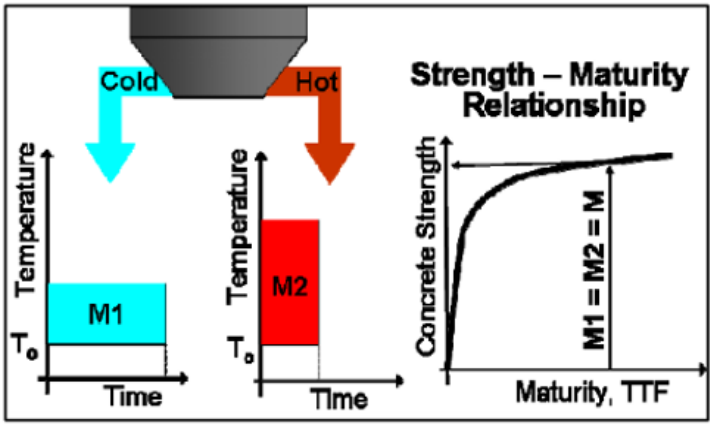

Figure 2.3: The Maturity Rule

(Source: Nixon et al., 2008)

The maturity method has been modified overtime by preceding studies and constructive measures have been developed to standardize its application in the concrete construction industry (ASTM C-1074-11, 2011). Some of the advantages of using the Maturity method include:

i. The method is a non-destructive approach that shows the continual strength gain of concrete compared to the convectional compressive strength method that involves crushing of samples at predetermined time intervals (Salama, 2008).
ii. Timely knowledge of the earliest strength of concrete enables the making of important decisions, which are required for work on site to proceed safely and effectively. Such decisions include; the earliest time to remove formwork and shores supporting structures, the appropriate time to do transverse jointing and post-tensioning of structures and to open concrete pavements to traffic.

Proper application of this relatively simple procedure can result in savings by allowing construction operations to be performed safely at the earliest possible time (Carino & Lew, 2001). The application of the maturity method in the construction industry is accompanied by several limitations:

i. The maturity curve for a particular mix cannot be used in another mix even though the design strength is the same.
ii. Any change in the mix in terms of quality or quantity changes the maturity index. Therefore, high precision is required during the production of CMA for construction.
iii. The maturity method only considers time and temperature as factors affecting strength development in concrete ignoring other important factors that affect

the strength of concrete like the mix design process and the heterogeneous nature of concrete (Carino & Lew, 2001; Nixon et al., 2008).

2.7.1 Maturity Functions

Maturity functions are mathematical expressions that calculate the index that is indicative of maturity of a cementitious mixture using temperature history and a predetermined curing period (ASTM C1074-11, 2011). The two mostly used maturity functions are; Nurse-Saul and Arrhenius maturity functions (Wilde, 2013).

i. Nurse-Saul Maturity Function

The Nurse-Saul maturity function computes the maturity of a concrete sample as a function of its curing temperature and time as illustrated by Equation 2.1.

$$M = \sum_{o}^{t}(T - T_o)\,\Delta t \qquad (2.1)$$

Where:

M = Maturity at age t (°C-hours or °C-days)

t = Elapsed time (hours or days)

Δt = Time interval (hours or days)

T = Average concrete temperature during the time interval Δt (°C)

T_o = Datum temperature - temperature below which no curing occurs (°C)

The maturity of concrete is the area between the curve and datum temperature in the temperature history graph (Figure 2.4, Nixon et al., 2008).

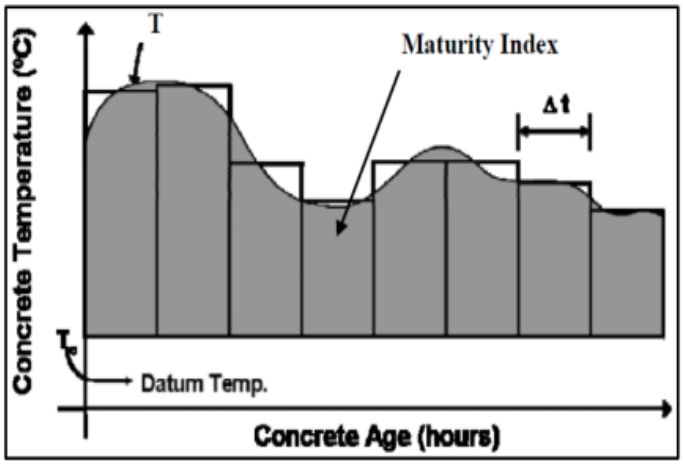

Figure 2.4: Nurse-Saul Maturity Function

(Source: Nixon et al., 2008)

The Nurse-Saul maturity function assumes a linear relationship between the rate of strength gain and the curing temperature (Carino, 1984). This is not realistic because concrete is a heterogeneous mix that undergoes complex chemical reactions during curing. As a result, Hansen & Pedersen (1977) proposed the Arrhenius maturity function that takes in to account the rate of chemical reaction during hydration with respect to material sensitivity to temperature.

ii. Arrhenius Maturity Function

The Arrhenius maturity function was developed to address the non-linear relationship between curing temperature of concrete and strength gain. It accounts for the rate of chemical reaction during concrete hydration with respect to material sensitivity to temperature (Carino & Lew, 2001; Hansen & Pedersen, 1977). The maturity of concrete is expressed as equivalent age illustrated by Equation 2.2.

$$t_e = \sum_0^t e^{\frac{E_a}{R}\left(\frac{1}{273+T}-\frac{1}{273+T_{ref}}\right)}\Delta t \quad (2.2)$$

Where:

t_e = Equivalent age at the reference temperature (hours or days)

t = Elapsed time (hours or days)

Δt = Time interval (hours or days)

E_a = Apparent activation energy (J/mol)

R = Universal gas constant (8.314 J/mol-K)

T = Average temperature of the concrete during time interval Δt (℃)

T_{ref} = Reference temperature (20℃ in Europe, Kenya 18 ℃)

2.7.2 Activation Energy

Instant chemical reactions within active chemical compounds like concrete are hindered because of low initial energy of dormant reactants. Therefore, Carino (1984) proposed the use of "activation energy" to activate dormant reactants from their low energy state. Activation energy also known as rate constant (k) illustrated by Equation 2.3 is the effect of curing temperature on the rate of strength development in concrete (Carino & Lew, 2001).

$$k = \beta(T - T_0) \quad (2.3)$$

Where:

k = Rate constant (1/days),

β = Regression coefficient

T = Average temperature of the concrete during time interval Δt (℃)

T_o = Datum temperature - temperature below which no curing occurs (℃)

The rate constant (k) can be obtained using empirical formulas (ASTM C-1074-11, 2011) or from typical values obtained from previous studies (Nixon et al., 2008). Further improvement of the rate constant led to the development of an exponential relationship between the rate constant and the curing temperatures as illustrated by Equation 2.4 (Carino & Tank, 1992).

$$k = A_o e^{BT} \tag{2.4}$$

Where:

k = Rate constant, initial slope of strength versus duration curve (1/days)

A_o = The value of the rate constant at 0 ℃ (1 / days)

B = Temperature sensitivity factor (1 / ℃)

T = Concrete temperature (℃)

T_{ref} = The reference temperature (20 ℃ in Europe, Kenya 18 ℃)

Temperature sensitivity factor (B) illustrate how the curing temperatures affect the rate constant (k) of concrete mixtures at varying curing temperature with respect to material used (Carino & Lew, 2001). It is obtained by fitting an exponential curve of Equation

2.4 to a plot of rate constants (k) versus the curing temperatures (ASTM C-1074 -11, 2011). Arrhenius Equivalent age is an exponential function of curing temperature, curing time and temperature sensitivity factor (Equation 2.5).

$$t_e = \sum_0^t e^{B(T-T_r)}\Delta t \qquad (2.5)$$

Where:

t_e = Equivalent age at the reference temperature (hours or days)

t = Elapsed time (hours or days)

B = Temperature sensitivity factor (1/°C)

T = Average concrete temperature during time interval Δt (°C)

T_r = Absolute reference temperature (20°C in Europe, Kenya 18°C)

Δt = Time interval (Hours or days)

2.7.3 Strength-Maturity Relationships

Strength-maturity functions are empirical relationships between strength and maturity. Strength-Maturity functions are developed by a series of experimental tests conducted simultaneously on a specific batch of concrete whose curing time and temperature history has been recorded up to the time of test (ASTM C1074-11, 2011). The procedure involves:

i. Concrete from the same batch are moulded in to a number of specimens.

ii. Temperature sensors, which are connected to temperature recording devices, are installed in some of the specimens during moulding.
iii. Specimen are subjected to isothermal curing regimes at varying time intervals.
iv. Maturity of concrete is calculated as a function of curing temperature and time using either the Nurse-Saul or the Arrhenius maturity functions.
v. Compressive strength of specimens are measured using the compressive tests after each curing regime.
vi. Strength-maturity functions are obtained either by a plot of compressive strength versus the maturity or by regression analysis using a computer (Kuna, 2015).

Strength-maturity functions are expressed as either exponential, logarithmic or hyperbolic equations shown by Equations 2.6, 2.7 and 2.8 (Carino & Lew, 2001; Kwon, 2013; Nixon et al., 2008; Wilde, 2013).

a) Exponential strength-maturity function

$$S = S_u e^{-\left[\frac{\tau}{M}\right]^{\beta}} \tag{2.6}$$

Where:

S = Strength at maturity (M)

S_u = Limiting strength

M = Maturity index (°C - hours/days)

τ = Characteristic time constant (°C - hours/days)

β = Shape parameter.

b) Logarithmic Strength-Maturity Function

$$S = \frac{a}{S_o} + \frac{a}{S_o} log(M) \quad (2.7)$$

Where:

S_o = Strength at the beginning of strength development

M = Maturity index (°C - hours/days)

a and b = Mixture-specific constants related to water cement ratio

c) Hyperbolic Strength-Maturity Function

$$S = S_u \frac{k(M-M_o)}{1+k(M-M_o)} \quad (2.8)$$

Where:

S = Strength at age t

S_u= Limiting strength

k = Rate constant - initial slope of strength-maturity curve (1/days)

M_o = Maturity index at the beginning of strength development (°C - hours/days)

M = Maturity index (°C-Hours or °C-days)

The logarithmic strength-maturity function illustrates a linear relationship between strength and maturity index. This does not well represent the complex chemical reactions in concrete mixture (Doyle et al., 2013). The hyperbolic strength-maturity function is recommended for isothermal curing regimes used in the laboratory during design (Carino & Lew 2001; Kuna et al., 2016) Therefore, the hyperbolic strength maturity function was used in this study.

Superior attributes of using the Arrhenius Equivalent-age strength-maturity functions to analyze curing CMA concrete with respect to other statistical models include: It takes in to account the non-linear relationship between curing temperature and strength gain in concrete. It demonstrates the rate of strength gain of concrete at a constant temperature using the rate constant (k) hence gradual strength gain in CMA cab be monitored during curing. It is able to predict mechanical properties of CMA like the stiffness modulus and fatigue strength (Chelelgo et al., 2019; Kuna et al., 2016; Doyle et al., 2013). It takes in to account the temperature sensitivity of the material at varying curing temperature.

2.7.4 Application of Maturity Method in Cold Mix Asphalt

Strength gain nature of cold mix asphalt concrete is similar to that of cement concrete because it occurs gradually through curing. Maturity method used in cement concrete takes into consideration two important factors that affect strength gain of CMA. These are the combined effect of curing time and temperature on the strength gain of CMA and gradual strength gain in CMA during curing (Carino & Lew, 2001; Doyle et al., 2013; Kuna et al., 2016; Chelelgo et al., 2019). Doyle et al. (2013) used emulsified cold mix asphalt cured isothermally in the laboratory at temperatures of 20, 40, 60 and 18 ºC. They used regression analysis to develop a logarithmic strength-maturity function. The model predicted the short-term stiffness of cold mix asphalt and overestimated long-term stiffness of CAEMs (Table 2.4).

Using a logarithmic strength-maturity function, Kuna et al. (2016) predicted early-age stiffness of foamed bituminous mixtures (FBMs) within the range of the measured stiffness but the model overestimated the stiffness of FBMs cured for 296 days beyond the expected realistic in situ stiffness. Moreover, FBMs cured for 296 days did not have a crossover effect, which is a phenomenon that occurs during curing of cement concrete whereby higher early-age curing temperatures result in higher initial strength and lower long-term strength (Carino & Lew, 2001). The study recommended the use of parabolic-hyperbolic strength maturity functions for the prediction of stiffness of FBMs. Chelelgo et al. (2019) concluded that there is a strong correlation between the fatigue maturity of emulsified cold mix asphalt and the actual fatigue strength using the parabolic-hyperbolic function (Table 2.4).

Table 2.4 Application of Maturity Method in Cold Mix Asphalt

Study	CMA Type	CMA test	Maturity function	Results
Doyle et al. (2013)	Emulsified	Stiffness modulus (ITSM)	Logarithmic function	**Estimated early age stiffness. Over predicted long term stiffness**
Kuna et al. (2016)	Foamed	Stiffness modulus (ITSM)	Logarithmic function. Parabolic-hyperbolic	**Over predicted long term stiffness. Predicted actual stiffness of FBMs**
Chelelgo et al. (2019)	Emulsified	Fatigue strength (4 Point bending test)	Parabolic-hyperbolic	**Strong correlation between fatigue-strength and maturity strength**

With regard to stiffness modulus, the Maturity method demonstrated the ability of CMA specimens to resist elastic deformation under load (Kuna et al., 2016; Doyle et al., 2013). Moreover, the repeated cyclic stresses that result to fatigue of CMA pavements

were modelled using the Maturity method (Chelelgo, 2019). There is however no literature correlating the Maturity method and the tensile strength of cold asphalt emulsion mixtures produced from siliceous basaltic aggregates and a cationic bitumen emulsion. Tensile strength measures the maximum load adhered by a material prior to permanent deformation or fracture failure (Figure 2.5).

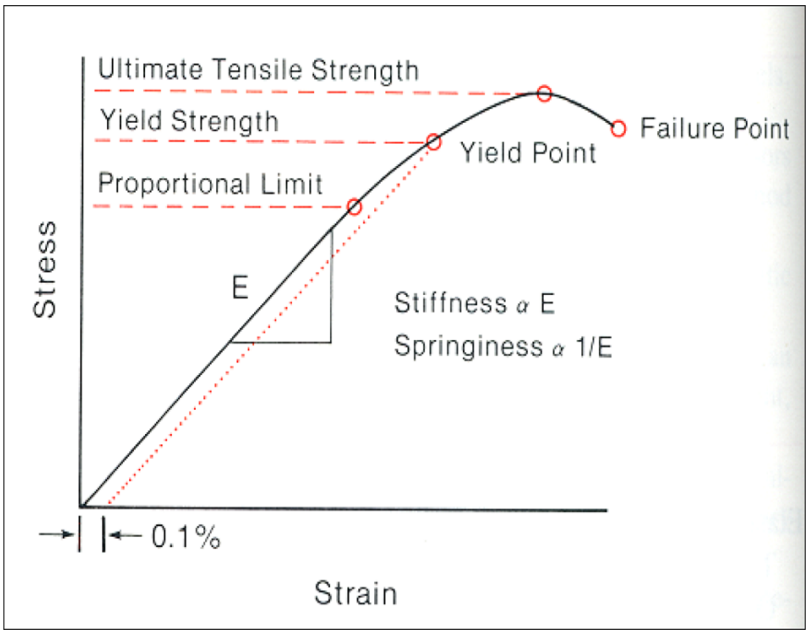

Figure 2.5: Stress and strain curve

In asphalt concrete, indirect tensile strength (ITS) test is used to illustrate cracking properties of flexible pavement layers by simulating the tensile stresses at the base of asphalt concrete surface course (Ma et al., 2015). Tensile stresses are determined by dividing the load at the point of failure with the cross sectional area. ITS demonstrates the adherence of asphalt concrete against fatigue failure, temperature cracking and rutting failure (Bouramia & Qiu, 2017). From the foregoing, the current use of the Maturity method in cold mix asphalt is still limited despite its ability to bridge the gap

between laboratory curing during design and actual curing during construction of CMA pavements.

2.8 Summary of the Literature Review and the Research Gap

The outlined Laboratory-Field Curing Correlation techniques and statistical models used to predict the strength of CMA by correlating isothermal curing regimes during design and actual curing of CMA pavements under construction are limited in several ways:

i. The isothermal curing regimes used during design are controlled and pre-determined in the laboratory and therefore they do not well represent the actual weather conditions appropriately of CMA pavements at in situ (Kuna et al., 2016; Doyle et al., 2013).
ii. Performance-based tests used like the stiffness, rutting and moisture resistance tests are done at the end of curing. Hence, they disregards the gradual strength gain nature of cold mix asphalt (Graziani et al. 2016). This causes delays in the making of decisions related to work progress like the earliest time to overlay the earliest time to overlay a CMA pavement layer with a wearing course or open a CMA pavement layer to traffic.
iii. Finally, the application of Maturity method in cold mix asphalt has not been studied with respect the tensile strength of emulsified asphalt.

From the foregoing, this study used the Maturity method to predict the indirect tensile strength of cold asphalt emulsion mixtures produced using siliceous basaltic aggregates commonly found in Kenya and a slow setting cationic bitumen emulsion. To achieve the study objectives, the independent variables considered included the materials used and the curing regimes while the outputs considered were mix design and strength functions (Figure 2.6). Specimens were subjected to isothermal curing regimes at temperatures of 25, 40 and 60 ºC. There are no universal standards for the design of CMA hence; curing temperatures were selected below the softening point of the bitumen

binder used in the study. This prevents flow of bitumen and change in its dispersion during curing (Kuna et al., 2016). The curing periods considered were 3, 8, 13, 18 and 23 days for each temperature (Figure 2.6). A range of 5 days per curing regime was used to determine a trend during curing. ITS was subsequently measured for each of those curing regimes

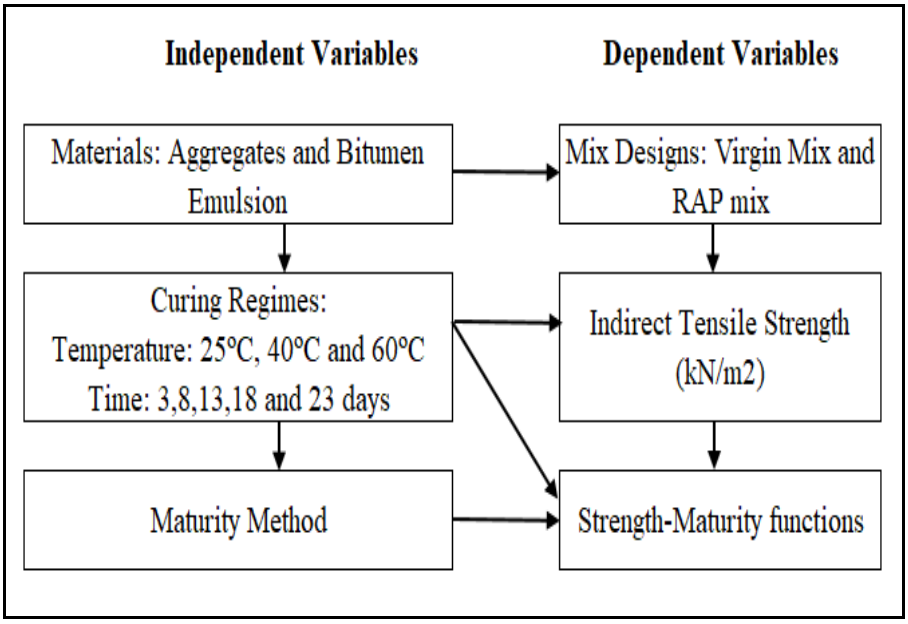

Figure 2.6: Conceptual framework

CHAPTER THREE

MATERIALS AND METHODS

3.1 Introduction

This chapter defines the materials and methods used in the study. The study was conducted at the Materials Testing & Research Division (MT&RD) of the Ministry of Transport, Infrastructure, Housing & Urban Development located at Industrial Area in Nairobi. The study was done in three sections as demonstrated by the research design (Figure 3.1). The first section outlines the material characterization and mix design procedures. Second section outlines the procedures used to mould, cure and test CAEMs specimens. The last section outlines the empirical procedure used to develop hyperbolic strength-maturity functions for the prediction of indirect tensile strength of CAEMs.

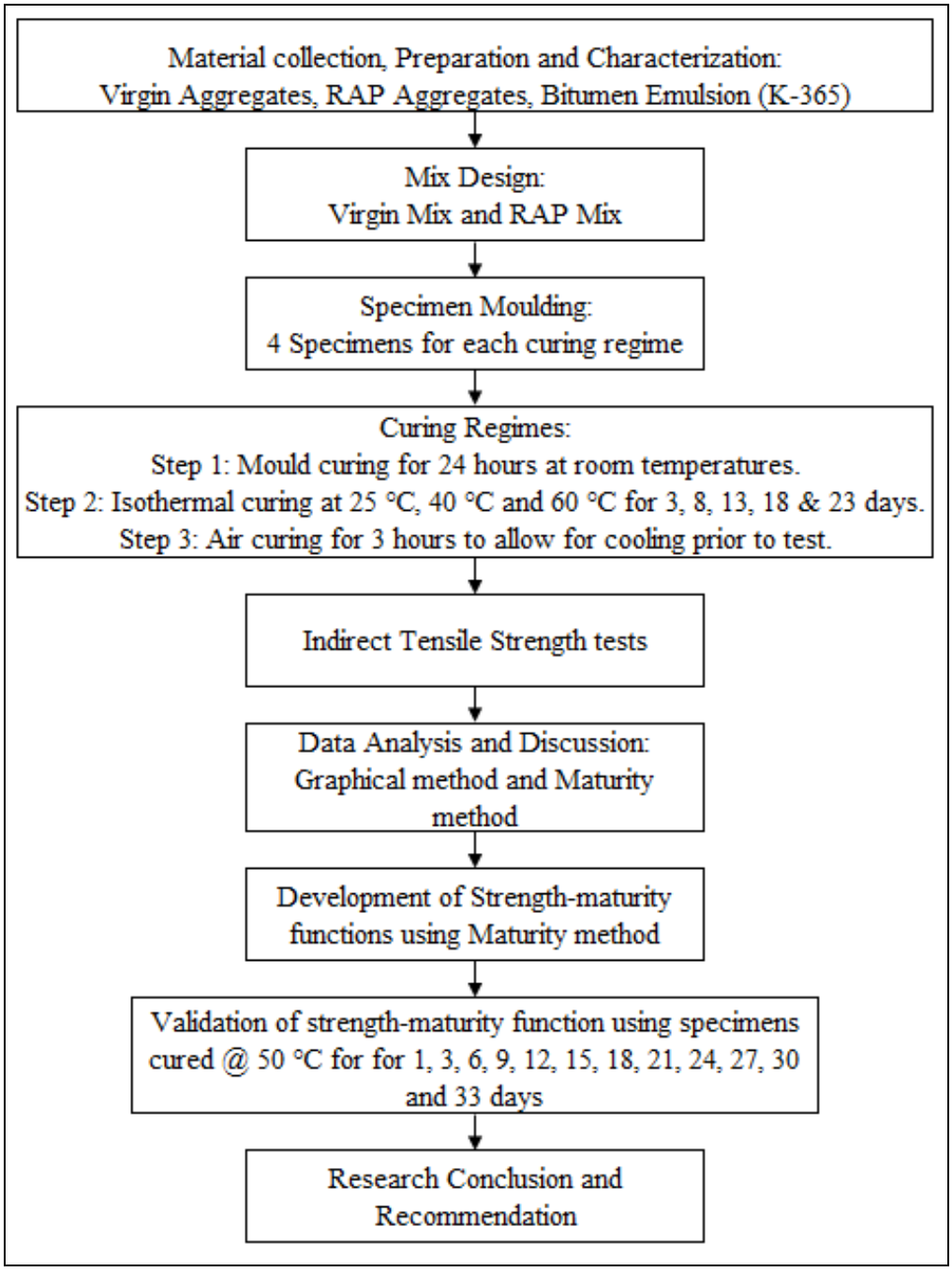

Figure 3.1: Research Design

3.2 Material Characterization and Mix Design

3.2.1 Material Collection

Virgin aggregates, recycled aggregates from reclaimed asphalt pavement (RAP) and a slow setting bitumen emulsion were collected for the study. The virgin aggregates of maximum nominal size 20 mm were obtained from D.M Quarries Limited located in Katani area of Machakos County. They were sourced from basaltic rocks, which are siliceous in nature. The virgin aggregates were packed in sacks at the collection point in sizes of 0/6, 6/10, 10/14 and 14/20 mm respectively (Figure 3.2a). Recycled aggregates from RAP were obtained from the Enterprise Road Expansion Project in Kenya. The RAP material was collected in large blocks (Figure 3.2b). Bitumen emulsion ($K_{3\text{-}65}$) was obtained from COLAS East Africa Limited located at Industrial Area in Nairobi.

Figure 3.2: Material Collection: (a) Virgin Aggregates; (b) RAP Aggregates

3.2.2 Research Equipment

Equipment used were a Hobart rotary mixer (A200-B3HE), Rotor Vapor (Buchi EL-131), Marshall compaction apparatus (UTAS 0082E), Genlab electric ovens

(MINO/18/SS), MATEST Tensile Splitting device (B047-02), Silverline Vernier calipers (380244), a set of standard sieves and a sieve shaker (ELE ISO3310-1:2000), an electronic weighing scale (KERN FCB-30KG), Automatic Digital Ring and Ball apparatus (MATEST - B070N1), bitumen penetrometer (NORMALB ANALYS P-734).

3.2.3 Preparation of Reclaimed Asphalt Pavement Aggregates

A hammer was used to break down the large recycled aggregates from RAP blocks to small blocks. The small RAP blocks were heated in the oven at a temperature of 50°C for 4 hours to enable the asphalt binding the aggregates to soften and allow the aggregates to separate. The recycled aggregates obtained after aggregate separation were sieved, packed and stored in sacks as per their sizes of 0/6, 6/10, 10/14, and 14/20 mm respectively (Figure 3.3). This was done to enhance homogeneity during mix design. No preparation was required with the virgin aggregates.

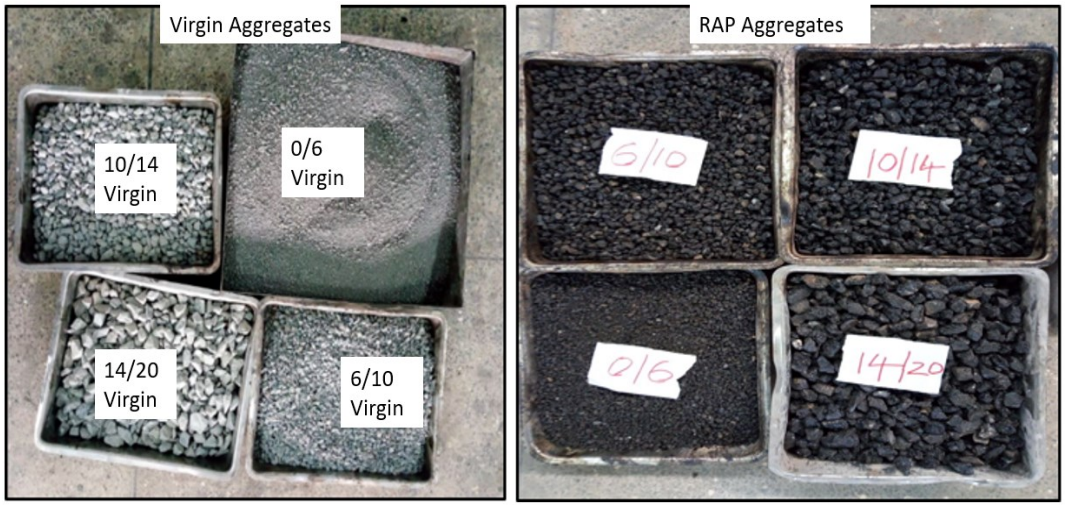

Figure 3.3: Research Materials: (a)Virgin Aggregates; (b) RAP Aggregates

3.2.4 Material Characterization Tests

Bitumen emulsion ($K_{3\text{-}65}$), virgin aggregates and the RAP aggregates were subjected to physical, mechanical and mineralogical tests to determine their quality and viability for the production of cold mix asphalt.

i. Aggregate Physical Tests

Aggregate physical tests done were specific gravity tests and moisture absorption (BSI 812:112, 1985). Aggregate specific gravity measures the materials density as compared to the density of water at 23 ℃. The specific gravity of fine aggregates was determined using the Pycnometer water method (ASTM D854 – 14, 2014). The weight of fine aggregates sample sets of size 0/6 – 6/10 mm were measured and their volume was determined by submerging them in a Pycnometer of known volume. Density was calculated by dividing mass with the volume. Specific gravity was the ratio of the aggregate density to the density of water at 23 ℃. For course aggregate, the specific gravity was determined by measuring the weight of sample aggregates in three different conditions, namely: oven dried, saturated surface dried and submerged. Specific gravities considered were bulk specific gravity, apparent specific gravity and bulk saturated gravity. They were used to determine the voids in mineral aggregates (VMA) and air void contents (Ogunbayo et al. 2018; FHWA, 2010).

Moisture absorption of aggregates was used to determine the permeability of aggregates that affects durability and determined binder absorption in asphalt concrete. It was determined by comparing the weight of dry aggregates to those of surface dry aggregates after submerging in water (BSI 812:112, 1985).

ii. Aggregate Mechanical Tests

The mechanical tests were done to assess aggregates toughness and abrasion characteristics with respect to traffic loads. The mechanical properties considered were: (1) Aggregate Crushing Value (ACV) where sample aggregates of size 14-20mm were subjected to a compressive load of 400 kN for 10 minutes. Resistance to crushing was assessed by sieving the crushed sample through sieve size 2.36 mm (BS 812:110, 1990). (2) Flakiness Index (FI) was illustrates the particle shape that affects the degree of parking of particles. FI of aggregates of size 6-20 mm was obtained as percentage by weight of particles whose thickness is less than three-fifths (0.6 times) of their mean dimension (BS 812:105, 1998). (3) Los Angeles Abrasion (LAA) was obtained by rotating coarse aggregates of size 10/14 and 14/20 mm in a steel drum containing 10 steel spheres at a speed of 30 revolutions per min. The abrasion loss value was assessed by sieving the sample aggregates through sieve size 1.7mm (BS EN 1097-2, 2010).

iii. Mineralogical Attributes

The mineralogical properties of the aggregate were obtained using a non-destructive elemental chemical analysis known as the X-Ray Fluorescence spectrometry method (X-RF). The virgin and the RAP aggregates were subjected to X-Rays interaction using the BRUKER XR-F spectrometer (ASTM E1621-13, 2013). The XR-F method involves interaction between the aggregates and X-Ray by either absorption, scattering or transmission (Moreno-Perez, et al., 2018). Mineral composition of aggregates were produced by the XR-F spectrometer done at the Ministry of mining located along Machakos Road in Nairobi County.

iv. Aggregates Grading

Grading also known as sieve analysis was done to determine of particle size distribution of aggregates. Sieve analysis involved sifting sample aggregates through a stack of wire mesh sieves. The set of standard sieve sizes considered were ranging from 0.075-20 mm The sieves were arranged in reducing size order; having the largest (sieve 20 mm) at the top to the smallest sieve (0.075 mm) at the bottom. They were vibrated using a sieve shaker for 60 seconds. The weight of aggregates passing and retained in each sieve were measured, recorded and grading curves was plotted (BSI 410-2, 2010).

v. Bitumen Characterization Tests

A slow setting bitumen emulsion (K_{3-65}) was used as the binder. K_{3-65} was composed of 65% bitumen and 35% water. K_{3-65} was selected because of its slow rate of setting (breaking) which enables effective mixing and coating of aggregates with binder. Bitumen coating the recycled aggregates from RAP was extracted using the solvent extraction method (BS EN 12697-1, 2012). The bitumen extraction process involved mixing the RAP aggregates with methylene chloride to form a solution of bitumen and methylene chloride. The extracted solution was subjected to Rotary Evaporator Method to separate the bitumen and the methylene chloride by distillation (Figure 3.4, BS EN 12697-3, 2013).

Figure 3.4: Rotary Evaporator Method

(BS EN 12697-3, 2013)

Binder tests considered for the bitumen emulsion (K_{3-65}) and the extracted bitumen from RAP were:

i. Bitumen penetration test involves the penetration of a needle under a load of 100g through sample bitumen binder at a fixed temperature of 25℃ for 5 seconds (Figure 3.5a). Penetration distance of the needle recorded in decimillimeter (0.1mm) illustrates the hardness/softness of the binder (BS 2000-49, 2007).
ii. Ring and Ball softening point test was done by placing a 3.5g steel ball on sample bitumen binder contained within a brass ring and submerged in a water bath. The temperature of the water bath was increased at 5℃ per minute until the point where the binder softens and deforms causing the ball to pass through the ring to the base plate located 25mm below (Figure 3.5b). The temperature at the point of binder deformation is called the softening point temperature (BS EN 1427, 2007).

(a)

(b)

Figure 3.5: Bitumen quality tests: (a) Penetration test; (b) Softening Point test. (BS 2000-49, 2007; BS EN 1427, 2007)

3.2.5 Mix Design

Two mix designs were developed using the virgin and the RAP aggregates respectively in accordance to the Asphalt Cold Mix manual - series No. 14 (The Asphalt Institute, 1989) and Basic Asphalt Emulsion Manual (Asphalt Institute, 2008). The mix design procedure was:

i. Combined aggregate grading.
ii. Determination of the initial emulsion content (IEC).
iii. The emulsion coating test.
iv. Determination of optimal total fluid content (OTFC).
v. Determination of aggregate pre-mix water.
vi. Variation of the bitumen content (BC)
vii. Selection of optimal bitumen content (OBC).
viii. Determination of optimal compaction properties.

i. Combined Aggregate Grading

Combined aggregate grading was calculated using Cooper's formula (Equation 3.1). The objective was to develop a cold mix asphalt with minimal air voids and maximum density (Asphalt Academy, 2009).

$$P = \frac{(100-F)(d^n - 0.075^n)}{(D^n - 0.075^n)} + F \qquad (3.1)$$

Where:

P = Material passing a sieve of size d (%),

d = Selected sieve size (mm),

D = Maximum aggregate size (mm),

F = Mineral filler content (%)

n = An exponent that dictate the concavity of the grading line for optimal aggregate packing (0.45 or 0.50)

The selected exponent (n) was 0.45 to enable optimal packing of aggregates that ultimately enhances the density of dense-graded asphalt mixtures (Thanaya et al., 2009). The maximum aggregate size (D) was 20 mm. No mineral filler (F) was used for this study. Proportions of fine virgin aggregates of size 0/6mm and RAP aggregates were calculated (Equation 3.2) and blended to reduce coarse grading in RAP mix. The study intended to produce combined aggregate grading curves that are within the grading envelope (Asphalt Academy, 2009).

$$P = aA + bB + c\,C \quad (3.2)$$

Where:

P = Combined aggregates passing a particular sieve (%)

a, b & c = Proportions of individual aggregates sizes used in the combination (%)

A, B & C = Aggregate passing a particular sieve for individual aggregates sizes (%)

ii. Determination of the initial emulsion content

Initial emulsion content (IEC) is the approximate amount of binder required to produce a cold mix asphalt. It can be obtained by using the Centrifuge Kerosene Equivalent test (CKE). In the absence of the CKE testing equipment as was the case in the laboratory, total binder demand (P_b) is calculated as a function of aggregate retained in sieve size 2.36mm, aggregate passing sieve size 2.36mm and filler passing sieve size 0.075 mm (Equation 3.3, Asphalt Institute, 1989).

$$P_b = (0.05A + 0.1B + 0.5C) \times 0.7 \quad (3.3)$$

Where:

P_b = Total binder demand by mass of the combined aggregates (%).

A = Aggregates retained on sieve size 2.36 mm (%).

B = Aggregates passing sieve 2.36 mm and retained on sieve 0.075 mm (%)

C = Filler passing sieve size 0.075 mm (%).

The initial emulsion content (IEC) was calculated using Equation 3.4.

$$IEC = \left(\frac{P_b}{X}\right) \times 100 \quad (3.4)$$

Where:

IEC = Initial Emulsion Content by mass of total mixture (%)

X = Bitumen content in the emulsion (65%)

For the RAP mix, existing binder coating the recycled aggregates was considered during design. Therefore, additional new binder required by the RAP mix was calculated using Equation 3.5.

$$P_{nb} = P_b - \frac{P_{sb}(100-r)}{100} \quad (3.5)$$

Where:

r = Virgin aggregates content blended with the RAP aggregates (%)

P_{sb} = Asphalt binder content in RAP (%)

P_{nb} = Additional new binder content (%)

P_b = Total binder demand by mass of the combined virgin aggregates (%)

iii. Emulsion Coating Test

The emulsion coating test was done to assess how the bitumen emulsion ($K_{3\text{-}65}$) would coat the aggregates at varying pre-mix (pre-wetting) water content. A suitable bitumen

emulsion should coat at least 50% of the aggregates at a specific pre-wetting water (Asphalt Institute, 2008; 1989). Five samples of blended aggregates of mass 200 grams were prepared for virgin mix and the RAP mix respectively. Aggregate pre-mix water was varied from 1 - 5% by mass of dry aggregates for the five samples respectively. Aggregates and the pre-mix water were mixed for 60 seconds. Bitumen emulsion equivalent to the pre-determined initial emulsion content was added to the virgin and the RAP samples respectively. Mixing was done for 60 seconds then the samples were placed on white filter papers and left to air cure for 24 hours (Figure 3.6). After 24 hours, the percentage of the aggregates coated by the bitumen emulsion was visually assessed. The coating test that guides the study on the range of bitumen content to be considered when determining the optimal bitumen content during mix design.

Figure 3.6: Coating test - Air curing of coated aggregates

(Asphalt Institute, 1989)

iv. Determination of optimal total fluid content

Optimal total fluid content (OTFC) also known as Optimum Moisture Content (OMC)was used to illustrate the moisture-density relationship of cold mix asphalt (BS 1377-4, 1990). Five sets of combined aggregates were prepared for the virgin and the

RAP mix respectively. Moisture contents of the virgin mix were varied from 7.7 to 11.5% while those of the RAP mix were varied from 5.2 to 9.5%. Each specimen was compacted in three layers by vertically pressing the vibratory hammer for 60 seconds per layer (Figure 3.7).

Figure 3.7: Vibrating Hammer Method

(BS 1377-4, 1990)

Dry density was calculated as a function of bulk density and moisture content (Equation 3.6). Dry density was plotted against moisture content. Maximum Dry Density (MDD) is the peak density at a specific moisture content. The moisture content at MDD is the optimal total fluid content (OTFC)

$$\gamma_d = \frac{100\gamma}{(100+w)} \qquad (3.6)$$

Where:

γ_d = Dry density $(\mathrm{Kg/m^3})$

γ = Bulk density$(\mathrm{Kg/m^3})$

w = Moisture content (%)

v. Determination of aggregate pre-mix water content

Specimens composed of 1100 grams of blended aggregates, bitumen emulsion content equivalent to the calculated IEC and varying pre-mix water were moulded and compacted using the Marshall Method (ASTM-D6926-10, 2010). The pre-mix water content was varied from 1% to 5% by mass of dry aggregates for both the virgin and the RAP aggregates. Three samples were prepared for each pre-mix water content. Curing was done in three stages: mould curing for 24 hours at ambient room temperatures, isothermal curing in the oven for 72 hours at 40 ^{o}C, then air curing for 3 hours at ambient room temperature prior to stability test (Oluwasenyi, 2011). Stability was obtained by loading the specimen diametrically using the Indirect Tensile Strength (ITS) apparatus up to the point of failure (ASTM D6931-12, 2012). The dial reading at the point of failure was multiplied by the ring factor (0.0228 KN) to get stability. Pre-mix water content was plotted against stability and optimal pre-mix water content was selected at the highest stability.

vi. Varying the bitumen content

Bitumen emulsion (BC) used was composed of 65% bitumen and 35% water. The percentage bitumen content was varied two points above and two points below the calculated Initial Bitumen Content (IBC). Six specimens were prepared for each bitumen content at a constant predetermined pre-mix water content. After compaction, specimen

were labelled and cured in three stages: mould curing for 24 hours at ambient room temperatures, isothermal curing in the oven for 72 hours at 40^{o}C, then air curing for 3 hours at ambient room temperature. Three specimens were subjected to moisture conditioning as outlined in the Asphalt Cold Mix manual MS-14 (Asphalt Institute, 1989) and were tested for stability as soaked specimens. The other three specimens were not subjected to moisture conditioning hence they were tested for dry stability. The effect of bitumen content on the performance of cold mix asphalt was analyzed in terms of the stability, stability loss, resistance to moisture absorption and porosity.

vii. Selection of optimal bitumen content

The optimal bitumen content (OBC) was selected based on its effect on stability, stability loss, resistance to moisture damage and porosity.

viii. Determination of optimal compaction properties.

Compaction properties of CAEMs was assessed based on the air void content obtained at different compaction levels. The study was targeting air voids contents ranging between 6-10% for the virgin mix and 10-15% for the RAP mix respectively. To achieve this, three compaction levels were considered: 50, 75 and 150 blows respectively. Six specimens: three for RAP mix and three for virgin mix were compacted using the Marshall hammer for each compaction level. Air voids were determined as per the Asphalt Cold Mix manual (Asphalt Institute, 1989). Air voids content were plotted against the compaction level for analysis.

From the mix design, specific mix proportions of combined aggregate grading, pre-mix water content, bitumen content and number of compaction blows were determined and were used for preparation of specimens to be used for the attainment of objectives two and three.

3.3 Determining the effect of curing time and temperature on the ITS of CAEMs.

3.3.1 Experimental Set-up

Using the mix proportions obtained from the mix design, cylindrical specimens of diameter 100 mm and thickness 63.5 mm were moulded and compacted using the Marshall Method (ASTM-D6926-10, 2010). They were cured in moulds for 24 hours at ambient temperatures. Specimens (4 replicates for each regime) were subjected to isothermal curing temperatures of 25, 40 and 60℃. There are no universal standards for the design of CMA therefore, curing temperatures were selected with respect to the softening point of the bitumen binder used in the study. This prevents flow of bitumen and change in its dispersion during curing (Chelelgo et al., 2019, Kuna et al., 2016, Doyle et al., 2013). Curing age considered were 3, 8, 13, 18 and 23 days for each curing temperature. A range of 5 days per curing regime was used to determine a trend during curing.

3.3.2 Data Collection and Analysis

Indirect tensile strength test was used to determine the strength of cold mix asphalt (ASTM D6931-12, 2012). Specimens were loaded diametrically at a rate of 50.8 mm/min up to a point of failure (Figure 3.8a). This loading configuration develops a relatively uniform tensile stress perpendicular to the direction of the applied load and along the vertical diametrical plane. Therefore, the specimen fail by splitting along the vertical diameter (Figure 3.8b). The dial reading at the failure point was recorded and multiplied with the ring factor 0.0228 kN to get maximum load (P_{ult}). Indirect tensile strength of the specimen was calculated using Equation 3.7.

$$S_t = \frac{2P_{ult}}{\pi \times d \times t} \tag{3.7}$$

Where:

S_t = Indirect tensile strength (N/mm^2)

$P_{ul}t$ = maximum load (N)

t = thickness of the specimen (mm)

d = diameter of specimen (mm)

(a)  **(b)** 

Figure 3.8: Indirect Tensile Strength test: (a) ITS Test; (b) Failed Specimens. (ASTM D6931-12, 2012)

3.4 Prediction of ITS of CAEMs using the Maturity method

3.4.1 Experimental set-up

Data required for the development of the strength-maturity function were indirect tensile strength (kN/m^2), curing temperature (^{o}C) and curing time (days). Data was obtained from specimens prepared, cured and tested in objective one.

3.4.2 Data Collection and Analysis

The Maturity Method was used to develop strength-maturity functions for cold asphalt emulsion mixtures. Strength-maturity functions are empirical relationships between strength and maturity that are obtained by testing specimens whose temperature history up to the time of test has been recorded (ASTM C1074-11, 2011). The strength-maturity functions were developed as follows:

a) Determination of the rate constant (k)
b) Determination of the temperature sensitivity factor (B)
c) Maturity in terms of equivalent age (t_e)
d) Modified Arrhenius maturity function.
e) Developing strength-maturity functions.
f) Validating the strength-maturity function.

a) Determination of the rate constant

Rate constant (k) is the rate of strength gain with respect to the curing temperatures (Carino & Lew, 2001). Strength-age relationships were used to determine the rate constant (ASTM C-1074-11, 2011). For isothermal curing regimes, a hyperbolic strength-age relationship (Equation 3.8) is recommended for the determination of the rate constant (Carino, 1984). The rate constants and the limiting strengths for each curing temperature were obtained by fitting ITS data to an appropriate equation using the least squares fitting technique of regression analysis (Equation 3.8).

$$S = S_u \frac{k(t-t_o)}{1+k(t-t_o)} \tag{3.8}$$

Where:

S = Strength at age t

S_u = Limiting strength

k = Rate constant (1/days)

t_0 = Curing age at start of strength development (days) ($t_0 = 0$)

t = Curing age (days).

Limiting strength (S_u) is the asymptotic value of the strength for the hyperbolic function that fits the data.

b) Determination of the temperature sensitivity factor

Temperature sensitivity factor (B) for the virgin and the RAP mix were determined by fitting an exponential curve of Equation 2.4 in a plot of rate constant against curing temperature.

c) Maturity in terms of Equivalent Age

The Maturity of cold asphalt emulsion mixtures was calculated using the Arrhenius equivalent-age (t_e) maturity function (Equation 2.5). Strength was plotted against Maturity.

d) Modified of the Arrhenius maturity function

Maturity rule states that concrete drawn from the same batch will have approximately the same strength at the same maturity index, despite being subjected to different

combinations of curing temperature and time (Carino & Lew, 2001). Curing mechanism of cold mix asphalt concrete and cement concrete differ in two major ways:

a) Curing of cold mix asphalt involves loss of water for strength gain while that of cement concrete requires addition of water for strength gain.
b) Cold mix asphalt concrete does not undergo crossover effect that occurs in cement concrete (Kuna et al., 2016).

A study on foamed bituminous mixtures (FBMs) proposed the incorporation of curing temperature in Arrhenius maturity function (Equation 2.5). For specimens cured under isothermal curing regimes, Kuna et al. (2016) recommended the calculation of maturity (M) of FBMs as a function of equivalent age and curing temperature (Equation 3.9).

$$M = t_e \times T \tag{3.9}$$

Where: M = Maturity index (°C - days)

T = Curing temperature (°C)

t_e = Equivalent age at the reference temperature (days)

e) Development of strength-maturity functions

For specimens cured under isothermal conditions, as was the case for this study, hyperbolic strength-maturity functions are recommended for strength prediction (Carino, 1984; Kuna et al., 2016). Linear-hyperbolic (Equations 3.10) and parabolic-hyperbolic (Equations 3.11) were considered for development of strength-maturity functions of CAEMs.

$$S = S_u \frac{kM}{1+kM} \quad (3.10)$$

$$S = S_u \left(\frac{\sqrt{kM}}{1+\sqrt{kM}}\right) \quad (3.11)$$

Where:

S = Strength at age t (kN/m^2)
M = Maturity index at age t (^{o}C - days)
S_u = Limiting strength (kN/m^2)
k = Rate constant (1/days)

The difference between Equations 3.10 and 3.11 is based on the rate of mix chemical reaction during the curing process (Knudsen, 1984). Regression analysis using the least square fitting technique was used to determine k and S_u.

f) Validating the strength-maturity functions

A set of virgin and RAP mix specimens (three replicates per curing regime) were prepared using the Marshall method (ASTM-D6926-10, 2010) and subjected to different isothermal curing regimes. Data required to calculate the maturity of CAEMs were curing temperature of 50 ^{o}C and curing age of 1, 3, 6, 9, 12, 15, 18, 27, 30 and 33 days. Indirect tensile strength was measured after every curing step and was recorded as measured strength (kN/m^2). Maturity index (M) of CAEMs was calculated as a function of equivalent age and curing temperature (Equation 3.9). The rate constant (k) and the limiting strength (S_u) were determined using hyperbolic strength-maturity functions for the virgin and the RAP mix respectively. The maturity index (M) of CAEMs was incorporated in the developed strength-maturity functions to predict the tensile strength

of cold asphalt emulsion mixtures. Measured strength (ITS) was plotted against predicted tensile strength for analysis.

CHAPTER FOUR

RESULTS AND DISCUSSIONS

4.1 Introduction

This section of the thesis covers detailed discussion of the results obtained in the study. The first section describes the mix design results; the components of the virgin and the RAP mix respectively. The second section elaborates how curing temperature and time affect the strength of cold asphalt emulsion mixtures. Lastly, strength-maturity functions are developed for prediction of strength of cold asphalt emulsion mixtures. The developed strength-maturity functions are validated by assessing their accuracy in predicting the indirect tensile strength of CAEMs specimens subjected to different curing regimes. Data in tables and graphs were summarized from the Appendices.

4.2 Material Characterization and Mix Design

4.2.1 Material Properties

The obtained specific gravities were within the recommended range of 2.5 to 2.9 kg/m^3 for flexible road pavements (BS 812 -112, 1985). The bulk, apparent and saturated specific gravities of virgin aggregates were higher than those of the RAP aggregates meaning that the virgin aggregates were denser than the RAP aggregates (Figure 4.1 a, b & c). High aggregate density depicts that the aggregate is tough and highly resistance to failure by mechanical action (Ogunbayo et al., 2018). The observed difference in the densities between the virgin and the RAP aggregates could have been contributed by difference in the geological formation process of their parent rock and differing environmental factors like nature of weathering and fluctuating climatic conditions (Zhang, Pei, Liu & Zou, 2019; Buertey, Atsrim & Offei, 2016).

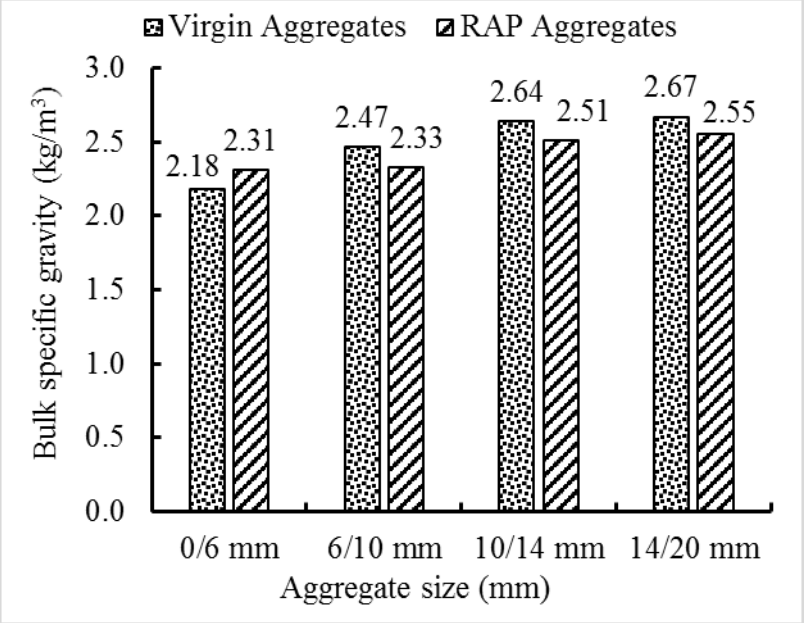

(a) Bulk specific gravities

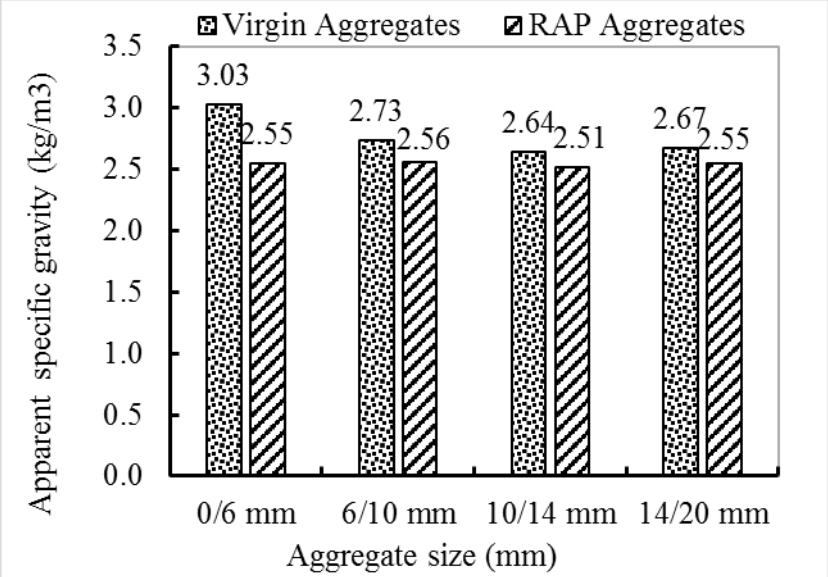

(b) Apparent Specific gravities

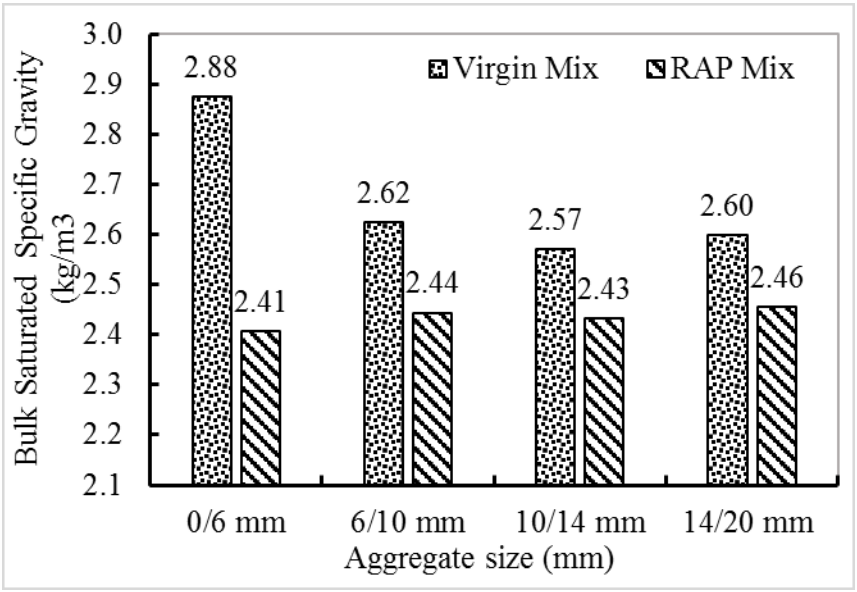

(c) Bulk Saturated Specific Gravities

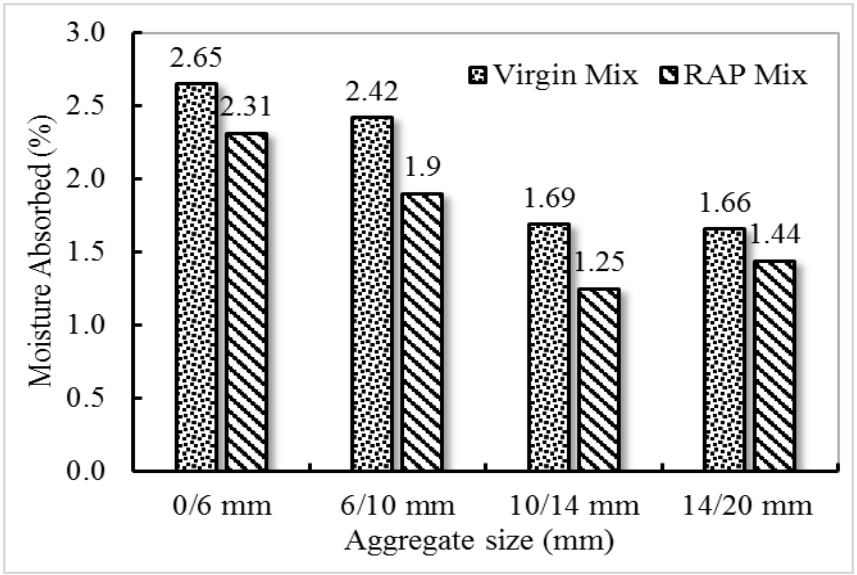

(d) Moisture absorbed

Figure 4.1: Aggregates physical properties

The virgin aggregates absorbed more moisture compared to the RAP aggregates for all the aggregate sizes (Figure 4.1d). The highest moisture content absorbed (2.65 %) was observed for the virgin mix of size 0/6 mm. High moisture absorption by 0/6 mm aggregates could have been contributed by of the fines that increased the surface required by water compared to that of the RAP aggregates. Fine RAP aggregates (0/6 mm) were agglomerated to each other or to the coarse aggregates by the existing aged binder hence surface area was reduced and water absorption was limited.

Irrespective of lower density values, the RAP aggregates was more resistance to crushing (ACV) and abrasion (LAA) compared to those of the virgin aggregates (Figure 4.2). This can be explained by the stiff nature of the RAP material because of aging during its service life (Taher & Aman, 2016). The virgin aggregates had a flakiness of 14.71%, which was higher than 13.4% of the RAP aggregates. This could have contributed to the observed low resistance of virgin aggregates to mechanical action compared to the RAP mix.

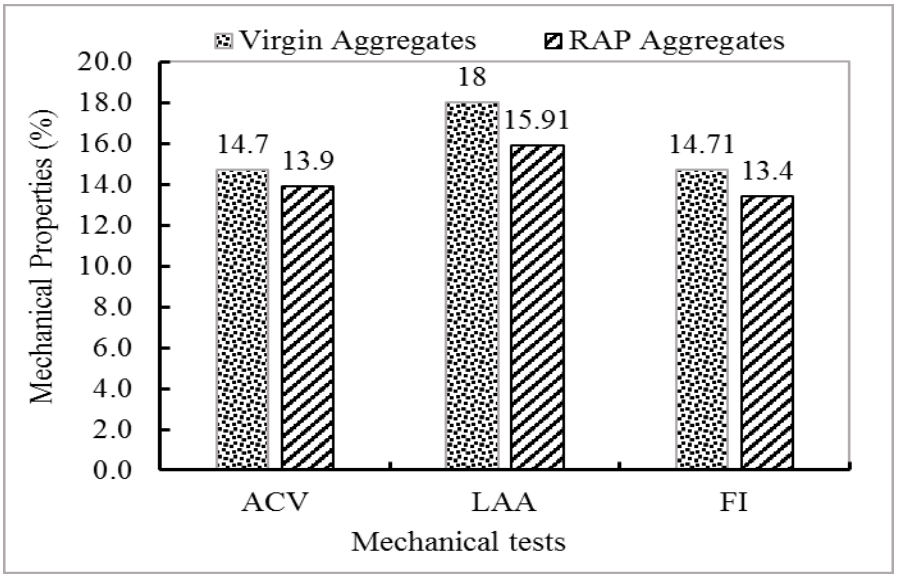

Figure 4.2: Aggregates Mechanical Properties

Both the virgin and the RAP aggregates had more than 65% of siliceous mineral component ($Si0_2$) (Figure 4.3). Aggregates with high siliceous ($Si0_2$) and Aluminum (Al_20_2) content have density and strength parameters (Pekala, 2015). $Si0_2$ is negatively charged hence a positively charged slow setting cationic bitumen emulsion ($K_{3\text{-}65}$) was used as a binder.

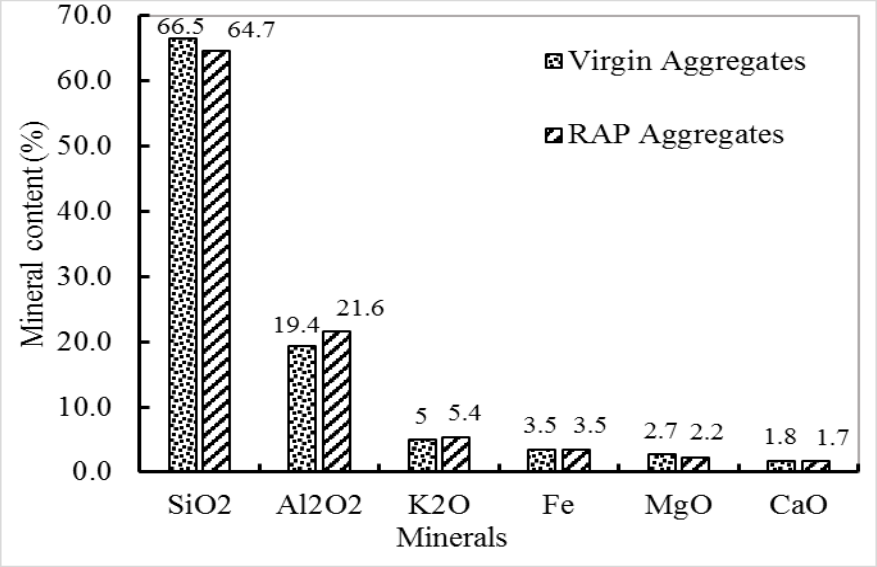

Figure 4.3: Aggregates mineral composition

The aged binder from the RAP aggregates had lower penetration distance of 18 dmm compared to 58.25 dmm of $K_{3\text{-}65}$ (Table 4.1). Moreover, the RAP binder had a higher softening point of 65.05 ºC compared to that of 60.90 ºC of the virgin binder. The results observed indicate that the aged binder from RAP was harder and required high temperatures to soften. Hardening of the RAP bitumen binder could have been as a result of aging during its service life (Norouzi, Sabouri & Kim, 2014).

Table 4.1: Properties of bitumen emulsion (K_{3-65}) and RAP bitumen

Property	Standards / Codes	Tests Result		Status
		K_{3-65}	RAP Bitumen	
Bitumen content	BS EN 12697-1:2012	65.0	-	**OK**
(%)		-	4.4%	**OK**
Penetration at 25°C (0.1 mm)	BS 2000-49:2007	58.25	18	**OK**
Softening Point - Ring and Ball (°C)	BS EN 1427:2007	60.90	65.05	**OK**
Particle charge	(Using litmus paper)	+ve	-	**OK**

Material properties suitable for the productions of CAEMs include: Specific gravities ranging between 2.4 – 3.0%, moisture absorption below 5%, aggregate crushing value below 25%, Flakiness Index below 20%, Los Angeles Abrasion below 30% (Asphalt Institute 2008; MoTC, 1987; FHWA, 2010). Aggregates with high siliceous content above 50% is recommended for strength improvement (Pekala, 2015). Binder properties suitable for the production of CAEMs are penetration above 40 dmm and softening point above 40 °C is recommended to prevent flow of binder. In summary, the physical, mechanical and mineralogical properties of the aggregates and the binder were within the limits of their respective standards. Hence, the materials were used for the production of CAEMs.

4.2.2 Aggregate Grading

Single sized grading of the RAP aggregates had coarse grading compared to the virgin aggregate with only 1% passing sieve size 0.425mm (Figure 4.4a) while the virgin mix had 19% passing sieve 0.425mm (Figure 4.4b). Fine virgin aggregates of size 0/6 mm

were blended with the RAP aggregates to improve the coarse grading of the RAP aggregates.

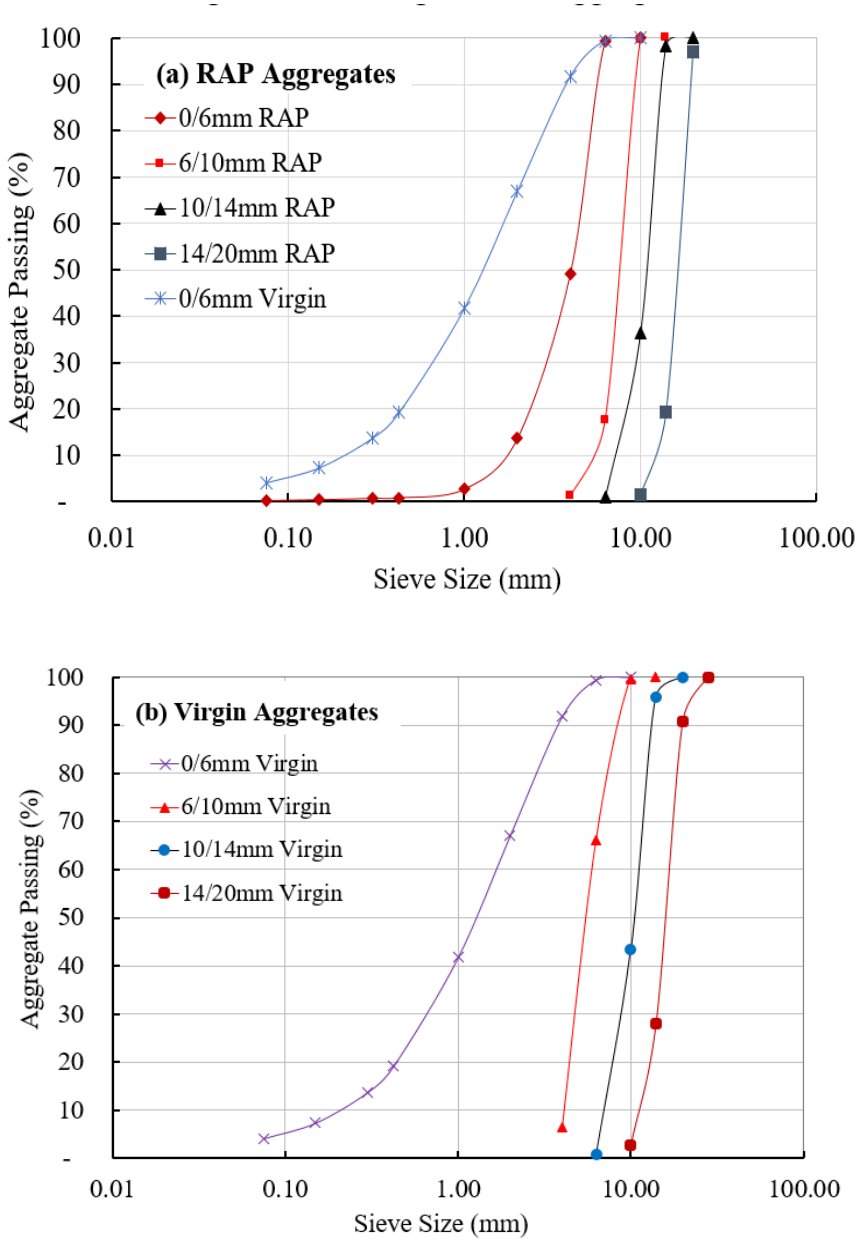

Figure 4.4: Single-size Aggregate Grading

Combined aggregate grading curves of the virgin and the RAP mix were within the upper and lower limits of the grading envelope (Figure 4.5) in accordance to the Technical Guide for bitumen stabilized materials (Asphalt Academy, 2009). Combined Virgin - RAP aggregates improved the fines passing sieve size 0.425mm by 10% (Figure 4.5). Hence, no filler was used to improve coarse grading of the RAP mix.

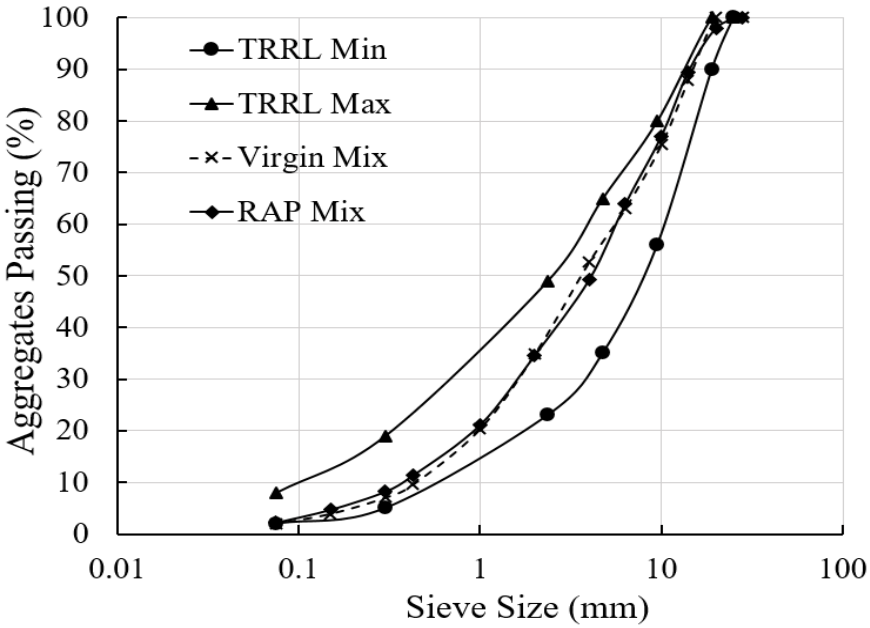

Figure 4.5: Combined aggregate grading

4.2.3 Initial Emulsion Content

RAP mix required a lower binder content of 3% compared to 5% of the virgin mix (Table 4.2). This could be contributed to the presence of the existing aged binder coating the RAP aggregates.

Table 4.2: Initial Emulsion Content

Parameters	Virgin Mix	RAP Mix
Binder demand (P_b)	5.285%	
Additional new binder (P_{nb})	-	**3.085%**
Initial emulsion content (IEC)	8.13%	**4.8%**
Bitumen Content	5%	**3%**

4.2.4 Emulsion Coating Test

The percentage of RAP aggregates coated was lower than that of the virgin aggregates coated for all pre-mix water contents (Figure 4.6). Moreover, increase in pre-mix water content increased the amount of aggregates coated for both the virgin and the RAP aggregates (Figure 4.6). The bitumen emulsion should coat at least 50% of the aggregates for it to be used for production of CMA (Asphalt Institute, 2008). The bitumen emulsion ($K_{3\text{-}65}$) coated 50% of the virgin and the RAP aggregates at 3% and 3.7% pre-mix water content respectively.

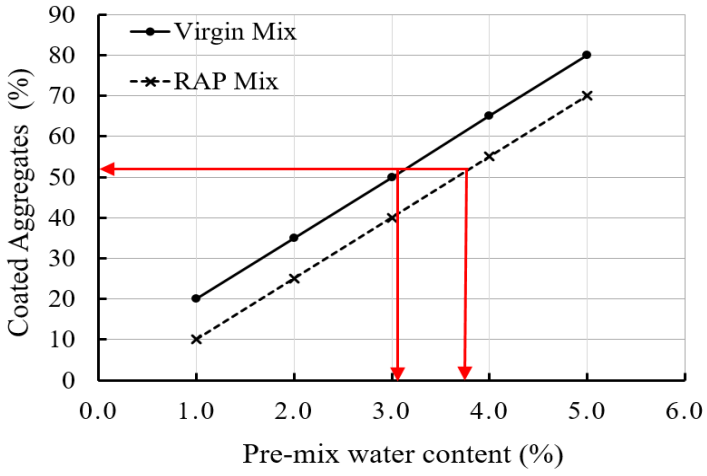

Figure 4.6: Emulsion coating test

4.2.5 Optimal Total Fluid Content (OTFC)

The virgin mix achieved a maximum of 2065 kg/m^3 at 9.6% moisture content while the RAP aggregates achieved a maximum dry density of 1945 kg/m^3 at 7.7% moisture content (Figure 4.7). The virgin MDD of the virgin mix was 6% higher than that of the RAP mix. Lower dry density of the RAP mix could have been contributed by the aging of the recycled aggregates during their service life. The virgin mix required higher moisture content of 9.6% compared to 7.7% of the RAP mix (Figure 4.7). High moisture requirement by the virgin aggregates could have been contributed the high content of size 0/6 mm fines in the virgin aggregates that increased the surface area required by water.

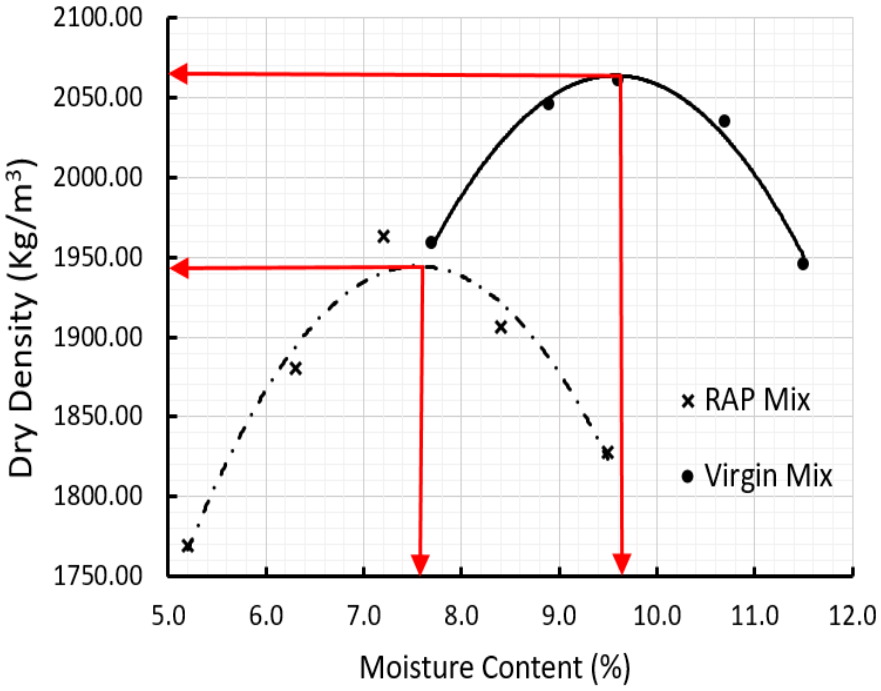

Figure 4.7: Moisture – Density relationships

4.2.6 Aggregate Pre-Mix water content

A plot of stability versus pre-mix water content illustrated that the RAP mix had a higher optimal stability of 2.81 kN at 4% pre-mix water content compared to that of the virgin mix of 2.64 kN at pre-mix water content of 2.8% (Figure 4.8). Optimal stability of RAP was 6% higher than that of the virgin mix. Higher stability in CAEMs illustrates high resistance to failure by mechanical action. This could have been contributed by the stiff nature of the binder coating the RAP aggregates that occurs by oxidation during their service life (Taher & Aman, 2016). At optimal stability, pre-mix water content of the RAP mix was 1.2 % higher than that required by the virgin mix. The presence of deleterious materials and fines agglomerated to the RAP aggregates by the aged binder could have absorbed moisture prior to coating and compaction hence the RAP mix required more pre-mix water than the virgin mix.

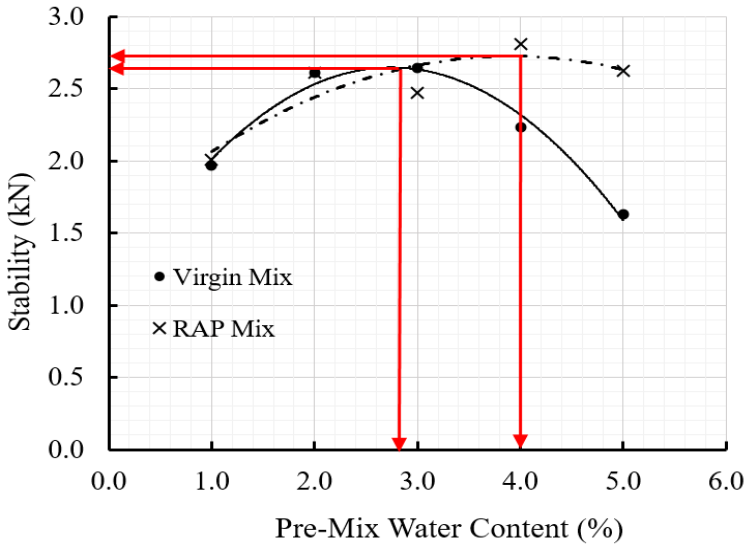

Figure 4.8: Pre-mix water content

4.2.7 Optimal Bitumen Content

At optimal bitumen contents of 5.2% and 3% for the virgin and the RAP mix respectively, the RAP aggregates improved the stability of CAEMs by 16% (Table 4.3). The RAP material is stiff as a result of in-situ aging during its service life and its recycling is recommended to reduce permanent deformation of asphalt pavements (Taher & Aman, 2016; Oluwasenyi, 2011). The RAP mix had a higher stability loss of 20.7% compared to 3% of the virgin mix. This means that the RAP mix was highly susceptible to moisture damage compared to the virgin mix. This was validated by the lower of tensile strength ratio (TSR) value of 0.79 of the RAP mix compared to 0.97 of the virgin mix. At the selected optimal bitumen content, more than 50% of the virgin and the RAP aggregates were coated (Table 4.3).

Table 4.3: Properties of selected optimal bitumen content

Mix Property	Virgin mix 5.2% OBC	RAP mix 3% OBC	Requirements MS-14 (1989)	Status
Stability – conditioned	3.52 kN	4.10 kN	2.2 kN (Minimum)	**OK**
Stability Loss (%)	3%	20.7%	50% (Maximum)	**OK**
Coating (%)	85%	60%	50% (Minimum)	**OK**
Tensile Strength Ratio	0.97	0.79	> = 0.7	**OK**

4.2.8 Optimal Compaction Properties.

The minimal air void contents of the virgin and the RAP mix were 9.2% and 12.9% respectively (Figure 4.9). Air void content of the RAP mix was higher than that of the virgin mix for the three compaction levels (Figure 4.9). This can be explained by the coarse grading of RAP aggregates caused by the agglomeration of fine aggregates in the

RAP mix by the existing aged binder (Valentin et al., 2016; Thanaya et al., 2014; Moloto, 2010).

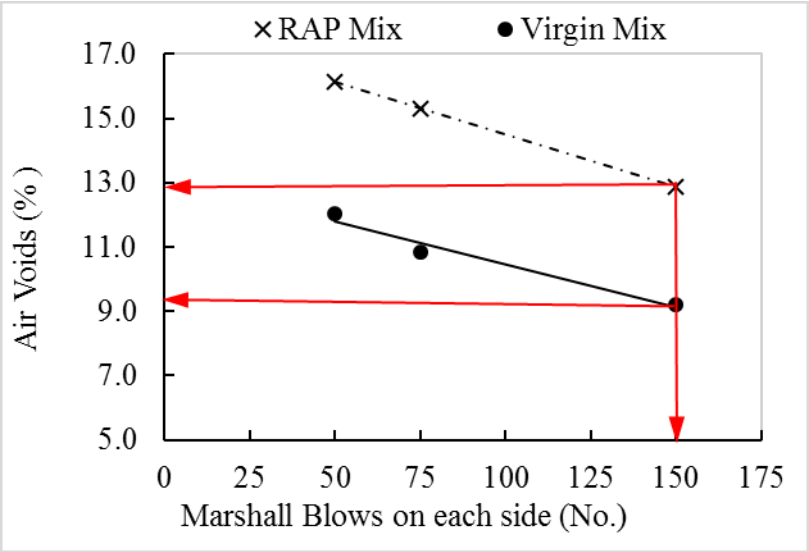

Figure 4.9: Effect of compaction on air voids in CAEMs

4.2.9 Mix Design Summary

Variables considered for mix design of CAEMs were combined aggregate grading, pre-mix water content, optimal bitumen content and number of compaction blows (Table 4.4). Combined aggregate grading of the RAP mix was improved by incorporating 50% of fine virgin aggregates of size 0/6 mm. The virgin mix design had lower pre-mix water content demand and a higher binder demand compared to the RAP mix. With respect to the targeted air void contents below 10% and 15% for the virgin and the RAP respectively, compaction level of 150 blows per face were used for both mixtures.

Table 4.4: Mix Design Summary

Mix design variables	Virgin Mix	RAP Mix
Combined Aggregate Grading	0/6 virgin – 55% - 6/10 virgin – 15% 10/14 virgin – 15% 14/20 virgin – 15%	0/6 virgin – 50% 0/6 RAP – 10% 6/10 RAP – 10% 10/14 RAP – 15% 14/20 RAP – 15%
Pre - mix water by mass of aggregate	2.8%	4.0%
OBC by mass of aggregate.	5.2%	3%
Bitumen Emulsion by mass of aggregate	8%	5%
Compaction level	150 Blows	150 Blows

Conclusions drawn from objective one include:

i. CAEMs produced from RAP aggregates have a coarser gradation compared to the virgin aggregates. However, the addition of fine virgin aggregates of size 0/6mm improved the combined aggregate grading of the RAP mix.

ii. The RAP mix required more pre-mix water content than the virgin mix. This could have been contributed by the presence of pores within the aged RAP aggregates that retained water during mixing.

iii. At optimal bitumen content, use of RAP aggregates improved the stability of CAEMs by 16%. However, RAP mix was more susceptible to moisture damage compared to the virgin mix.

iv. CAEMs produced from RAP aggregates had a higher air void content above 10% for the three compaction levels.

4.3 Effect of curing temperature and time on ITS of CAEMs.

The indirect tensile strength of CAEMs increased with moisture loss as illustrated in Figure 4.10. Virgin mix specimens cured at temperatures of 25 ℃ and 40 ℃ did not lose more than 3% moisture during the 23 days curing periods. However, RAP mix specimens cured at 40 ℃ lost more 3.5% moisture. Specimens cured at 60 ℃ experienced the highest moisture loss ranging between 2- 4% depending on the curing period (Figure 4.10).

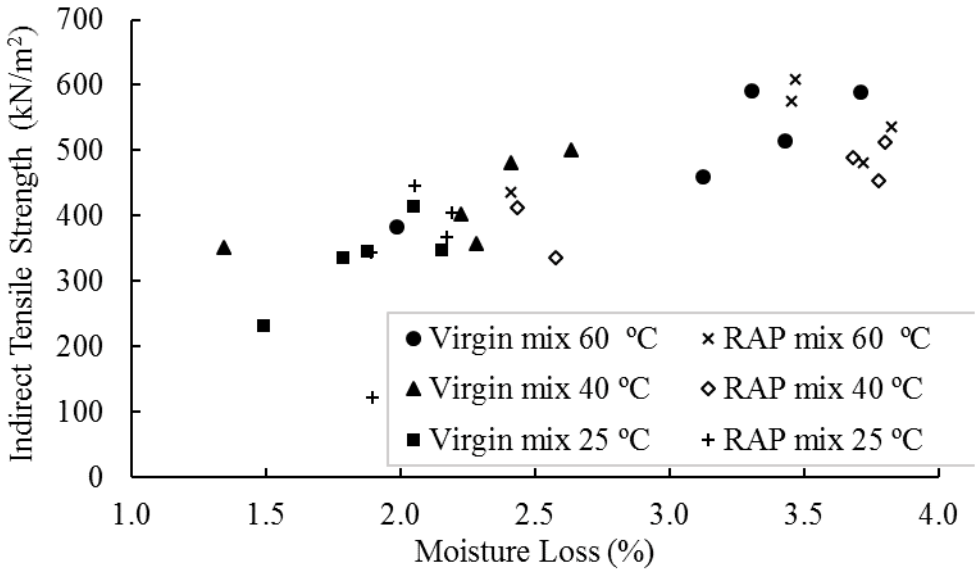

Figure 4.10: Effect of moisture loss on the strength of CAEMs

For all curing regimes, specimens cured at 25 ℃ had the lowest strength ranging between 122 - 414kN/m^2, while those cured at 60 ℃ had the highest strength ranging between 383 - 609 kN/m^2 (Figure 4.11). At high curing temperatures high amount of moisture loss was observed. Moreover, enhanced binder adhesion that increases strength in CMA could have been contributed by high curing temperatures (Thanaya et al., 2014; Kuna et al., 2016).

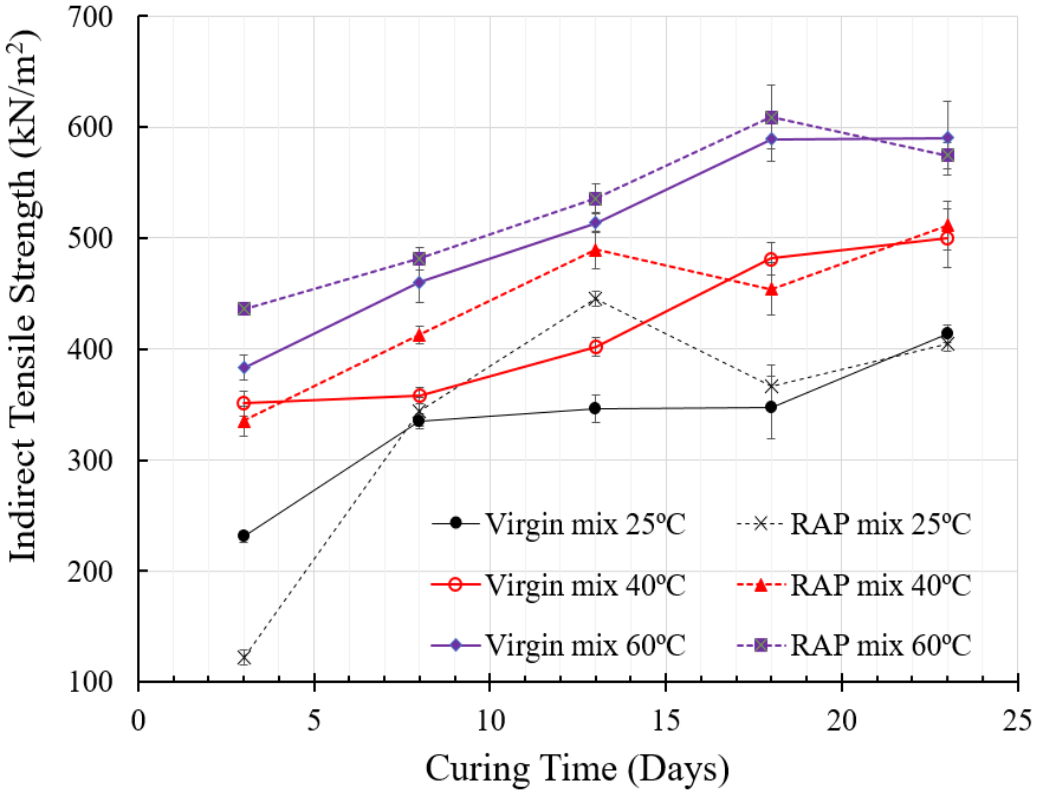

Figure 4.11: Effect of curing time and temperature on the strength of CAEMs

This study observed that at Early-age of 3 days the ITS of RAP mix cured at low temperatures of 25 ºC was 47.04% lower than that of the virgin mix. However, for all temperature regimes, the difference in ITS between the virgin and RAP mix was 3% for specimens cured for 23 days and a maximum of 6% for specimens cured for 18 days. (Figure 4.11). Virgin mix demonstrated consistent gain in tensile strength for all curing regimes while the RAP mix had consistent gain in tensile strength up to 13 days for specimen cured at 25 ℃ and 40 ℃ (Figure 4.11). At 13 days of curing, the ITS of RAP mix cured at 25 ℃ and 40 ℃ were 27% and 22% higher than those of the virgin mix. Moreover, the ITS of the RAP mix dropped at 18 days of curing followed by increase in ITS at 23 days of curing. Additional studies are required to establish the cause of this

phenomenon. After 13 days of curing, the study observed minimal difference in ITS ranging from 3-6% for specimens cured for 18 days and 23 days. With respect to the tensile strength of pavement construction, there is no difference of using virgin aggregates or recycled materials (Norouzi et al., 2014; (Oluwasenyi, 2011). Specimens cured at 60 ℃ had optimal ITS at 18 days of curing.

Specimens cured for 3 days had the lowest strength for the three curing temperatures and the strength increased gradually with increase in curing time (Figure 4.11). This was probably because loss of moisture from CAEMs is a gradual process that takes time (Graziani et al., 2017; Serfass et al., 2004).

Conclusions drawn from specific objective two were:

i. Increase in curing temperature and time increases the amount of moisture expelled from cold asphalt emulsion mixtures irrespective of the materials used.
ii. Early-age (3 days) strength of RAP mix cured at low temperatures of 25 ºC was 47.04% lower than that of the virgin mix. However, for all temperature regimes, the difference in ITS between the virgin and RAP mix was 3% for specimens cured for 23 days and a maximum of 6% specimens cured for 18 days.

4.4 Prediction of ITS of CAEMs using the Maturity method

The strength-maturity functions of cold asphalt emulsion mixtures were developed mathematically using a series of empirical formulas outlined in section 3.5.2 (Carino & Lew, 2001; Doyle et al., 2013; Kuna et al., 2016). Factors determined during the development of the strength-maturity functions are outlined below.

i. The rate constant (k)
ii. The temperature sensitivity factor (B)

iii. Maturity in terms of equivalent age (t_e)

iv. Modified maturity function

v. Strength-Maturity relationships

vi. Validation of the strength-maturity function

4.4.1 The Rate Constant

The rate constant (k) of the RAP mix increased with increase in curing temperatures while for the virgin mix, increase in temperature had minimal effect on k (Figure 4.12a). The virgin mix rate constant k varied between 0.4 and 0.6 1/day. The limiting strength (S_u) of the virgin and the RAP mix generally increased with increase in the curing temperature (Figure 4.12b). Therefore, no crossover effect was observed during the 23 days of curing of cold asphalt emulsion mixtures (Carino & Lew, 2001). Kuna et al. (2016) did not observe a crossover effect after curing cold-foamed bituminous mixtures for 296 days. Therefore, it can be concluded that cold mix asphalt concrete does not experience a crossover effect during curing.

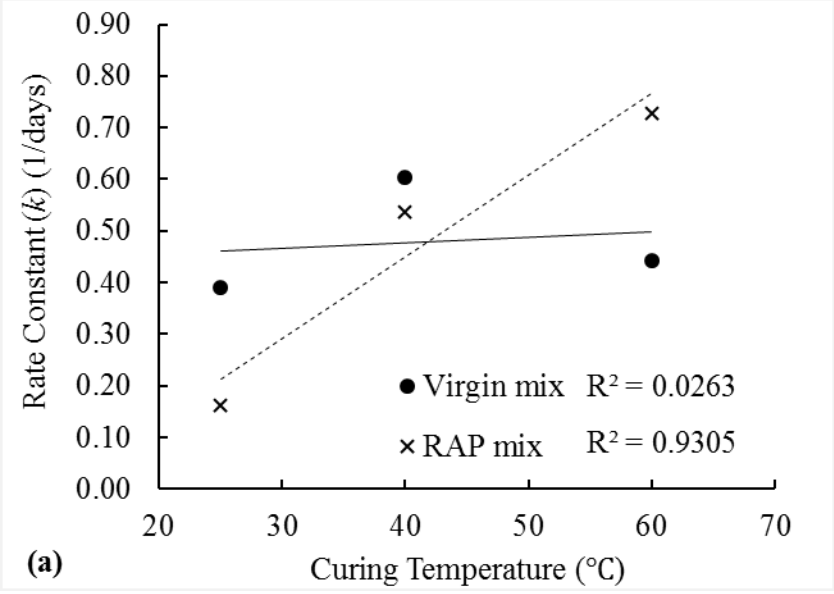

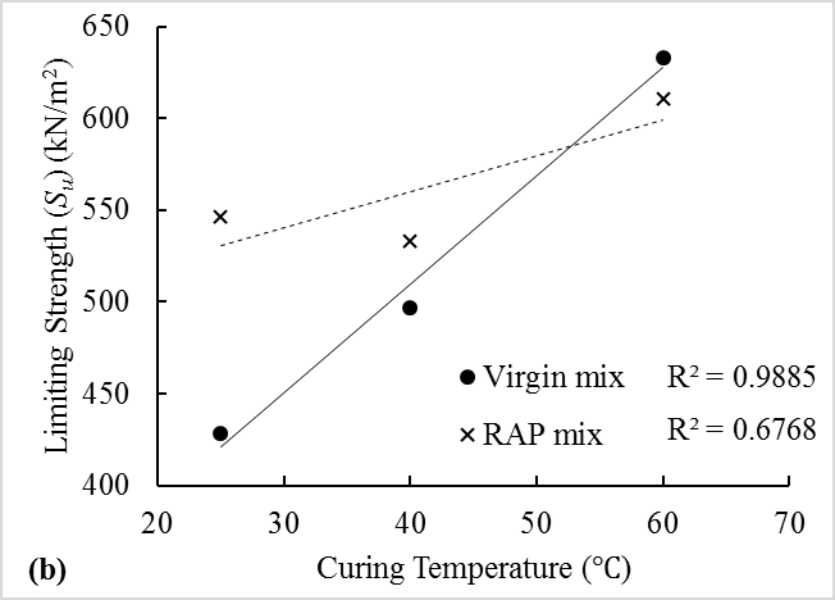

Figure 4.12: Effect of curing temperature on;(a) rate constant; (b) limiting strength

4.4.2 Temperature Sensitivity Factor

The RAP mix temperature sensitivity (*B*) was 94% higher than that of the virgin mix (Table 4.5). This was probably caused by the rejuvenation of the aged bitumen in the RAP mix (Oluwasenyi, 2011).

Table 4.5: Rate constant at 0°C (A_0) and temperature sensitivity factor (*B*)

Mix	A_o (1/day)	B	R^2
Virgin mix	0.4378	0.0021	0.9999
RAP mix	0.0931	0.0361	0.9681

4.4.3 Maturity in terms of Equivalent age

The study observed difference in ITS at the same equivalent age (t_e) (Figure 4.13). For example, at equivalent age of 13 days the ITS of the virgin mix cured at 25, 40 and 60℃ were 347 kN/m^2, 402 kN/m^2 and 514 kN/m^2 respectively, giving a ITS difference of 167 kN/m^2 (Figure 4.13a). However, at any equivalent age the difference in ITS of the RAP mix subjected to different curing regimes was lower compared to that of the virgin mix. An example is at day 17 equivalent age, RAP mix cured at 25 ℃ and 40 ℃ had ITS difference of 32kN/m^2 (Figure 4.13b). The above results disregard the maturity rule (Carino & Lew, 2001).

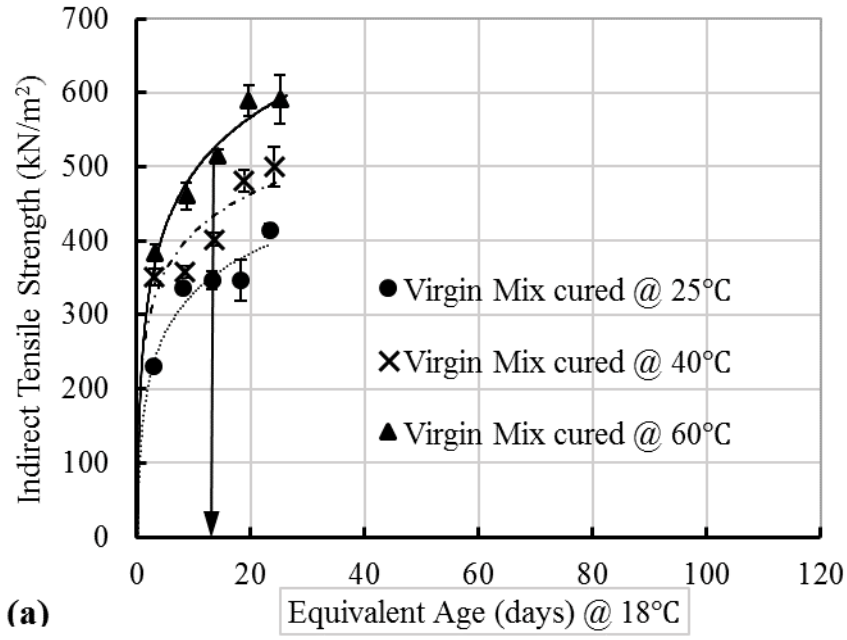

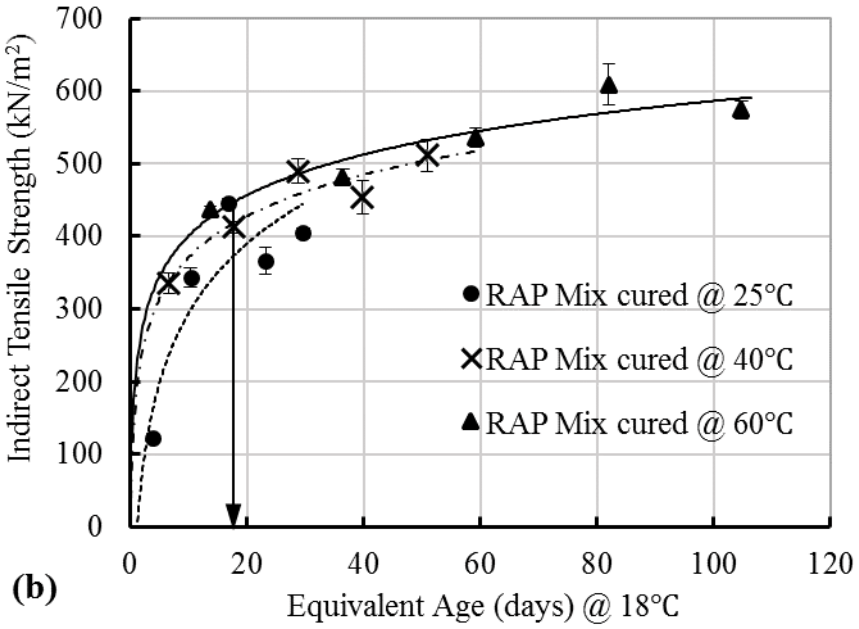

Figure 4.13: Effect of Equivalent age on ITS: (a) Virgin mix; (b) RAP mix

4.4.4 Modified Arrhenius Maturity

A plot of indirect tensile strength against maturity shows that, the indirect tensile strength CAEMs specimens subjected to different curing regimes was the same at the same maturity (Figure 4.14).

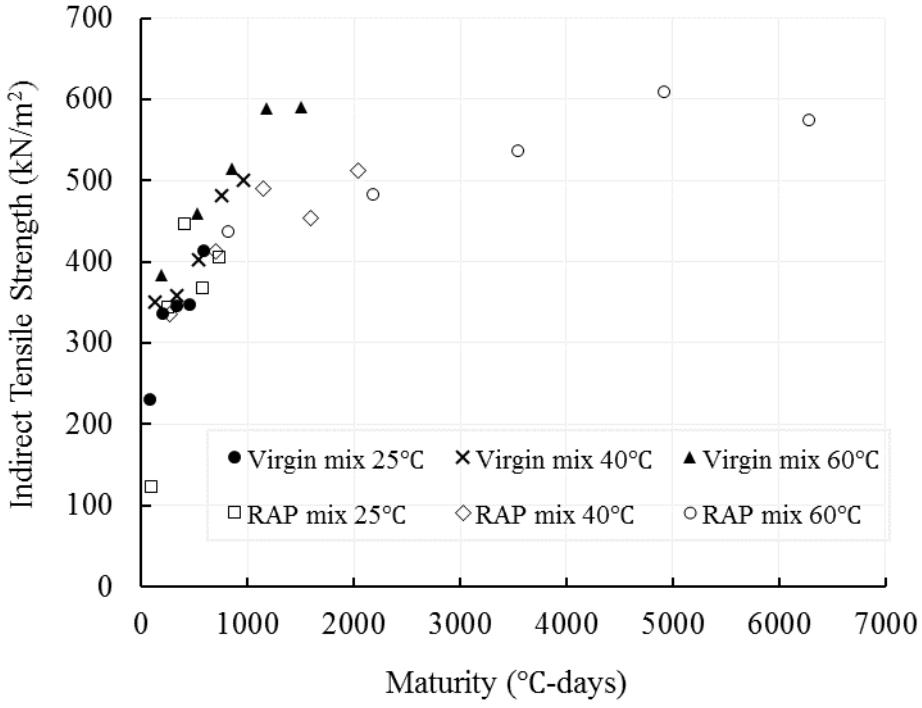

Figure 4.14: Effect of Maturity on indirect tensile strength

Maturity beyond 3000°C-days was only observed for RAP specimens cured at 60 °C. The temperature sensitivity factor of the RAP mix was found to be higher than that of the virgin mix (section 4.4.2, Table 4.5). High maturity of the RAP mix could have been contributed by combined effect of high curing temperatures of 60 °C and high RAP material temperature sensitivity factor.

4.4.5 Strength-Maturity Relationships

The linear-hyperbolic function (Equation 3.10) predicted limiting strengths (S_u) of the virgin mix (576.10 kN/m^2) and the RAP mix (558.63 kN/m^2) within the observed tensile strength range of 231-591 kN/m^2 for the virgin and 122-609 kN/m^2 for the RAP mix respectively. However, the limiting strengths (S_u) of the virgin mix (990.73 kN/m^2) and

the RAP mix (763.04 kN/m^2) predicted by the parabolic-hyperbolic function (Equation 3.11) were beyond the observed tensile strength range (Table 4.6, Appendix 14).

Table 4.6: Rate constant and limiting strength of strength-maturity functions

Function	Virgin Mix		RAP Mix	
	k	***S_u***	***k***	***S_u***
Measured ITS (kN/m^2)		231-591		122-609
Linear-hyperbolic function	0.0070	576.10	0.0043	558.63
Parabolic-hyperbolic function	0.0012	990.73	0.0019	763.04

Therefore, the linear-hyperbolic function was used to develop two strength-maturity functions for the virgin mix (Equations 4.1) and the RAP mix (Equation) 4.2.

$$S = 576.10 * \left(\frac{0.007M}{1+0.007M}\right) \quad (4.1)$$

$$S = 558.63 * \left(\frac{0.0043M}{1+0.0043M}\right) \quad (4.2)$$

Strength-maturity functions in Equations 4.1 and 4.2 are specific to the mix design parameters. The rate constant (k) which was developed using specimens subjected to different curing regimes illustrates the rate of strength gain for a particular mix. Limiting strength (S_u) is the asymptotic value of the tensile strength for the hyperbolic function that fits the data. Tensile strength (S) of specimens subjected to different curing regimes can be determined by incorporating Maturity (M) calculated as a function of curing time and temperature in Equations 4.1 and 4.2. Therefore, strength-maturity functions can be able to predict the tensile strength of CAEMs provided accurate curing time and temperatures are provided.

4.4.6 Validation of strength-maturity functions

The linear-hyperbolic strength-maturity functions predicted the actual strength of cold asphalt emulsion mixtures accurately and achieved an R^2 value of 99% for the virgin mix and an R^2 value of 95% for the RAP mix (Figure 4.15). This suggests that the Maturity method can be confidently used to predict the tensile strength of cold mix asphalt pavements.

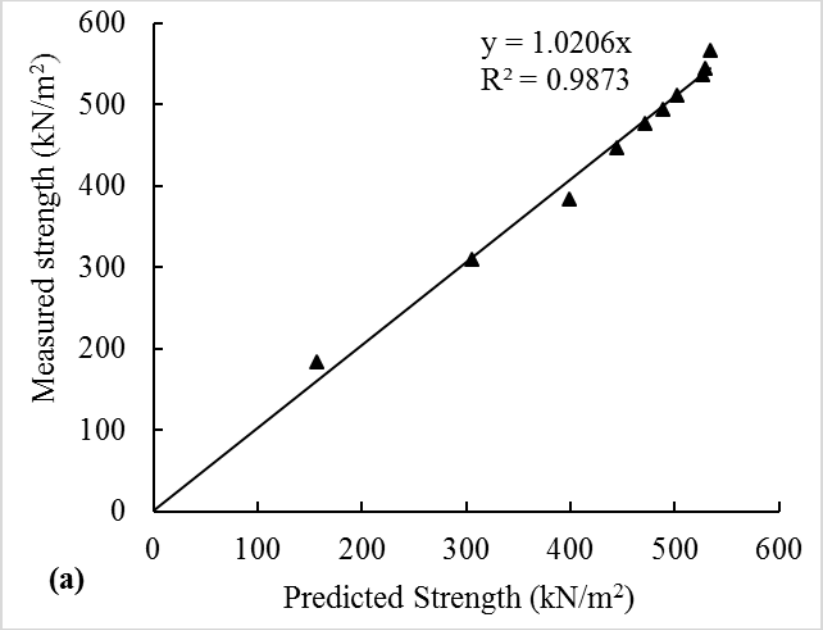

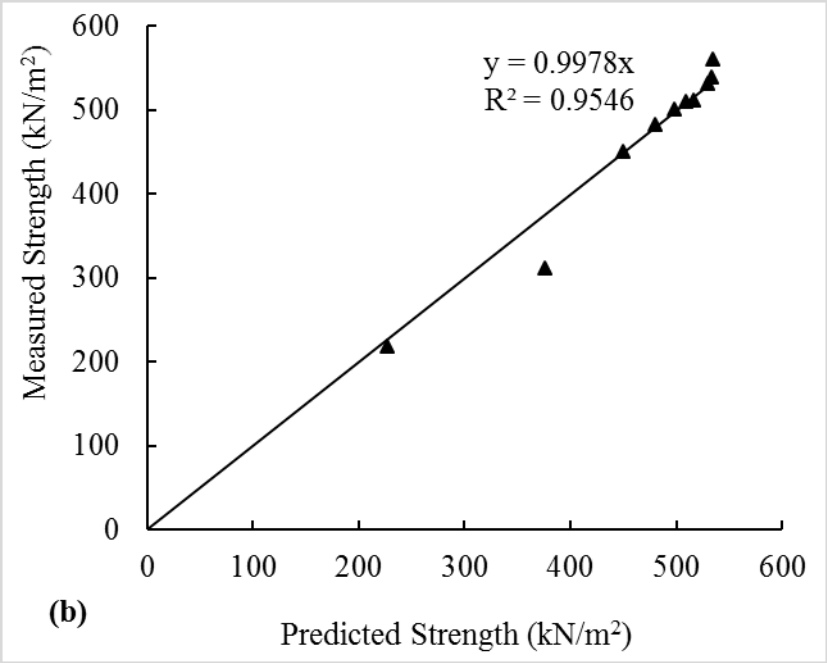

Figure 4.15: Validation of strength-maturity functions: (a) virgin mix; (b) RAP mix

Conclusions drawn from specific objective three were:

i. The temperature sensitivity factor (*B*) of the RAP mix was 94% higher than that of the virgin mix. This probably explains why maturity beyond 3000°C-days was only observed for RAP specimens cured at 60°C.
ii. Maturity of CAEMs as a function of Equivalent age and curing temperature simulated similar indirect tensile strength of CAEMs subjected under different curing regimes.
iii. Linear-Hyperbolic strength-maturity function predicts the strength of CAEMs composed of a cationic bitumen emulsion and siliceous aggregates with an accuracy of 99% for the virgin mix and 95% for the RAP mix.

CHAPTER FIVE

SUMMARY, CONCLUSIONS AND RECOMMENDATIONS

5.1 Summary

The main objective of this study was to predict the strength of cold asphalt emulsion mixtures using the Maturity method. Two mix designs were developed using the virgin and the RAP aggregates respectively. The effect of moisture loss, curing time and temperature on indirect tensile strength of cold asphalt emulsion mixtures was analyzed. Linear-hyperbolic strength-maturity functions predicted the indirect tensile strength of CAEMs with an accuracy of more than 95%. Use Maturity method as a performance-based tool for gradual strength prediction in cold mix asphalt during construction is recommended for effective project management: like determination of the earliest time to overlay a CMA pavement layer with a wearing course or open a CMA pavement layer to traffic. The study concludes as follows:

5.2 Conclusions

5.2.1 Conclusions for objective one

1. CAEMs produced from RAP aggregates have a coarser gradation compared to the virgin aggregates. However, the addition of fine virgin aggregates of size 0/6mm improved the combined aggregate grading of the RAP mix.
2. The RAP mix required more pre-mix water content than the virgin mix. This could have been contributed by the presence of pores within the aged RAP aggregates that retained water during mixing.

3. At optimal bitumen content, use of RAP aggregates improved the stability of CAEMs by 16%. However, RAP mix was more susceptible to moisture damage compared to the virgin mix.
4. CAEMs produced from RAP aggregates had a higher air void content above 10% for the three compaction level.

5.2.2 Conclusions for objective two

1. Increase in curing temperature and time increases the amount of moisture expelled from cold asphalt emulsion mixtures irrespective of the materials used.
2. At early-age of 3 days the ITS of RAP mix cured at low temperatures of 25ºC was 47.04% lower than that of the virgin mix. However for all temperature regimes, the difference in ITS between the virgin and RAP mix was 3% for specimens cured for 23 days and a maximum of 6% specimens cured for 18 days.

5.2.3 Conclusions for objective three

1. The temperature sensitivity factor (B) of the RAP mix was 94% higher than that of the virgin mix. This probably explains why maturity beyond 3000℃-days was only observed for RAP specimens cured at 60 ℃.
2. Maturity of CAEMs as a function of Equivalent age and curing temperature simulated similar ITS of CAEMs subjected under different curing regimes.
3. Linear-Hyperbolic Strength-Maturity functions predicts the strength of CAEMs composed of a cationic bitumen emulsion and siliceous aggregates with an accuracy of 99% for the virgin mix and 95% for the RAP mix. With accurate curing time and temperature data, strength-maturity functions can predict actual tensile strength in CAEMs pavement layers under in situ conditions.

5.3 Recommendations

5.3.1 Recommendations for use

1. For consistency indirect tensile strength of CAEMs subjected under isothermal curing temperatures of 25 ℃ and 40 ℃ virgin and RAP mix should be cured for at least 23 days. However, CAEMs cured at 60 ℃ have optimal indirect tensile strength after 18 days of curing.
2. Gradual gain of tensile strength of CMA during construction can be monitored using the Maturity method provided accurate curing time and temperatures are recorded. This study recommends the use of the Maturity method during design to predict the performance (tensile strength) of CAEMs and monitor curing during construction.

5.3.2 Recommendations for future studies

1. For all curing regimes, virgin mix demonstrated consistent gain in indirect tensile strength. However, the RAP mix had a consistent drop in ITS at day 18 for specimens cured at 25℃ and 40℃ followed by a rise in ITS at day 23 of curing. Additional studies are required to establish the cause of this phenomenon.

Maturity beyond 3000℃-days was only observed for RAP specimens cured at 60℃. This study suggests that this phenomenon could be contributed by high rate constant and temperature sensitivity factor observed for RAP mix cured at 60℃. Additional studies are required to establish the cause of this phenomenon.

REFERENCES

Acott, S. M. (1979). Sand stabilization using foamed bitumen. *3rd Conference on Asphalt Pavements for South Africa*. Durban.

Al-Hdabi, A. (2014). *High strength cold rolled asphalt surface course mixtures*. (Unpublished Doctoral Dissertation). Liverpool John Moores University.

Aragão, F. T. S., Kim, Y., Lee, J., & Allen, D. H. (2011). Micromechanical Model for Heterogeneous Asphalt Concrete Mixtures Subjected to Fracture Failure. *Journal of Materials in Civil Engineering, 23*, 30–38.

Arimilli, S., Jain, P. K., & Nagabhushana, M. N. (2016). optimization of Recycled Asphalt Pavement in Cold Emulsified Mixtures by Mechanistic Characterization. *Journal of Materials in Civil Engineering, 28*(2), 1–10.

Asphalt Institute. (1989). *Asphalt Cold Mix Manual* (3rd edition*)*. Lexington KY 40512–4052 USA: Asphalt Institute.

Asphalt Institute. (2008). *Basic Asphalt Emulsion Manual* (2nd edition). Lexington KY 40512–4052 USA: Asphalt Institute.

Asphalt Academy. (2009). *Technical Guideline 2 : Bitumen Stabilised Materials* (TG2-2009). Petroria, South Africa: Asphalt Academy.

ASTM (American Society for Testing and Materials). (2013). Standard Guide for Elemental Analysis by Wavelength Dispersive X-Ray Fluorescence Spectrometry (ASTM E1621-13). *ASTM International, West Conshohocken*, PA, 2013, www.astm.org

ASTM (American Society for Testing and Materials). (2010). *Standard practice for preparation of bituminous specimens using Marshall Apparatus* (ASTM-D6926-10). ASTM International.

ASTM (American Society for Testing and Materials). (2011). *Standard Practice for Estimating Concrete Strength by the Maturity Method* (ASTM- C1074-11), ASTM International. https://doi.org/https://doi.org/10.1520/C1074-11.2

ASTM (American Society for Testing and Materials). (2012). *Standard Test Method for Indirect Tensile (IDT) Strength of Asphalt Mixtures* (ASTM-D6931-12), ASTM International.

ASTM (American Society for Testing and Materials). (2014). *Standard Test Methods for Specific Gravity of Soil Solids by Water Pycnometer* (ASTM-D854-14), ASTM International.

Bessa, I. S., Almeida, L. R., Vasconcelos, K. L., & Bernucci, L. L. B. (2016). Design of cold recycled mixes with asphalt emulsion and portland cement. *Canadian Journal of Civil Engineering, 43*(9), 773–782. https://doi.org/10.1139/cjce-2016-0111

Bouramia, M., B., and Qiu, Y. (2017). Investigation of influential factors on the tensile strength of cold recycled mixture with bitumen emulsion due to moisture conditioning. *Journal of traffic and transport engineering (English edition),* 4(2), 198-201. doi: http://creativecommons.org/licenses/by-nc-nd/4.0/

Bouteiller, E. (2010). Asphalt Emulsion For Sustainable Pavements. *First International Conference on Pavement Preservation.* NewPort Beach, California, USA

British Standards Institution. (1990). *Methods of test for soils for civil engineering purposes - Compaction-related tests* (BSI. BS 1377-4:1990). British Standards.

British Standards Institution. (1985). Test*ing Aggregates - Aggregate physical tests* (BS 812:112:1985). British Standards.

British Standards Institution. (1990). *Methods for Determination of Aggregate Crushing Value (ACV)* (BS812:110:1990). British Standards.

British Standards Institution. (1998). *Testing aggregates-Part 105: Methods for determination of particle shape - Flakiness index* (BS 812:105-1:1998). BSI.

British Standards Institution. (1995). *Testing aggregates. Methods for determination of density* (BS 812-2:1995). British Standards.

British Standards institution. (2007*). Bitumen and bituminous binders- Determination of needle penetration* (BS 2000:49:2007). British Standards.

British Standards institution. (2007). *Bitumen and bituminous binders: Determination of the softening point. Ring and Ball method* (BS EN 1427:2007). British Standards.

British Standards Institution. (2010). *Tests for mechanical and physical properties of aggregates. Methods for the determination of resistance to fragmentation* (BS EN 1097-2:2010). British Standards. Doi: https://doi.org/10.1016/j.ccr.2011.01.056

British Standards Institution. (2012). *Bituminous mixtures - Test methods for hot mix asphalt. Soluble binder content.* (BS EN 12697-1: 2012). British Standards. Doi: https://doi.org/10.3141/2127-15

British Standards Institution. (2013). *Bituminous mixtures. Test methods for hot mix asphalt. Bitumen recovery: Rotary evaporator* (BS EN 12697-3:2013). British Standards

Brown, S., & Needhem, D. (2000). A study of cement modified bitumen emulsion mixtures. Proceedings of the annual meeting of the Association of Asphalt Paving Technologist, AAPT. (1-22).

Buertey, J., I., T., Atsrim, F., Offei, S., W. (2016). An Examination of the Physio-mechanical Properties of Rock Lump and Aggregates in Three Leading Quarry Sites Near Accra. *American Journal of Civil Engineering.* 4 (6), 264-275. doi: 10.11648/j.ajce.20160406.1

Bullen, F., John, B., Lancaster, J., Maccarrone, S., Mungan, D., & Rebbechi, J. (1997). *Cold Mixed Granular Materials Guide*. (AAPA Implementation Guide G-2). Australian Asphalt Pavement Association.

Carino, N. J. (1984). The Maturity Method: Theory and Application. Cement, *Concrete and Aggregates, 6*(2), 61–73. Retrieved from https://doi.org/10.1520/CCA10358J

Carino, N. J., & Lew, H. S. (2001). *The Maturity Method: From Theory to Application*. *Structures 2001*, (pp. 1–19). Reston, VA: American Society of Civil Engineers. https://doi.org/10.1061/40558(2001)17

Carino, N. J., & Tank, R. C. (1992). Maturity functions for concrete made with various cements and admixtures. *American Concrete Institute (ACI), 89*(2), 188–196.

Chelelgo, K., Gariy, Z., C., A., & Shitote, S., M. (2019). Modeling of Fatigue-Strength Development in Cold-Emulsion Asphalt Mixtures Using Maturity Method. *Molecular Diversity Preservation International and Multidisciplinary Digital Publishing Institute (MDPI). Appl. Sci. 9*(13), 2694; https://doi.org/10.3390/app9132694

D'Angelo, J., Harm, E., Bartoszek, J., Baumgardner, G., Corrigan, M., Cowsert, J., … Yeaton, B. (2008). Warm-Mix Asphalt : European Practice. *International technology Scanning Program*. http://international.fhwa.dot.gov/pubs/pl08007/pl08007.pdf

Dash, S. S. (2013). *Effect of Mix Parameters on Performance and Design of Cold Mix Asphalt* (Unpblished Masters dissertation). National Institute of Technology.

Doyle, T. A., Gibney, A., McNally, C., & Tabakovic, A. (2010). Development of maturity methods for predicting performance of cold-mix pavement materials. *Proceedings of 9th international conference, sustainable construction materials and technology in asphalt pavement engineering and maintenance*. Liverpool.

Doyle, T. A., McNally, C., Gibney, A., & Tabaković, A. (2013). Developing maturity methods for the assessment of cold-mix bituminous materials. *Construction and Building Materials, 38,* 524–529.

Du, S. (2015). Performance Characteristic of Cold Recycled Mixture with Asphalt Emulsion and Chemical Additives. *Advances in Materials Science and Engineering, 2015*. https://doi.org/10.1155/2015/271596

Graziani, A., Godenzoni, C., Cardone, F., & Bocci, M. (2016). Effect of curing on the physical and mechanical properties of cold-recycled bituminous mixtures. *Materials and Design, 95,* 358–369. https://doi.org/10.1016/j.matdes.2016.01.094

Graziani, A., Godenzoni, C., Cardone, F., Bocci, E., & Bocci, M. (2017). An application of the Michaelis–Menten model to analyze the curing process of cold recycled bituminous mixtures. *International Journal of Pavement Research and Technology, 10*(1), 62–74. https://doi.org/10.1016/j.ijprt.2016.09.002

Federal Highway Administration (FHWA). (2010) *A review of aggregate and asphalt mixture specific gravity measurements and their impacts on asphalt mix design properties and mix acceptance* (FWHA-HIF-11-033). Pavement Technology.

Hansen, P., & Pedersen, J. (1977). Maturity Computer for Controlled Curing and Hardening of Concrete. *Nordisk Beton,* 19–34.

https://doi.org/doi:10.1061/40558(2001)17

Kim, Y., Lee, H. D., & Heitzman, M. (2007). Validation of new mix design procedure for cold-in-place recycling with foamed asphalt. *Journal of Materials in Civil Engineering, 19*(11), 1000–1010.

Kim, Y., Im, S., & Lee, H. (2011). Impacts of Curing Time and Moisture Content on Engineering Properties of Cold In-Place Recycling Mixtures Using Foamed or Emulsified Asphalt. *Journal of Materials in Civil Engineering, 23*(5), 542–554. https://doi.org/10.1061/(ASCE)MT.1943-5533.0000209

Kishore, K. C., Amar, K. D., Amarantha, R. M., & Sudhakar, R. K. (2008). Investigation of cold in place recycled mixes in india. *International Journal Pavement Engineering, 9*(4), 265–274.

Knudsen, T. (1984). The dispersion model for hydration of portland cement I. General concepts. *Cement and Concrete Research, 14*(5), 622–630. https://doi.org/https://doi.org/10.1016/0008-8846(84)90024-3

Kuna, K. (2015). *Mix design considerations and performance characteristics of foamed bitumen mixtures (FBMs)* (Published Doctorial Dessertation). University of Nottingham. United Kingdom.

Kuna, K., Airey, G., & Thom, N. (2016). Development of a tool to assess in-situ curing of Foamed Bitumen Mixtures. *Construction and Building Materials, 124*, 55–68. https://doi.org/10.1016/j.conbuildmat.2016.07.086

Kwon, O. (2013). *Application of the Maturity Method for the Prediction of Early Strength of concrete under various curing conditions* (Unpublished doctorial dissertation). University of Florida

Lee, D. Y. (1981). Treating marginal aggregates and soil with foamed asphalt. *Proceedings of the Association of Asphalt Paving Technologists 50*, 211–150.

Ma, T., Wang, H., Zhao, Y., Huang, X., & Pi, Y. (2015). Strength Mechanism and Influence Factors for Cold Recycled Asphalt Mixture. *Advances in Materials Science and Engineering, 2015*, 1-10. https://doi.org/10.1155/2015/181853

Maccarone, S., Holleran, G., & Ky, A. (1995). Cold Asphalt System as an Alternative to Hot Mix. *9th conference proceeding of AAPA International Asphalt Conference*.

McIntosh, J. (1949). Electric Curing of Concrete. *Magazine of Concrete Research, 1*(1), 21–28. Retrieved from https://doi.org/10.1680/macr.1959.1.1.21

Meyer, M. D. (1999). Bitumen emulsion. *Akzonobel Surface Chemistry* (p. 31). https://sc.akzonobel.com/en/asphalt/Documents/AN_Asphalt_Emulsion_TB_eng.df

Ministry of Roads and Public Works. (1986). *Standard Specifications for Road and Bridge Construction* (Road Note 31). Kenya.

Ministry of Transport & Communication. (1987). *Road Design Manual Part III: Materials and Pavement Design for New Roads*. MoTC, Nairobi, Kenya.

Moghadam, B. B., & Farhad, M. M. (2017). Suggesting a simple design method for cold recycled asphalt mixes with asphalt emulsion. *Journal of Civil Engineering and Management, 23*(7), 966–976. https://doi.org/10.3846/13923730.2017.1343200

Moloto, K. P. (2010). *Accelerated curing protocol for bitumen stabilized materials* (Masters Dessertation). Stellenbosch University.

Moreno-Pérez, E., Hernández-Ávila, J., Rangel-Martínez, Y., Cerecedo-Sáenz, E., Arenas-Flores, A., Reyes-Valderrama, M., I., & Salinas-Rodríguez, E. (2018). Chemical and Mineralogical Characterization of Recycled Aggregates from Construction and Demolition Waste from Mexico City. *Molecular Diversity Preservation International and Multidisciplinary Digital Publishing Institute (MDPI).* 8(6), 237; https://doi.org/10.3390/min8060237

National Roads Authority. (2011). *Low Energy Pavements* (Interim Advice Note 01/1). Dublin.

Needham, D. (1996). *Developments in bitumen emulsion mixtures for roads* (Unpublished Doctorial Dessertation). University of Nottingham.

Nixon, J. M., Schindler, A. K., Barnes, R. W., & Wade, S. A. (2008). Evaluation of the maturity method to estimate concrete strength in field applications. *ALDOT Research Project*, 930-950.

Norouzi, A., Sabouri, M., & Kim, Y. R. (2014). Evaluation of the fatigue performance of high RAP asphalt mixtures. *Proceedings of 12th International Society for Asphalt Pavements, Raleigh, NC, 3,* 1–17.

Nurse, R. W. (1949). Steam Curing of Concrete. *Magazine of Concrete Research, 1*(2), 79–88. https://doi.org/10.1680/macr.1949.1.2.79

O'Flaherty, C. A. (2002). Highways the location design construction and maintenance of road pavements. *Elsevier, 4,* 553.

https://books.google.co.uk/books/about/Highways.html?id=Ren4sWQ3jKkC&pgis=1

Ogunbayo, B., F., Ajao, A., M., Ogundipe, K., E., Joshua, O., Durotoye T., O. & Bamigboye, G., O. (2018) Study of aggregate dormancy and its effects on the properties of aggregates and concrete, Cogent Engineering, 5:1,

doi: 10.1080/23311916.2018.1519944

Ojum, C., Kuna, K., Thom, N. H., & Airey, G. (2014). An investigation into the effects of accelerated curing on Cold Recycled Bituminous Mixes. *Asphalt Pavements - Proceedings of the International Conference on Asphalt Pavements, ISAP 2014, 2,* 1177–1188.

Oluwasenyi, O. O. (2011). *A study on the development of guidelines for the production of bitumen emulsion stabilised RAPs for roads in the tropics* (Unpublished doctorial dissertation).The University of Nottingham. United Kingdom.

Pekala, A. (2015). The influence of siliceous mineral phases on the mechanical properties of transitional rocks in the belchatow lignite deposit. *Archives of Civil Engineering, LXI(4).* Doi: 10.1515/ace-2015-0035

Plotnikova, I. A. (1993). Control of the Interaction process between bitumen emulsions and mineral aggregates by means of physico-chemical modification of their surfaces. *1st World congress on emulsion* (p. 9). Paris: CME.

Read, J., & Whiteoak, D. (2003). *The Shell Bitumen Handbook*. Shell Bitumen , UK, Chertsey.

Ruckel, P. J., Acott, S. M., & Bowering, R. H. (1983). Foamed - asphalt paving mixture: Preparation of Design mixes and treatment of test specimens. *Transportation Research Record, (911)*, 88–95.

Salama, A. E. (2008). The Use of Maturity Method in Estimating Early Concrete Strength. *International Conference on Durability of Building Materials and Components ISTANBUL*, 11, Turkey.

Saul, A. G. (1951). Principles Underlying of The Steam Curing of Concrete at Atmospheric pressure. *Magazine of Concrete Research, 2*(6), 127–140. Retrieved from https://doi.org/10.1680/macr.1951.2.6.127.

Serfass, J. P., Poirier, J. E., Henrat, J. P., & Carbonneau, X. (2004). Influence of curing on cold mix mechanical performance. *Materials and Structures, 37*(269), 365–368. https://doi.org/10.1617/14130

Serfass, J. P. (2012). Emulsified Asphalt Mixes: Proposed Mix Design Method and Performance Based Specifications. *Proceedings of the International Symposium on Asphalt Emulsion Technology.* Virginia.

Sterling, A. B., & Zamhari, K. A. (1997). Designing asphalt mixes to last. *3rd Annual Bitumen Conference*. Singapore: Transport Research Laboratory.

Taher, M. N. M., & Aman, M. Y. (2016). An overview of reclaimed asphalt pavement (RAP) materials in Warm Mix Asphalt using foaming technology. *ARPN Journal of Engineering and Applied Sciences, 11*(16), 9874–9881.

Tebaldi, G., Dave, E. V., Marsac, P., Muraya, P., Hugener, M., Pasetto, M., … Canestrari, F. (2014). Synthesis of standards and procedures for specimen preparation and in-field evaluation of cold-recycled asphalt mixtures. *Road*

Materials and Pavement Design, 15(2), 272–299. https://doi.org/10.1080/14680629.2013.8667o7

Thanaya, N. A. (2007). Review and Recommendation of Cold Asphalt Emulsion Mixtures Caems. Design. *Civil Engineering Dimension, 9*(1), 49–56. Retrieved from http://puslit2.petra.ac.id/ejournal/index.php/civ/article/view/16590

Thanaya, I. N. A., Zoorob, S. E., & Forth, J. P. (2009). A laboratory study on cold-mix, cold-lay emulsion mixtures. *Proceedings of the Institution of Civil Engineers - Transport, 162*(1), 47–55. https://doi.org/10.1680/tran.2009.162.1.47

Thanaya, N. A., Negara, I. N. W., & Suarjana, I. P. (2014). Properties of Cold Asphalt Emulsion Mixtures (CAEMs) using materials from old road pavement milling. *Procedia Engineering, 95*(Scescm), 479–488.

https://doi.org/10.1016/j.proeng.2014.12.208

Transportation Research Board (TRB). (2006). *Asphalt emulsion technology: Characteristics of Bituminous Materials.* (Transportation Research Circular - E-C102)*,* Washington D.C, (pp. 1–24). http://onlinepubs.trb.org/onlinepubs/circulars/ec102.pdf

Transport Research Laboratory. (2002). *A guide to the design of hot mix asphalt in tropical and sub-tropical countries* (Overseas Road Note 19) (p. 94).

Valentin, J., Čížková, Z., Suda, J., Batista, F., Mollenhauer, K., & Simnofske, D. (2016). Stiffness Characterization of Cold Recycled Mixtures. *Transportation Research Procedia,* 14 (2016), 758–767. Elsevier B.V. https://doi.org/10.1016/j.trpro.2016.05.065

West, R., Dukatz, E., Haddock, J., Hall, K., Kliever, J., Marek, C., … Regimand, A. (2010). *A review of aggregate and asphalt mixture specific gravity measurements and their impacts on asphalt mix design properties and mix acceptance* (TechBrief FHWA-HIF-11-033).

Wilde, W. J. (2013). Development of a Concrete Maturity Test Protocol. *Center for Transportation Research and Implementation.* Minnesota State University, Mankato

You, Z., Goh, S. W., & Qingli, D. (2011). *Laboratory Evaluation of Warm Mix Asphalt* (Technical Report, 108). Michigan Technological University.

Zaumanis, M., Poulikakos, L. D., & Partl, M. N. (2018). Performance-based design of asphalt mixtures and review of key parameters. *Materials and Design, 141,* 185–201. https://doi.org/10.1016/j.matdes.2017.12.035

Zhang, S., Pei, J., Li, R., Zhou, J., & Hu, D. (2019). Effect of Coarse Aggregate Composition on Physical and Mechanical Properties. Journal of Materials in Civil Engineering, 31(10), https:// ascelibrary.org/doi/pdf/10.1061/(ASCE)MT.1943-5533.0002886

APPENDICES

Appendix I: Aggregates Physical Properties

Properties: BS 812 Part 112: 1985	0/6mm		6/10mm		10/14mm		14/20mm	
	VA	RAP	VA	RAP	VA	RAP	VA	RAP
Bulk specific gravity (kg/m^3)	2.18	2.31	2.47	2.33	2.64	2.51	2.67	2.55
Apparent specific gravity (kg/m^3)	3.03	2.55	2.73	2.56	2.64	2.51	2.67	2.55
Bulk saturated gravity (kg/m^3)	2.88	2.49	2.62	2.46	2.52	2.46	2.60	2.49
Water absorption	2.65	2.31	2.42	1.9	1.69	1.25	1.66	1.44

Appendix II: Aggregates Mechanical Properties

Properties	Aggregates	0/6mm	6/10 mm	10/14 mm	14/20 mm	KRDM (Part 3) (MoTC, 1987)
Aggregate crushing value (%)	VA	14.7				Maximum = 25
	RAP	13.9				
Flakiness Index (%)	VA	-	12.8	14.3	13.4	Maximum = 20
	RAP	-	13.7	15.6	14.84	
Value (LAA)%	VA	18.0				Maximum = 30
	RAP	15.91				

Appendix III: Virgin aggregates mineralogical components

00297-GeoChem.pdz	AssayTime: 20/12/2018 10:18:12	ElapsedTime: 25
Alloy 1:	Match No:	

Field Info			
LAB NO.	Virgin aggregate	SENDER`S NAME	

Element Name	Min	%	Max	+/- [*3]
MgO	0	2.699	0	2.435
Al2O3	0	19.374	0	0.691
SiO2	0	66.488	0	0.763
P2O5	0	0.068	0	0.050
S	0	0.000	0	0.023
Cl	0	0.052	0	0.018
K2O	0	4.999	0	0.049
CaO	0	1.768	0	0.030
Ti	0	0.625	0	0.012
V	0	0.000	0	0.005
Cr	0	0.000	0	0.003
Mn	0	0.226	0	0.015
Fe	0	3.519	0	0.042
Co	0	0.000	0	0.005
Ni	0	0.002	0	0.003
Cu	0	0.000	0	0.001
Zn	0	0.021	0	0.002
As	0	0.000	0	0.001
Se	0	0.000	0	0.001
Rb	0	0.016	0	0.002
Sr	0	0.000	0	0.001
Y	0	0.011	0	0.002
Zr	0	0.093	0	0.002
Nb	0	0.031	0	0.002
Mo	0	0.003	0	0.002
Rh	0	0.000	0	0.003
Ag	0	0.000	0	0.003

Appendix IV: RAP aggregates mineralogical components

00300-GeoChem.pdz	AssayTime: 20/12/2018 10:25:18	ElapsedTime: 25
Alloy 1:	Match No:	

Field Info			
LAB NO.	RAP aggregate	SENDER`S NAME	

Element Name	Min	%	Max	+/- [*3]
MgO	0	2.196	0	3.403
Al2O3	0	21.595	0	0.819
SiO2	0	64.741	0	0.870
P2O5	0	0.037	0	0.055
S	0	0.000	0	0.023
Cl	0	0.000	0	0.022
K2O	0	5.345	0	0.058
CaO	0	1.667	0	0.032
Ti	0	0.527	0	0.012
V	0	0.000	0	0.004
Cr	0	0.000	0	0.003
Mn	0	0.183	0	0.016
Fe	0	3.537	0	0.048
Co	0	0.000	0	0.004
Ni	0	0.006	0	0.003
Cu	0	0.001	0	0.001
Zn	0	0.018	0	0.002
As	0	0.000	0	0.001
Se	0	0.000	0	0.001
Rb	0	0.019	0	0.002
Sr	0	0.007	0	0.001
Y	0	0.009	0	0.002
Zr	0	0.077	0	0.002
Nb	0	0.026	0	0.002
Mo	0	0.002	0	0.002
Pd	0	0.000	0	0.005
Ag	0	0.004	0	0.003

Appendix V: Virgin aggregates - Single sized grading

0/6mm Virgin Aggregates			
Sieve Size (mm)	Mass Retained (g)	Mass Passing (g)	Percentage Passing (%)
10	-	1,004	100
6	6	998	99
4	77	921	92
2	248	673	67
1	254	419	42
0.425	226	193	19
0.300	55	137	14
0.150	64	74	7
0.075	32	41	4
	41	-	-
	1,004		

6/10mm Virgin Aggregates			
Sieve Size (mm)	Mass Retained (g)	Mass Passing (g)	Percentage Passing (%)
14	-	1,013	100
10	3	1,010	100
6	340	669	66
4	603	66	7
2	66	-	-
	1,013		

10/14mm Virgin Aggregates			
Sieve Size (mm)	Mass Retained (g)	Mass Passing (g)	Percentage Passing (%)
20	-	1,009	100
14	42	967	96
10	530	437	43
6	429	8	1
4	8	-	-
	1,009		

14/20mm Virgin Aggregates			
Sieve Size (mm)	Mass Retained (g)	Mass Passing (g)	Percentage Passing (%)
28	-	1,030	100
20	96	934	91
14	644	289	28
10	260	29	3
6.3	29	-	-
	1,030		

Appendix VI: RAP aggregates - Single sized grading

0/6mm RAP Aggregates			
Sieve Size (mm)	Mass Retained (g)	Mass Passing (g)	Percentage Passing (%)
10	-	1,038	100
6	8	1,030	99
4	519	511	49
2	370	141	14
1	114	28	3
0.425	19	8	1
0.300	1	7	1
0.150	3	4	0
0.075	2	2	0
	2	-	-
	1,037.67		

6/10mm RAP Aggregates			
Sieve Size (mm)	Mass Retained (g)	Mass Passing (g)	Percentage Passing (%)
14	-	1,027	100
10	5	1,022	100
6	841	181	18
4	167	14	1
2	14	-	-
	1,027		

10/14mm RAP Aggregates			
Sieve Size (mm)	Mass Retained (g)	Mass Passing (g)	Percentage Passing (%)
20	-	1,023	100
14	18	1,006	98
10	635	371	36
6	360	11	1
4	11	-	-
	1,023		

14/20mm RAP Aggregates			
Sieve Size (mm)	Mass Retained (g)	Mass Passing (g)	Percentage Passing (%)
20	-	991	100
14	27	964	98
10	772	192	19
6	176	16	2
4	16	-	-
	991	-	-

Appendix VII: Aggregate combined grading

Laboratory blended samples A, B, C, D						
Virgin Aggregates				RAP Aggregates		
Sieve Size (mm)	Mass Retained (g)	Mass Passing (g)	Percentage Passing (%)	Mass Retained (g)	Mass Passing (g)	Percentage Passing (%)
28.000	-	997.00	100	-	995.75	100
20.000	21.00	976.00	98	-	995.75	100
14.000	85.00	891.00	89	121.75	874.00	88
10.000	93.50	797.50	77	123.00	751.00	75
6.300	127.50	670.00	64	124.50	626.50	63
4.000	140.75	529.25	49	102.50	524.00	53
2.000	151.00	378.25	35	178.25	345.75	35
1.000	139.25	239.00	21	144.00	201.75	20
0.425	119.00	120.00	11	107.00	94.75	10
0.300	29.50	90.50	8	24.75	70.00	7
0.150	39.00	51.50	5	31.00	39.00	4
0.075	22.75	28.75	2	19.00	20.00	2
	28.75	-	-	20.00	-	-
	997.00			**995.75**		

A = Aggregates retained on sieve size 2.36 mm

= 100 % – 35 % = 65 %

B = Aggregates passing sieve size 2.36 mm and retained on sieve size 0.075 mm

= 35 % - 2 % = 33 %

C = Filler passing sieve size 0.075 mm = 2 %

Appendix VIII: Emulsion Coating Test

Pre-mix water (%)	Coated Aggregates (%)	
	Virgin Mix	RAP Mix
1	20	10
2	35	25
3	50	40
`4	65	55
5	80	70

Appendix IX: Virgin mix Moisture-Density relationship (VH-Method)

MINISTRY OF TRANSPORT, INFRASTRUCTURE, HOUSING URBAN DEVELOPMENT MATERIAL, TESTING AND RESEARCH DEPARTMENT

DRY DENSITY/MOISTURE CONTENT RELATIONSHIP — Standard Specification used: **Vibrating Hammer Method - BS 1377 - 4**

Sample No. :		Date	16/2/2018
Sample source :	DM QUARRIES		
Sample description :	Virgin Aggregates		

MOISTURE CONTENT	Unit	1%	2%	3%	4%	5%		
Tin Nº.	-	3A	81A	2C	24C	81C		
Wt of sample + Tin	g	488.1	477.1	517.1	473.3	478.0		
Wt of sample + Tin	g	459.0	446.0	479.0	435.0	434.0		
Wt of Water	g	29.1	31.1	38.1	38.3	44.0		
Wt of Tin	g	28.0	24.8	30.2	30.6	23.6		
Wt of Dry Soil	g	431.0	421.2	448.8	404.4	410.4		
Moisture Content MC	%	6.8	7.4	8.5	9.5	10.7		
Average MC	%	7.7	8.9	9.6	10.7	11.5		
DRY DENSITY								
Test no	g	100	330	325	328	1000		
mass of Sample (A)		6000	6000	6000	6000	6000		
Water content (B)	%	300	360	420	480	540		
Water content PMC = 2.9%	%	5	6	7	8	9		
Wt of Mould + specimen	g	12055	12301	12416	12317	12200		
Wt of Mould	g	6962	6962	6962	6962	6962		
Height of specimen	mm	133	132	133	131	133		
Wt of Compacted specimen	g	5093	5339	5454	5355	5238		
Volume of Mould	cc	2378	2414	2342	2324	2396		
Wet Density	Kg/m^3	2110	2228	2259	2252	2170		
Dry Density	Kg/m^3	1959	2046	2061	2035	1946		

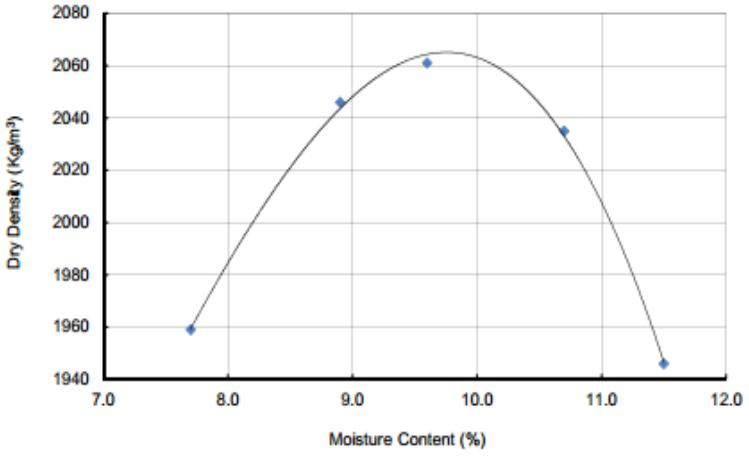

MDD = 2065 Kg/m^3

OMC = 9.7 %

Observations :

Preparation procedure :

2.5kg rammer	
4.5kg rammer	
vibrating hamme	√
3 layers	√
5 layers	

Appendix X: RAP mix Moisture-Density relationship (VH-Method)

MINISTRY OF TRANSPORT, INFRASTRUCTURE, HOUSING URBAN DEVELOPMENT MATERIAL, TESTING AND RESEARCH DEPARTMENT

DRY DENSITY/MOISTURE CONTENT RELATIONSHIP	Standard Specification used:	Vibrating Hammer Method - BS 1377 - 4
Sample No. :	Date	16/2/2018
Sample source :	DM QUARRIES	
Sample description :	Reclaimed Asphalt Pavement (RAP) Aggregates	

MOISTURE CONTENT	Unit	1%	2%	3%	4%	5%		
Tin Nº.	-	3A	81A	2C	24C	81C		
Wt of sample + Tin	g	488.1	477.1	517.1	473.3	478.0		
Wt of sample + Tin	g	459.0	446.0	479.0	435.0	434.0		
Wt of Water	g	29.1	31.1	38.1	38.3	44.0		
Wt of Tin	g	28.0	24.8	30.2	30.6	23.6		
Wt of Dry Soil	g	431.0	421.2	448.8	404.4	410.4		
Moisture Content MC	%	6.8	7.4	8.5	9.5	10.7		
Average MC	%	5.2	6.3	7.2	8.4	9.5		
DRY DENSITY								
Test no	g	100	330	325	325	1000		
Mass of Sam (A)	g	6000	6000	6000	6000	6000		
Water conten (B)	%	180	240	300	360	420		
Water conten PMC = 2.2%	%	3	4	5	6	7		
Wt of Mould + specimen	g	11420	11750	12043	11950	11794		
Wt of Mould	g	6962	6962	6962	6962	6962		
Height of specimen	mm	132	132	133	133	133		
Wt of Compacted specimen	g	4458	4788	5081	4988	4832		
Volume of Mould	cc	2378	2414	2342	2324	2396		
Wet Density	Kg/m^3	1862	1998	2105	2066	2002		
Dry Density	Kg/m^3	1769	1880	1963	1906	1828		

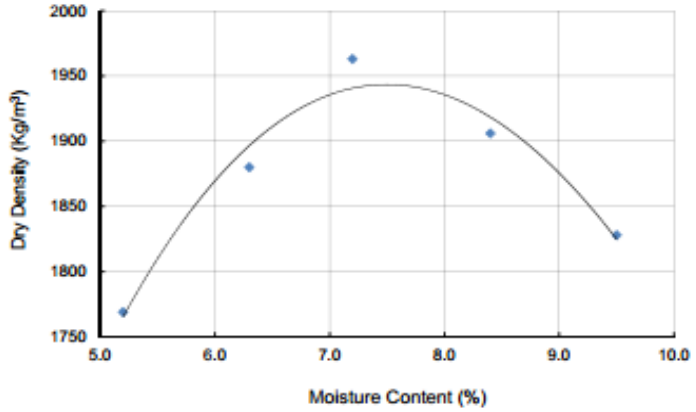

MDD = 1945 Kg/m^3

OMC = 7.5 %

Preparation procedure :

2.5kg rammer	
4.5kg rammer	
vibrating hamme	√
3 layers	√
5 layers	

Appendix XI: Pre-Mix Water Content

Virgin Mix Pre-Mix Water Content at 8 % IEC

Sample No.	Water content (%)	Wt in AIR (g)	Wt in H2O (g)	Wt in SSD (g)	Volume (Kg/m3)	Bulk Specific Gravity (BSG)	Ave BSG	(D) Diameter (mm)	(D) Ave (mm)	(H) Height (mm)	(H) Ave mm	(P) Dial Reading	(P) Ave	Stability (0.0228 X P)
5VA	0.7	1122.2	585.6	1128.7	543.1	2.07		101.1		69.4		98		
5VB	0.7	1134.9	593.8	1144.6	550.8	2.06	2.05	101.6	101.3	69.0	70.1	90	86.33	1.97
5VC	0.7	1138.4	591.6	1152.9	561.3	2.03		101.2		71.9		71		
6VA	1.7	1143.8	598.6	1147.2	548.6	2.08		101.0		69.3		99		
6VB	1.7	1149	605	1152.6	547.6	2.10	2.09	101.1	101.1	69.5	69.4	129	114.33	2.61
6VC	1.7	1143.9	596.9	1147.9	551	2.08		101.1		69.6		115		
7VA	2.7	1144.8	609.4	1150.1	540.7	2.12		101.4		68.3		122		
7VB	2.7	1149.8	605.6	1152	546.4	2.10	2.11	101.1	101.2	69.4	68.7	105	115.67	2.64
7VC	2.7	1150	607.5	1153.6	546.1	2.11		101.0		68.5		120		
8VA	3.7	1140.3	600.6	1143.7	543.1	2.10		101.0		68.1		100		
8VB	3.7	1144.9	603.8	1146	542.2	2.11	2.11	101.1	101.0	67.9	67.8	89	97.67	2.23
8VC	3.7	1141.8	605.6	1142.9	537.3	2.13		101.0		67.5		104		
9VA	4.7	1131.8	600	1132.4	532.4	2.13		100.6		67.6		75		
9VB	4.7	1111.9	585.9	1114.8	528.9	2.10	2.11	101.3	101.1	67.8	67.4	64	71.33	1.63
9VC	4.7	1127.2	594.9	1128.6	533.7	2.11		101.5		66.8		75		

RAP Mix Pre-Mix Water Content at 5% IEC

Sample No.	Water content (%)	Wt in AIR (g)	Wt in H2O (g)	Wt in SSD (g)	Volume (Kg/m3)	Bulk Specific Gravity (BSG)	Ave BSG	(D) Diameter (mm)	(D) Ave (mm)	(H) Height (mm)	(H) Ave mm	(P) Dial Reading	(P) Ave	Stability (0.0228 X P) (kN)
4RA	1.3	1127.4	594	1149.9	555.9	2.03		100.8		70.3		79		
4RB	1.3	1121.4	580.5	1133.6	553.1	2.03	2.03	100.9	100.9	70.1	69.7	87	88.00	2.01
4RC	1.3	1121.5	579.2	1129.8	550.6	2.04		101.0		68.8		98		
5RA	2.3	1128.4	588.2	1133.4	545.2	2.07		101.1		68.3		117		
5RB	2.3	1133.3	591.3	1139	547.7	2.07	2.07	101.2	101.1	68.8	69.0	117	114.33	2.61
5RC	2.3	1131.4	591.3	1140.9	549.6	2.06		100.9		69.9		109		
6RA	3.3	1125.7	594.1	1132.6	538.5	2.09		101.2		67.4		103		
6RB	3.3	1119.8	588.8	1125.7	536.9	2.09	2.10	100.9	100.9	67.7	67.5	102	108.33	2.47
6RC	3.3	1138.6	611.3	1144.7	533.4	2.13		100.8		67.6		120		
7RA	4.3	1126.3	603.2	1130.6	527.4	2.14		101.0		66.3		125		
7RB	4.3	1131.5	603	1136.4	533.4	2.12	2.13	100.8	100.9	67.8	66.6	124	123.33	2.81
7RC	4.3	1114.4	598.2	1117.4	519.2	2.15		100.9		65.6		121		
8RA	5.3	1118.9	598.6	1121.7	523.1	2.14		100.6		66.7		120		
8RB	5.3	1114.8	599.9	1117.7	517.8	2.15	2.13	100.7	100.8	66.1	66.7	110	115.00	2.62
8RC	5.3	1137.4	603.3	1142.8	539.5	2.11		101.1		67.3		115		

Appendix XII: Bitumen content

Virgin Mix Bitumen Content at 2.8 % Pre-mix Water Content - (Dry tested Specimens)

Sample No.	Bitumen Content (%)	Wt in AIR (g)	Wt in H2O (g)	Wt in SSD (g)	Volume (Kg/m3)	Bulk Specific Gravity (BSG)	Ave BSG	(D) Diameter (mm)	(D) Ave (mm)	(H) Height (mm)	(H) Ave mm	(P) Dial Reading	(P) Ave	Stability (0.0228 X P) (kN)
5VA	3.3	1114.8	594.3	1117.9	523.6	2.13		101.8		66.1		182		
5VB	3.3	1115.7	594.4	1119.3	524.9	2.13	2.13	101.7	101.7	66.1	66.0	178	176.50	4.02
5VC	3.3	1115.3	594.5	1120.1	525.6	2.12		101.6		65.9		175		
6VA	3.9	1126.3	597.2	1129.2	532	2.12		101.5		67.2		180		
6VB	3.9	1120.7	591.9	1124.3	532.4	2.10	2.11	101.4	101.5	67.2	67.3	135	171.00	3.90
6VC	3.9	1128.8	599.5	1133	533.5	2.12		101.4		67.5		162		
7VA	4.6	1134.7	602.6	1137.1	534.5	2.12		101.3		67.7		175		
7VB	4.6	1132.4	598.6	1136.3	537.7	2.11	2.12	101.7	101.6	68.1	67.5	177	176.00	4.01
7VC	4.6	1135.6	604.5	1140.1	535.6	2.12		101.6		66.9		188		
8VA	5.2	1140.1	594.2	1143.7	549.5	2.07		101.5		70.2		121		
8VB	5.2	1135.3	598.5	1138	539.5	2.10	2.09	102.1	101.7	66.9	68.2	162	159.00	3.63
8VC	5.2	1126	588.2	1130	541.8	2.08		101.5		67.7		156		
9VA	5.9	1137.2	598.1	1140.3	542.2	2.10		101.6		67.9		151		
9VB	5.9	1132.8	589.9	1136.1	546.2	2.07	2.09	101.5	101.6	68.9	68.0	130	154.00	3.51
9VC	5.9	1124.5	592	1127.2	535.2	2.10		101.6		67.1		157		

Virgin Mix Bitumen Content at 2.8 % Pre-mix Water Content - (Moisture-Conditioned Specimens)

Sample No.	Bitumen Content (%)	Wt in AIR (g)	Wt in H2O (g)	Wt in SSD (g)	Volume (Kg/m3)	Bulk Specific gravity	Ave BSG	(D) Diameter (mm)	(D) Ave (mm)	(H) Height (mm)	(H) Ave mm	(P) Dial Reading	(P) Ave	Stability (0.0228 X P) (kN)
5VA	3.3	1193.9	651.2	1193.9	542.7	2.20		101.3		66.9		50		
5VB	3.3	1173.5	635.2	1173.5	538.3	2.18	2.19	101.3	101.2	66.9	66.9	80	80.00	1.82
5VC	3.3	1174.6	639.1	1174.6	535.5	2.19		101.1		66.8		80		
6VA	3.9	1166.5	630.4	1166.5	536.1	2.18		101.6		66.6		102		
6VB	3.9	1181.4	636.4	1181.4	545	2.17	2.16	101.0	101.3	67.7	67.3	114	116.50	2.66
6VC	3.9	1169	624.8	1169	544.2	2.15		101.2		67.6		119		
7VA	4.6	1172.6	628	1172.6	544.6	2.15		101.6		66.9		133		
7VB	4.6	1182.8	632.4	1182.8	550.4	2.15	2.15	101.1	101.2	67.9	67.4	122	127.50	2.91
7VC	4.6	1173.2	630.1	1173.2	543.1	2.16		101.0		67.5		158		
8VA	5.2	1177.4	630.4	1177.4	547	2.15		101.9		68.9		136		
8VB	5.2	1179.7	633	1179.7	546.7	2.16	2.16	101.8	101.8	68.0	68.3	157	154.50	3.52
8VC	5.2	1181.8	634.2	1181.8	547.6	2.16		101.9		68.2		152		
9VA	5.9	1183.7	637.1	1183.7	546.6	2.17		101.9		68.0		141		
9VB	5.9	1179.7	631.2	1179.7	548.5	2.15	2.15	101.8	101.7	68.1	68.4	150	141.50	3.23
9VC	5.9	1180.5	627.3	1180.5	553.2	2.13		101.5		69.3		142		

RAP Mix Bitumen Content at 4.0 % Pre-mix Water Content - (Dry tested Specimens)

Sample No.	Bitumen Content (%)	Wt in AIR (g)	Wt in H2O (g)	Wt in SSD (g)	Volume (Kg/m3)	Bulk Specific Gravity (BSG)	Ave BSG	(D) Diameter (mm)	(D) Ave (mm)	(H) Height (mm)	(H) Ave mm	(P) Dial Reading	(P) Ave	Stability (0.0228 X P) (kN)
2RA	1	1102.1	582.8	1103.7	520.9	2.12		102.0		65.5		220		
2RB	1	1090.3	585	1096.5	511.5	2.13	2.13	100.9	101.5	64.6	65.1	170	186.67	4.26
2RC	1	1107.4	594	1113.7	519.7	2.13		101.7		65.3		170		
3RA	2	1108.2	590.5	1110.3	519.8	2.13		101.6		65.0		220		
3RB	2	1108.3	590.5	1112.6	522.1	2.12	2.13	101.5	101.6	65.5	65.2	235	218.33	4.98
3RC	2	1111.4	596.8	1115.6	518.8	2.14		101.7		65.0		200		
4RA	3	1121.3	595.1	1123.3	528.2	2.12		101.8		66.6		240		
4RB	3	1063.1	563.7	1065.9	502.2	2.12	2.12	101.4	101.7	64.2	65.5	225	226.67	5.17
4RC	3	1119.8	592.9	1124.3	531.4	2.11		101.8		65.7		215		
5RA	4	1137.1	598.1	1138.1	540	2.11		101.6		68.0		220		
5RB	4	1133.3	598.5	1136.6	538.1	2.11	2.11	102.2	101.9	67.2	67.6	214	215.33	4.91
5RC	4	1134.2	599.4	1136.6	537.2	2.11		101.8		67.7		212		
6RA	5	1141.2	595.1	1145.1	550	2.07		101.7		69.2		185		
6RB	5	1142.6	596.9	1144.3	547.4	2.09	2.09	101.8	101.7	68.3	68.4	202	195.67	4.46
6RC	5	1136.1	595.8	1138.3	542.5	2.09		101.6		67.8		200		

RAP Mix Bitumen Content at 4.0 % Pre-mix Water Content - (Moisture-Conditioned Specimens)

Sample No.	Bitumen Content (%)	Wt in AIR (g)	Wt in H2O (g)	Wt in SSD (g)	Volume (Kg/m3)	Bulk Specific gravity	Ave BSG	(D) Diameter (mm)	(D) Ave (mm)	(H) Height (mm)	(H) Ave mm	(P) Dial Reading	(P) Ave	Stability (0.0228 X P) (kN)
2RA	1	1126.3	609.3	1126.3	517	2.18		100.7		65.8		182		
2RB	1	1142	625.6	1142	516.4	2.21	2.20	100.9	100.9	65.0	65.0	178	178.33	4.07
2RC	1	1137.8	625.2	1137.8	512.6	2.22		101.2		64.3		175		
3RA	2	1139.5	613.2	1139.5	526.3	2.17		101.0		65.9		180		
3RB	2	1131.4	614.2	1131.4	517.2	2.19	2.17	101.0	101.0	64.5	65.6	135	171.00	3.90
3RC	2	1138.7	612.1	1138.7	526.6	2.16		100.9		66.3		162		
4RA	3	1144.9	613.2	1144.9	531.7	2.15		101.0		67.1		175		
4RB	3	1136.9	610.1	1136.9	526.8	2.16	2.15	100.8	101.0	66.4	66.6	177	180.00	4.10
4RC	3	1138.4	604.7	1138.4	533.7	2.13		101.2		66.4		188		
5RA	4	1157.2	617.6	1157.2	539.6	2.14		101.2		67.9		121		
5RB	4	1151.1	612.2	1151.1	538.9	2.14	2.14	101.0	101.1	67.2	67.6	162	159.00	3.63
5RC	4	1150.7	614.9	1150.7	535.8	2.15		101.0		67.8		156		
6RA	5	1151.6	604.5	1151.6	547.1	2.10		101.3		67.9		151		
6RB	5	1153.9	607.7	1153.9	546.2	2.11	2.11	101.1	101.1	68.3	68.0	130	146.00	3.33
6RC	5	1151.6	605.2	1151.6	546.4	2.11		101.0		67.8		157		

Appendix XIII: Air Voids at different compaction levels

Air Voids calculation sheet: MS-14, Appendix F (Asphalt Institute, 1989)

	RAP Mix			Virgin Mix		
Compaction blows (No.)	**50**	**75**	**150**	**50**	**75**	**150**
A(Residual asphalt content by wt. of agg.)	3	3	3	5	5	5
G(Bulk SpecificGravity)	2.07	2.09	2.15	2.18	2.21	2.25
Gd(Dry BSG)	1.987	2.006	2.064	2.129	2.159	2.198
Dry Bulk Density	1987	2006	2064	2129	2159	2198
K1(Water content at by wt. of agg.)	4.3	4.3	4.3	2.5	2.5	2.5
C (apparent sp.Gr.)	2.76	2.76	2.76	2.78	2.78	2.78
(100+A+K)/G	51.84	51.34	49.91	49.31	48.64	47.78
(100/C)	36.23	36.23	36.23	35.97	35.97	35.97
(A/B)	2.94	2.94	2.94	4.90	4.90	4.90
VMA,%	30.10	29.43	27.40	27.05	26.05	24.71
V (Total voids),%	24.43	23.70	21.51	17.11	15.97	14.45
(K*100)/L	430	430	430	250	250	250
Air Voids%	16.1	15.3	12.9	12.0	10.8	9.2
Dry Stability(KN)	2.96	3.25	3.48	2.96	2.96	2.96

Appendix XIV: Air Voids at different compaction levels

Indirect Tensile Strength of Virgin Mix Cured at 25 °C

Curing time (days)	Sample No.	Wt in Air (g)	Wt in water (g)	SSD Weight (g)	Volume (m3)	Bulk Specific Gravity (BSG)	Ave. BSG (Kg/m3)	(D1) Diameter (mm)	(D2) Diameter (mm)	(D3) Diameter (mm)	D Average (mm)	(H1) Height (mm)	(H2) Height (mm)	(H3) Height (mm)	H Average (mm)	(P) ITS Dial Reading	(Pu) Stability (P*0.0028) (kN)	ITS (2*Pu*10^6*)/ (3.14DH	Average ITS (kN/m2)
3 days	8V1	1154.3	614.9	1157.2	542.3	2.13		101.6	101	101.4	101.3	67	67.6	67.7	67.4	109	2.49	231.65	
	8V3	1160.3	621.7	1162.5	540.8	2.15	2.14	101.6	101.6	101.7	101.6	67.1	66.4	67	66.8	111	2.53	237.32	231.04
	8V5	1159.7	619.7	1161.1	541.4	2.14		101	101	101.1	101.0	67	67.6	67.4	67.3	105	2.39	224.15	
8 days	3V2	1153.9	611.2	1156.4	545.2	2.12		101.3	101	101.3	101.2	68.5	67	67.3	67.6	154	3.51	326.91	
	3V12	1158.6	620.3	1160	539.7	2.15	2.14	100.8	101	101	100.9	68	66.6	67	67.2	157	3.58	336.15	335.50
	3V16	1155.3	618	1156.8	538.8	2.14		101.4	101.4	101.5	101.4	66.5	67.4	66.2	66.7	160	3.65	343.44	
13 days	3V5	1157.2	613.8	1059.7	445.9	2.60		101	100.8	101	100.9	68	68	67.5	67.8	155	3.53	328.77	
	3V7	1158.4	618.1	1160.6	542.5	2.14	2.29	101.5	101.3	101.4	101.4	66.7	67	67.5	67.1	167	3.81	356.62	346.34
	3V15	1089.2	582.9	1090.9	508	2.14		101.5	101.5	101.5	101.5	67.8	67.5	67.4	67.6	167	3.81	353.63	
18 days	3V6	1155.9	616	1157.4	541.4	2.14		101.1	101.2	101.1	101.1	67.7	67.5	67.8	67.7	160	3.65	339.54	
	3V9	1158.6	617.6	1159.8	542.2	2.14	2.14	101	101.1	100.8	101.0	67.6	68.4	68.2	68.1	150	3.42	316.97	347.04
	3V13	1154.2	614.9	1155.7	540.8	2.13		101.1	100.7	101	100.9	66.9	67.8	67.3	67.3	180	4.10	384.63	
23 days	3V4	1146.2	607.6	1147.7	540.1	2.12		101	101	100.8	100.9	67.1	66.6	67	66.9	194	4.42	417.23	
	3V11	1163.7	619.7	1165.2	545.5	2.13	2.13	101	100.6	101.2	100.9	67.7	67.3	68.7	67.9	190	4.33	402.61	413.90
	3V14	1143.9	608.9	1146.2	537.3	2.13		101.3	101.3	101.6	101.4	65.6	66.8	66.2	66.2	195	4.45	421.87	
Indirect Tensile Strength of RAP Mix Cured at 25 °C																			
3 days	4R2	1125.5	600.6	1129.2	528.6	2.13		101.2	100.6	101.1	101.0	66.6	66.7	66.7	66.7	53	1.21	114.35	
	4R3	1127.2	603.3	1130.1	526.8	2.14	2.13	101.1	101.2	100.9	101.1	66.3	66	66	66.1	56	1.28	121.73	122.35
	4R4	1118.2	596.6	1121.8	525.2	2.13		101.5	101.7	101.8	101.7	65.1	65.8	65.4	65.4	60	1.37	130.98	
8 days	4R2	1120.4	595	1122.6	527.6	2.12		101	100.6	101	100.9	65.3	65.5	65.4	65.4	163	3.72	358.84	
	4R3	1123.2	593.9	1126.4	532.5	2.11	2.11	101.2	101.6	101.4	101.4	65.6	66	65.6	65.7	150	3.42	326.82	343.60
	4R15	1117.6	588.9	1121.8	532.9	2.10		100.7	100.8	101	100.8	66.5	67.3	66.5	66.8	160	3.65	345.14	
13 days	4R5	1123.9	597.5	1127.3	529.8	2.12		101.5	101.3	101.2	101.3	65.6	65.1	66	65.6	208	4.74	454.64	
	4R9	1130.4	600.5	1133.7	533.2	2.12	2.12	101.6	101.5	101.3	101.5	66.3	66	65.7	66.0	202	4.61	438.05	445.42
	4R11	1127.7	597.2	1130.4	533.2	2.11		101.5	101.4	101.6	101.5	65.6	65.8	66	65.8	204	4.65	443.58	
18 days	4R4	1120.7	582	1122.1	540.1	2.07		101	101.1	101.1	101.1	66	67	66.5	66.5	166	3.78	358.69	
	4R12	1131.9	589.7	1134.7	545	2.08	2.07	101	100.8	101	100.9	67	67	66.9	67.0	162	3.69	348.06	366.43
	4R16	1123.4	580.4	1125.2	544.8	2.06		100.9	100.8	101	100.9	65.8	66	66.2	66.0	180	4.10	392.53	
23 days	4R7	1123.3	595.7	1126.7	531	2.12		101	101	101	101.0	66	66.1	65.7	65.9	190	4.33	414.35	
	4R8	1123.1	596	1128.6	532.6	2.11	2.12	101.3	101	101.1	101.1	66.2	66.3	66.3	66.3	184	4.20	398.72	404.67
	4R10	1124	598.8	1128.4	529.6	2.12		101.4	101.2	101.6	101.4	65.7	65.5	64.9	65.4	183	4.17	400.95	

Indirect Tensile Strength of Virgin Mix Cured at 40 °C

Curing time (days)	Sample No.	Wt in Air (g)	Wt in water (g)	SSD Weight (g)	Volume (m3)	Bulk Specific Gravity (BSG)	Ave. BSG (Kg/m3)	(D1) Diameter (mm)	(D2) Diameter (mm)	(D3) Diameter (mm)	D Average (mm)	(H1) Height (mm)	(H2) Height (mm)	(H3) Height (mm)	H Average (mm)	(P) ITS Dial Reading	(Pu) Stability (P*0.0028) (kN)	ITS (2*Pu*10^6*)/ (3.14DH	Average ITS (kN/m2)
3 days	8V1	1154.3	609	1156.6	547.6	2.11		101.6	101.8	101.5	101.6	67.2	68	68.2	67.8	165	3.76	347.74	
	8V6	1156.3	612.7	1159	546.3	2.12	2.12	101	101	101.2	101.1	68.3	68.6	68.8	68.6	162	3.69	339.49	351.12
	8V11	1155.1	614.1	1157.2	543.1	2.13		101	101	101	101.0	69.2	67.2	68.6	68.3	174	3.97	366.13	
8 days	8V1	1146.1	601.7	1150.7	549	2.09		101	100.8	101	100.9	67.8	69.7	67.6	68.4	170	3.88	357.77	
	8V2	1150.9	606.1	1153.1	547	2.10	2.10	101.3	101.3	101.5	101.4	67.9	67.7	67.4	67.7	165	3.76	349.34	357.96
	8V3	1143.7	605.7	1146	540.3	2.12		101	101.3	101.4	101.2	67.6	67	68.4	67.7	173	3.94	366.76	
13 days	8V3	1146.7	602.9	1149.7	546.8	2.10		101.3	100.6	101	101.0	68	67	68.8	67.9	189	4.31	400.16	
	8V10	1147.9	611	1150.3	539.3	2.13	2.11	101.3	101.5	101.5	101.4	68	67	67.5	67.5	185	4.22	392.39	401.83
	8V15	1146.1	605.4	1149.2	543.8	2.11		101.2	101	101.1	101.1	69	67.3	67.2	67.8	195	4.45	412.93	
18 days	8V5	1144.8	600.9	1148.1	547.2	2.09		101.4	101	101	101.1	67.8	67.7	68.3	67.9	229	5.22	484.05	
	8V13	1145.4	603.1	1148.6	545.5	2.10	2.10	101	101	101	101.0	67.7	68	67.7	67.8	235	5.36	498.37	481.45
	8V14	1147.9	604.8	1152.3	547.5	2.10		101.2	101	101	101.1	68	68.6	68.7	68.4	220	5.02	461.94	
23 days	8V2	1141.5	595.6	1144.2	548.6	2.08		101.2	101.1	100.8	101.0	69.2	69.7	68.6	69.2	239	5.45	496.67	
	8V4	1141.1	600	1144	544	2.10	2.10	101.4	101.6	101.7	101.6	67.7	67.4	67.9	67.7	253	5.77	534.60	500.28
	8V12	1137.8	602.6	1140.1	537.5	2.12		101.6	101.5	101.7	101.6	66.4	68	66.5	67.0	220	5.02	469.58	
Indirect Tensile Strength of RAP Mix Cured at 40 °C																			
3 days	3RA	1110.1	596.3	1113.6	517.3	2.15		101.5	101.7	102	101.7	66	67.1	65	66.0	150	3.42	324.26	
	3RB	1104	594.1	1107	512.9	2.15	2.15	101.3	100.6	101	101.0	63.7	65	63.7	64.1	146	3.33	327.44	335.42
	3RD	1101.1	591.6	1103.5	511.9	2.15		101.3	101.1	101	101.1	64.6	65	64.8	64.8	160	3.65	354.56	
8 days	8R2	1132.6	597	1135.8	538.8	2.10		101	101	101.8	101.3	68.2	67	67.5	67.6	190	4.33	403.26	
	8R3	1121.2	592.5	1123	530.5	2.11	2.11	101.3	101	101.1	101.1	65.7	67	66	66.2	190	4.33	411.92	412.79
	8R4	1126.8	595.1	1129.1	534	2.11		101.3	101	101.1	101.1	66.6	66	65.9	66.2	195	4.45	423.19	
13 days	4R2	1103.8	593.3	1110.5	517.2	2.13		101	101	101.1	101.0	65.8	64.3	66	65.4	214	4.88	470.57	
	4R6	1092	586.1	1095.8	509.7	2.14	2.14	101	101.3	101.6	101.3	64	62.8	65	63.9	228	5.20	511.25	489.46
	4R15	1101.1	590.8	1105.5	514.7	2.14		101	100.8	101.3	101.0	64	64.2	65	64.4	218	4.97	486.57	
18 days	4R4	1102.5	589.1	1105.1	516	2.14		101	101	101.4	101.1	64.3	64.9	64.5	64.6	191	4.35	424.78	
	4R9	1099.8	592.4	1100.9	508.5	2.16	2.15	101.2	100.9	101.2	101.1	63.8	64	64.2	64.0	215	4.90	482.55	454.15
	4R11	1108.8	596.1	1110.8	514.7	2.15		101	101	101	101.0	65	64.7	64.6	64.8	205	4.67	455.11	
23 days	4R7	1093.9	582	1098.5	516.5	2.12		101.4	101	101	101.1	64.5	66	64.4	65.0	232	5.29	512.79	
	4R12	1109.9	593	1112.2	519.2	2.14	2.13	101	101	101.5	101.2	64.4	65.5	65.8	65.2	220	5.02	484.12	511.67
	4R5	1092	587.2	1095.4	508.2	2.15		101	101	101.3	101.1	64	64.2	64	64.1	240	5.47	538.10	

Indirect Tensile Strength of Virgin Mix Cured at 60 °C

Curing time (days)	Sample No.	Wt in Air (g)	Wt in water (g)	SSD Weight (g)	Volume (m3)	Bulk Specific Gravity (BSG)	Ave. BSG (Kg/m3)	(D1) Diameter (mm)	(D2) Diameter (mm)	(D3) Diameter (mm)	D Average (mm)	(H1) Height (mm)	(H2) Heigh t (mm)	(H3) Height (mm)	H Average (mm)	(P) ITS Dial Reading	(Pu) Stability (P*0.0028) (kN)	ITS (2*Pu*10^6*)/ (3.14DH	Average ITS (kN/m2)
3 days	7V1	1148.6	607	1152.5	545.5	2.11		101.2	101.3	101.4	101.3	67.6	67.7	68	67.8	180	4.10	380.79	
	7V3	1154.7	607.9	1158.9	551	2.10	2.10	101.2	101.2	101.3	101.2	68	68.1	68.9	68.3	177	4.04	371.58	383.42
	7V4	1157.5	612.8	1161.2	548.4	2.11		101.1	101.2	101.1	101.1	68.8	68.9	68	68.6	190	4.33	397.91	
8 days	7V3	1145.5	592.2	1145.8	553.6	2.07		101	101	101.1	101.0	68	67.1	67.5	67.5	225	5.13	478.89	
	7V5	1140.6	588.5	1142.6	554.1	2.06	2.06	101	101.1	101.1	101.1	68.3	67.5	67.4	67.7	220	5.02	466.71	460.16
	7V7	1141.3	588.2	1143.7	555.5	2.05		101	101.3	101.2	101.2	68	68.3	66.7	67.7	205	4.67	434.89	
13 days	7V2	1137.7	594.2	1140.8	546.6	2.08		101.8	101.6	101.4	101.6	67	68.6	67	67.5	243	5.54	514.32	
	7V4	1139.9	596.4	1143.4	547	2.08	2.09	101	100.9	101.1	101.0	68.6	68.9	68.2	68.6	240	5.47	503.28	514.02
	7V8	1137.1	597	1140.4	543.4	2.09		101.2	101.3	101.2	101.2	67.1	68.9	67.5	67.8	248	5.65	524.47	
18 days	6V2	1137	591.3	1139.5	548.2	2.07		101	101.2	101.2	101.1	68	69	68.6	68.5	269	6.13	563.63	
	6V4	1139.1	595.1	1140.6	545.5	2.09	2.08	101	101	101	101.0	68.4	67.5	68.3	68.1	280	6.38	591.48	589.40
	6V6	1139.3	595.8	1141.4	545.6	2.09		101.5	101.5	101.7	101.6	66.8	67.9	68.2	67.6	290	6.61	613.09	
23 days	6V1	1138.1	584.1	1128.7	544.6	2.09		101.6	101.5	101.6	101.6	67.2	67.6	67.6	67.5	280	6.38	593.41	
	6V5	1140.8	591.9	1143.8	551.9	2.07	2.07	101.4	101.2	101.2	101.3	68.1	68.6	68	68.2	261	5.95	548.55	590.52
	6V7	1138.2	591.2	1142	550.8	2.07		101.3	101.1	101.1	101.2	68.2	68	69	68.4	300	6.84	629.60	
Indirect Tensile Strength of RAP Mix Cured at 60 °C																			
3 days	4R1	1124.1	587.1	1152.5	565.4	1.99		101.4	101.1	101.5	101.3	66.7	67.1	67.4	67.1	207	4.72	442.33	
	4R2	1111.6	583.2	1126.9	543.7	2.04	2.00	101	101.4	101	101.1	67	67.3	66.9	67.1	200	4.56	428.22	436.40
	4R3	1121.3	586.6	1158.9	572.3	1.96		101.8	101.8	101.8	101.8	66.7	66.5	66.8	66.7	205	4.67	438.66	
8 days	7R4	1105.5	569.1	1106.8	537.7	2.06		100.8	101	101	100.9	65.8	66.3	66	66.0	226	5.15	492.43	
	7R6	1109.4	568.6	1112.7	544.1	2.04	2.04	100.6	101	101.1	100.9	67.2	67	67	67.1	218	4.97	467.84	481.76
	7R8	1101	563.5	1104.3	540.8	2.04		100.6	101	100.8	100.8	67.2	66.3	67	66.8	225	5.13	485.02	
13 days	7R3	1104.5	580.7	1107.9	527.2	2.10		100.7	101.1	100.9	100.9	66	65.2	66.6	65.9	250	5.70	545.73	
	7R5	1101.5	574.2	1101	526.8	2.09	2.09	100.2	101.1	101	100.8	66	67.7	66.3	66.7	239	5.45	516.66	535.56
	7R7	1114	585	1117.2	532.2	2.09		101	100.9	101	101.0	66	66.2	66	66.1	250	5.70	544.27	
18 days	6R3	1119.3	579.2	1122.3	543.1	2.06		101.5	101.2	101.1	101.3	67.9	67.7	67	67.5	296	6.75	628.55	
	6R5	1115.7	536	1017.8	481.8	2.32	2.15	101	101.2	101	101.1	61	61.2	61.1	61.1	268	6.11	630.26	609.13
	6R7	1113.7	577.4	1117.4	540	2.06		101	101.1	101.4	101.2	68	67.5	69	68.2	270	6.16	568.58	
23 days	6R2	1112.7	575.2	1117.2	542	2.05		101.7	101.7	101.9	101.8	66.8	67.7	67.3	67.3	275	6.27	583.39	
	6R4	1118.7	576.9	1123.9	547	2.05	2.05	101.2	101.2	101.3	101.2	67.7	68	69	68.2	277	6.32	582.36	574.50
	6R8	1115.8	580.3	1121.4	541.1	2.06		101.1	101.3	101.5	101.3	68	67.7	67.1	67.6	263	6.00	557.74	

Appendix XV: Rate constant (k) and limiting strength (Su)

Curing Temperature	Virgin Mix		RAP-Mix	
(°C)	k	S_u	k	S_u
25	0.3878	429.77	0.1617	547.38
40	0.5575	499.64	0.4187	554.45
60	0.5635	610.24	0.7515	601.76

Appendix XVI: Equivalent Age (*te*) and Modified Arrhenius function (*M*)

Curing Regimes			Virgin Mix				RAP Mix			
(t) Curing time (days)	(T) Curing Temperature °C	(Tr) Reference Temperature °C	Indirect tensile strength (kN/m2)	(B) Temperature Sensistivity Factor	(te) Equivalent age (°C-days)	(M) Maturity ($te \times T$)	Indirect tensile strength (kN/m2)	(B) Temperature Sensistivity Factor	(te) Equivalent age (°C-days)	(M) Maturity ($te \times T$)
3	25	18	231.04	0.0021	3.04	76.11	122.35	0.0361	3.86	96.56
8	25	18	335.50	0.0021	8.12	202.96	343.60	0.0361	10.30	257.50
13	25	18	346.34	0.0021	13.19	329.81	445.42	0.0361	16.74	418.44
18	25	18	347.04	0.0021	18.27	456.66	366.43	0.0361	23.17	579.37
23	25	18	413.90	0.0021	23.34	583.51	404.67	0.0361	29.61	740.31
3	40	18	351.12	0.0021	3.14	125.67	335.42	0.0361	6.64	265.52
8	40	18	357.96	0.0021	8.38	335.13	412.79	0.0361	17.70	708.05
13	40	18	401.83	0.0021	13.61	544.59	489.46	0.0361	28.76	1150.59
18	40	18	481.45	0.0021	18.85	754.04	454.15	0.0361	39.83	1593.12
23	40	18	500.28	0.0021	24.09	963.50	511.67	0.0361	50.89	2035.66
3	60	18	383.42	0.0021	3.28	196.60	436.40	0.0361	13.66	819.88
8	60	18	460.16	0.0021	8.74	524.26	481.76	0.0361	36.44	2186.34
13	60	18	514.02	0.0021	14.20	851.92	535.56	0.0361	59.21	3552.81
18	60	18	589.40	0.0021	19.66	1179.58	609.13	0.0361	81.99	4919.27
23	60	18	590.52	0.0021	25.12	1507.25	574.50	0.0361	104.76	6285.74

Appendix XVII: Model Validation

Curing Regimes			Virgin Mix							RAP Mix						
(*t*) Curing time (days)	(T) Curing Temp. ℃	(*Tr*) Ref. Temp ℃	(*B*) Temperature Sensistivity Factor	(*te*) Equivalent age (℃-days)	(*M*) Maturity (*te x T*)	(k) Rate Constant (1/day)	(Su) Limiting Strength (kN/m2)	Predicted Strength (kN/m2)	Measured ITS (kN/m2)	(*B*) Temperature Sensistivity Factor	(*te*) Equivalent age (℃-days)	(*M*) Maturity (*te x T*)	(k) Rate Constant (1/day)	(Su) Limiting Strength (kN/m2)	Predicted Strength (kN/m2)	Measured ITS (kN/m2)
1	50	18	0.0021	1.07	53.48	0.007	576.1	156.91	183.00	0.0361	3.17	158.73	0.0043	558.63	226.62	219.00
3	50	18	0.0021	3.21	160.43	0.007	576.1	304.74	309.00	0.0361	9.52	476.20	0.0043	558.63	375.33	311.00
6	50	18	0.0021	6.42	320.85	0.007	576.1	398.62	383.00	0.0361	19.05	952.40	0.0043	558.63	448.99	451.00
9	50	18	0.0021	9.63	481.28	0.007	576.1	444.24	447.00	0.0361	28.57	1428.60	0.0043	558.63	480.42	483.00
12	50	18	0.0021	12.83	641.71	0.007	576.1	471.20	476.00	0.0361	38.10	1904.79	0.0043	558.63	497.85	501.00
15	50	18	0.0021	16.04	802.13	0.007	576.1	489.01	494.00	0.0361	47.62	2380.99	0.0043	558.63	508.92	511.00
18	50	18	0.0021	19.25	962.56	0.007	576.1	501.65	512.00	0.0361	57.14	2857.19	0.0043	558.63	516.58	512.00
27	50	18	0.0021	28.88	1443.84	0.007	576.1	524.23	537.00	0.0361	85.72	4285.79	0.0043	558.63	529.88	531.00
30	50	18	0.0021	32.09	1604.26	0.007	576.1	528.99	544.00	0.0361	95.24	4761.99	0.0043	558.63	532.62	540.00
33	50	18	0.0021	35.29	1764.69	0.007	576.1	532.96	567.00	0.0361	104.76	5238.19	0.0043	558.63	534.88	561.00